Myocardial Fatty Acid Metabolism in Normal Ovine Development and Intrauterine Growth Restriction

Rachel R. Drake

Bachelor of Science / Bachelor of Arts

A thesis submitted for the partial fulfillment of the requirements of the degree of Doctor of Philosophy

Dissertation Advisor: Kent L. Thornburg, PhD

Department of Chemical Physiology and Biochemistry
Program in Physiology and Pharmacology
School of Medicine
Oregon Health & Science University
Portland, OR, 97239

April 2021

CERTIFICATE OF APPROVAL

This is to certify that the PhD dissertation of

Rachel Rae Drake

has been approved

Mentor: Kent L. Thornburg, PhD

Committee Chair: George Giraud, MD PhD

Member: Melanie Gillingham, PhD

Member: Cindy

Member: Laura Brown, MD

TABLE OF CONTENTS

LIST OF FIGURES

LIST OF TABLES

LIST OF ABBREVIATIONS AND SYMBOLS

ACAT1	Acetyl-CoA acetyltransferase
ACSL1	Acyl-CoA synthetase long chain 1
ACSL3	Acyl-CoA synthetase long chain 3
ATP	Adenosine triphosphate
ATP5A	ATP synthase F1 subunit alpha
BSA	Bovine serum albumin
BODIPY	4,4-Difluoro-5,7-Dimethyl-4-Bora-3a,4a-Diaza-*s*-Indacene
CD36	Platelet glycoprotein 4, also known as fatty acid translocase (FAT)
CPT1a	Carnitine palmitoyltransferase 1a (fetal isoform)
CPT1b	Carnitine palmitoyltransferase 1b (adult isoform)
CS	Citrate synthase
dGA	days gestational age
DGAT	Diacylglycerol acyltransferase
dPN	days postnatal
FAT	Fatty acid translocase, also known as CD36
FATP6	Fatty acid transport protein 6, also known as SLC27A6
GPAT	Glycerol phosphate acyltransferase
HADH	Hydroxy-acyl dehydrogenase; also HADH/sc or medium, short-chain HAD
HDL	High density lipoprotein
IDH	Isocitrate dehydrogenase

IUGR	Intrauterine growth restriction
LCAD	Long chain acyl-CoA dehydrogenase
LCFA	Long chain fatty acid
LD	Lipid droplet
LDL	Low density lipoprotein
LPL	Lipoprotein lipase
MTCO1	Cytochrome c oxidase subunit 1
NDUFB8	NADH ubiquinone oxidoreductase subunit B8
PAP	Phosphatidic acid phosphatase
PDK4	Pyruvate dehydrogenase kinase 4
PI	Placental insufficiency
PL	Perilipin
SCFA	Short chain fatty acid
SDHB	Succinate dehydrogenase complex subunit B
SGA	Small for gestational age
SLC27A6	Solute carrier family 27 member 6, also known as FATP6
T3	Triiodothyronine
T4	Thyroxine
TAG	Triacylglycerol, also known as Triglyceride
TCA	Tricarboxylic acid
UQCRC2	Ubiquinol cytochrome b-c1 complex subunit 2
VLCAD	Very long chain acyl-CoA dehydrogenase
VLCFA	Very long chain fatty acid

VLDL	Very low density lipoprotein
>	Greater than
<	Less than
~	Approximately
±	Plus or minus

PUBLICATIONS

† data in this manuscript is described in this thesis

data presented in these manuscripts are not discussed in this thesis.

Published manuscripts

Spencer JH, Larson AA, **Drake R**, Iaizzo PA (2014). A detailed assessment of the human coronary venous system using contrast computed tomography of perfusion-fixed specimens. *Heart Rhythm*. **11(2),** 282-8. PMC24144884.

Karunadharma PP, Basisty N, Chiao YA, Dai DF, **Drake R**, Levy N, Koh, WJ, Emond MJ, Kruse S, Marcinek D, Maccoss MJ, Rabinovitch (2015). Respiratory chain protein turnover rates in mice are highly heterogeneous but strikingly conserved across tissues, ages, and treatments. *FASEB J*, **29(8),** 3582-92. PMC4511201.

Thornburg KL, Kolahi K, Pierce M, Valent A, **Drake R**, Louey S (2016). Biological features of placental programming. *Placenta*, **48 [Supplement 1],** S48-S53. PMC5278807.

Lindgren I, **Drake R**, Thornburg KL (2019). MEIS1 promotes the maturation of oxidative phosphorylation in perinatal cardiomyocytes. *FASEB J*, **33(6),** 7417-7426. PMC6529342.

Thornburg KL, **Drake R**, Valent AM (2020). Maternal hypertension affects heart growth in offspring. *J Am Heart Assoc*, **9(9),** e016538. PMC7428588.

Manuscripts under Review

† **Drake RR**, Louey S, Thornburg KL. Intrauterine growth restriction elevates circulating acylcarnitines and suppresses fatty-acid metabolism genes in the fetal sheep heart. *Submitted for review, March 2021.*

† **Drake RR**, Louey S, Thornburg KL. Lipid metabolism gene expression pattern prepares for birth in the ovine heart. *Submitted for review, March 2021.*

Abstracts & Conference Presentations

Drake RR, Louey S, Thornburg KL. "Fatty acid transport gene expression increases before birth in the ovine myocardium." Poster accepted for the 67th Annual Society for Reproductive Investigation Conference, Vancouver, British Columbia (March 2020). Event cancelled due to COVID-19.

Drake R, Louey S, Thornburg KL. "Placental insufficiency suppresses fatty acid transport proteins in the fetal heart." Oral presentation at the 66th Annual Society for Reproductive Investigation Conference, Paris, France (March 2019).

Drake R, Plubell DL, Fenton AM, Wilmarth PA, Bergstrom P, Minnier J, Hassan W, Varlamov O, Pamir N. "Epicardial adipose depot specific proteome and secretome signatures reveal distinct biology and nutrient utilization." Oral presentation at the Cascadia Proteomics Symposium, Seattle, WA (July 2018).

Drake R, Louey S, Lindgren IL, Thornburg KL "Fatty acid handling is altered in cardiomyocytes from growth restricted fetuses." Poster presented at the Knight Cardiovascular Institute Retreat, Portland, OR (May 2018).

Drake R, Thornburg KL. "Maturation of lipid metabolism in the developing sheep heart." Poster presented at the Knight Cardiovascular Institute Retreat, Portland, OR (May 2017). Oral presentation at the Physiology and Pharmacology departmental seminar (June 2017).

Drake R, Chiao YA, Basisty N, Karunadharma P, Levy N, MacCoss M, Rabinovitch P. "Protein homeostasis in the electron transport chain is regulated in a complex and dynamic manner: Implications for human health and disease." Poster presented at the LifeScience Alley Conference, Minneapolis, MN (November 2013).

Drake R, Phillips J, Wegner J, Westerfield M. "Exploring functional regions of Usher syndrome gene USH2A in zebrafish." Poster presented at the LifeScience Alley Conference, Minneapolis, MN (December 2012) and at Experimental Biology, Boston, MA (April 2013).

ACKNOWLEDGEMENTS

I owe a debt of gratitude to my knowledgeable, encouraging and enthusiastic mentor, Kent Thornburg. Thank you to my lab mate Samantha Louey, for your patience, countless hours spent counselling me, helping immensely with my development as a scientist and writer and for the tough love. Fellow MD/PhD student Kevin Kolahi, thanks for showing me the ropes while we overlapped in the lab and continuing to be a valuable resource for experimental troubleshooting. To Amy Valent, for being an amazing trailblazer and setting an example for female physician scientists. To Isa Lindgren, for aiding in my learning on how to think like a scientist and the importance of work life balance. To Haeri Choi and Natasha Chattergoon for being wonderful lab mates and a joy to work with. To Sonnet Jonker, for your honesty and setting a great example for what it takes to be a successful scientist. And Karthik! To my dissertation advisory committee: George Giraud, Melanie Gillingham and Cindy McEvoy, for your guidance and commitment to my learning. To Crystal Chaw, Aurelie Snyder and Stefanie Kaech Petrie, for all your help with designing, executing and analyzing the imaging experiments. To my MD/PhD classmates Jim Goodman, Sam Huang and Ali Pincus, for weathering numerous storms with me these past 7 years, I wouldn't have made it this far without you. To Louisa Chatroux, for being a great listener and encourager. To my pals Jessie Vickers and Marianne Falk, you've kept my soul afloat during quarantine and my heart swells with gratitude for your friendship. To my

parents Craig and Gloria, and brother Ryan for always urging me to work hard and play hard. To my dog Teddy, for the laughs and breakfast snatches. Lastly, to my partner Tyler, for keeping me well fed and well loved.

ABSTRACT

The human heart starts beating at 21 days gestation and does not stop until death. This posits an incessant metabolic demand that must be met despite abrupt changes to cardiac load, nutritional substrates and oxygenation that occurs at birth. Fetal cardiomyocytes rely on lactate and glucose for ATP production, while healthy adult cardiomyocytes utilize mostly fatty acids. In precocial species there is a rapid transition to fatty acid metabolism around the time of birth, but temporal regulation of the machinery required to do so remains poorly characterized. Using fluorescent-tagged long chain fatty acids (BODIPY C_{12}), we demonstrated that fetal sheep (0.85 gestation) cardiomyocytes produce 59% larger lipid droplets ($p<0.05$) compared to newborn (8 day) cardiomyocytes. We found gene expression of CD36, ACSL1, CPT1, HADH, ACAT1, IDH and GPAT progressively increase through the perinatal period (0.65 gestation versus 0.90 gestation versus newborn) whereas several genes FATP6, ACSL3, LCAD, VLCAD, HADH, PDK4, PAP and DGAT have lower expression in fetal hearts than after birth. These components are sensitive to suboptimal intrauterine conditions as experiences in placental insufficiency leading to intrauterine growth restriction (IUGR). IUGR fetuses had 50% (C14) and 60% (C18) higher circulating long chain fatty acylcarnitines compared to controls indicative of impaired fatty acid metabolism. mRNA levels of sarcolemmal fatty acid transporters, acylation enzymes,

mitochondrial transporter, ß-oxidation enzymes, tricarboxylic acid cycle enzyme, esterification enzymes and regulator of lipid droplet formation were all suppressed ($p < 0.05$) in IUGR myocardium without a concomitant suppression of protein levels.

This thesis provides new insights into the normal developmental profile of the myocardial fatty acid metabolic pathway in the perinatal period in a precocial species, and the impact of IUGR on this pathway.

Chapter 1. Introduction

This thesis was undertaken to begin filling a large gap in knowledge regarding the maturation of fatty acid metabolic machinery in the perinatal mammalian heart and the impact of a suboptimal intrauterine environment. While many resources have been invested into furthering our understanding of physiological processes in the adult heart, less emphasis has been placed on investigating heart development. This is unfortunate as it is now recognized that a person's risk for acquiring heart disease can be amplified by suboptimal conditions encountered during development, including in the fetal and early postnatal environment. The idea that suboptimal intrauterine conditions can elevate the risk for disease in adulthood was cemented by David Barker and colleagues when they found that infants born small were more likely to suffer from heart disease as adults. The molecular changes and underlying mechanisms responsible for these epidemiological observations are gradually being elucidated. However, many questions remain. For example, we do not understand how many critical processes are regulated in normal development, let alone how prenatal insults modify their normal program. This includes how the immature heart develops its ability to metabolize fatty acids, a critical process in mammalian hearts from birth onward.

Lipid Transport and Metabolism: An Overview

Lipids are an incredibly diverse and heterogeneous group of organic compounds characterized by their insolubility in water. They act as structural building blocks for cell membranes and organelles, signaling molecules and substrates for energy production. Free fatty acids are the most energy dense metabolic substrate, providing 9 kilocalories (kcal) per gram compared to 4 kcal per gram of either protein or carbohydrate. The majority of circulating free fatty acids are constituents of triacylglycerols within lipoprotein particles including low density lipoprotein (LDL), very low density lipoprotein (VLDL) and high density lipoprotein (HDL). Before free fatty acids can enter myocytes through sarcolemmal transporters, they must be cleaved from the glycerol backbone by lipoprotein lipases (LPL). Metabolism of these free fatty acids to yield ATP depends on a series of transporters and enzymes that contribute to one of two main fates: production of ATP in the mitochondrion by β-oxidation or sequestration into cytoplasmic lipid droplet stores. The key components involved in the transport, esterification, and oxidation of fatty acids are shown in Figure 1-1 and are summarized below (Lopaschuk *et al.*, 2010).

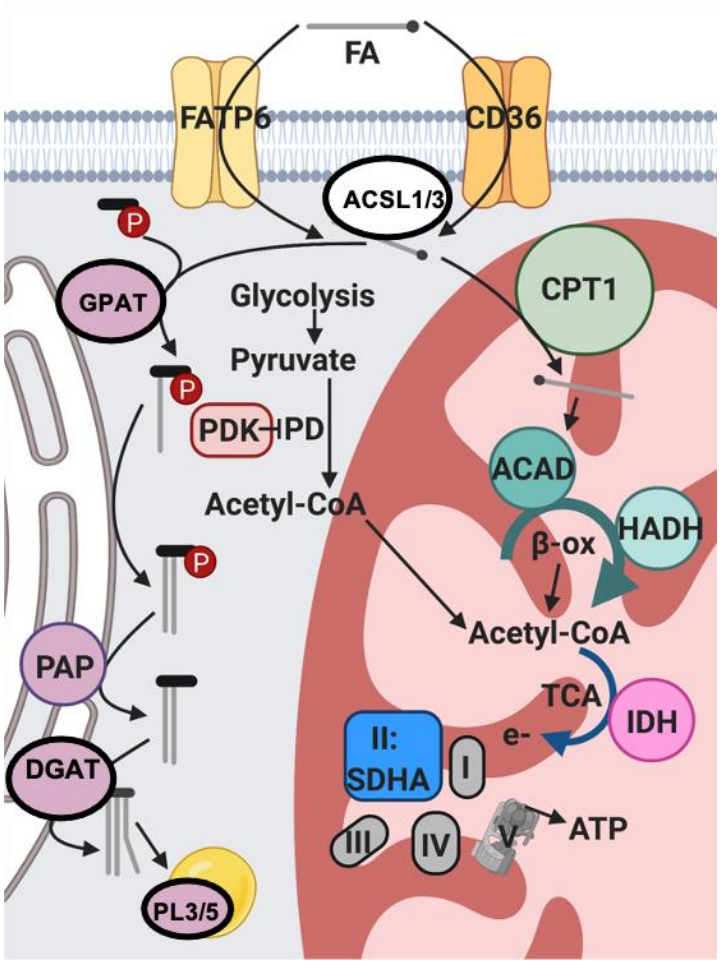

Figure 1-1 Cardiomyocyte fatty acid metabolism pathway.

FA: fatty acid, FATP6: fatty acid transport protein 6, CD36: fatty acid translocase, ACSL1/3: acyl-CoA synthetase long chain, PDK4: pyruvate dehydrogenase kinase, PD: pyruvate dehydrogenase, CPT1: carnitine palmitoyltransferase 1, VLCAD/LCAD: very long/long chain acyl-CoA dehydrogenase, HADH: hydroxyacyl-coenzyme A dehydrogenase, ACAT: acetyl-CoA acetyltransferase, CS: citrate synthase, IDH: isocitrate dehydrogenase, SDHA: succinate dehydrogenase, GPAT: glycerol phosphate acyltransferase, PAP: phosphatidic acid phosphatase, DGAT: diacylglycerol acyltransferase. PL3/5 perilipin 3/5.

Transport

CD36 (also known as Fatty acid translocase or Platelet glycoprotein 4) and Fatty acid transport protein (FATP) are the 2 key sarcolemmal transporters of long chain fatty acids. Within the family of FATP transporters, FATP6 (also known as solute carrier family 27 member 6, SLC27A6) is specific to the heart (Gimeno *et al.*, 2003). Once free fatty acids enter the cell, they are acylated by acyl-CoA synthetase long chain (ACSL) to form fatty acyl-CoA. There are five ACSL isoforms (1, 3, 4, 5 and 6), each differing in their expression in various organs, with ACSL1 being the most highly expressed isoform in the heart (Mashek *et al.*, 2006; Uhlen *et al.*, 2015).

Oxidation versus Esterification

Once fatty acyl-CoA is formed, it has five potential fates, it can be (1) degraded via β-oxidation in the mitochondrion, (2) trafficked to the endoplasmic reticulum (ER) to be esterified into a triacylglycerol and incorporated into a lipid droplet or used to produce phospholipids, ceramides, cholesterol and other lipids, (3) elongated or desaturated, (4) used for protein acylation or (5) used for transcriptional regulation (Grevengoed *et al.*, 2014). For the purposes of this work we will focus on the first two: (1) mitochondrial degradation and (2) ER triacylglycerol synthesis. The fate of the fatty acyl-CoA is determined by the balance of energy production and storage which is constantly in flux and is modulated by malonyl CoA and ACSL isoform. Malonyl CoA is produced by acyl-CoA carboxylase, the first committed step in fatty acid synthesis, and directly inhibits CPT1. ACSL isoforms direct these fatty acyl-CoAs to distinct

organelles, with ACSL1 targeting fatty acyl-CoA to mitochondria (Ellis *et al.*, 2011) and ACSL3 targeting fatty acyl-CoA to the ER (Chang *et al.*, 2011).

Oxidation Within the Mitochondrion

The mitochondrial fatty acid transporter CPT1 is the rate-limiting step in fatty acid oxidation because it is required for free fatty acids to enter the mitochondrion. Acyl-CoA dehydrogenase (LCAD or VLCAD for long chain or very long chain fatty acids) catalyzes the first step of β-oxidation. In humans, VLCAD is the primary acyl-CoA dehydrogenase for long chain fatty acids. We expect this is similar in sheep. The next three steps in the β-oxidation process are catalyzed by mitochondrial trifunctional protein (MTP), a multi-enyzme complex containing α (HADHA) and β (HADHB) subunits. The α subunit of MTP carries out both the long-chain enoyl-CoA hydratase and long-chain hydroxyacyl-CoA dehydrogenase activities which hydrates the double bond between the second and third carbon and then converts the 3-hydroxyl group to a keto group to produce 3-ketoacyl CoA. HADH/sc acts on acts short and medium chain fatty acids to convert the 3-hydroxyacyl-CoA to 3-ketoacyl-CoA. The β subunit of MTP liberates acetyl-CoA from long-chain 3-ketoacyl CoA while β-ketothiolase cleaves acetyl-CoA from medium and short-chain 3-ketoacyl groups. During periods of high fatty acid oxidation, acetyl-CoA molecules can condense forming ketone bodies in the liver. Ketone bodies are released into circulation and provide an alterative energy substrate for multiple tissues including the heart. The breakdown of ketones to acetyl-CoA occurring in the mitochondrion. Acetyl-CoA acetyltransferase (ACAT1) catalyzes the last step of ketone breakdown by cleaving acetoacetyl-CoA into two

molecules of acetyl-CoA. It is important to recognize that acetyl-CoA can also enter the TCA cycle from glycolysis by pyruvate dehydrogenase (PD) converting pyruvate to acetyl-CoA. Pyruvate dehydrogenase kinase 4 (PDK4) regulates acetyl-CoA flux from β-oxidation and glycolysis through PD inhibition, permitting more acetyl-CoAs to enter the TCA cycle from fatty acid oxidation. Two critical TCA cycle enzymes are citrate synthase (CS) which conducts condensation of acetyl-CoA and oxaloacetate to form citrate (the first committed step of the TCA cycle), and isocitrate dehydrogenase (IDH) which catalyzes the decarboxylation of isocitrate to produce α-ketoglutarate and yields the first reducing equivalent of the cycle. NADH and $FADH_2$ reducing equivalents are used to power the electron transport chain to generate a proton motive force and drive oxidative phosphorylation and ATP production. The electron transport chain is comprised of 5 complexes (I – V), with key subunits in each being I: NDUFB8, II: SDHA, III: UQCRC2, IV: MTCO1, V: ATP5A.

Esterification in the Endoplasmic Reticulum for Storage

Fatty acyl-CoA directed to the ER for esterification enters the first committed step of triacylglycerol (TAG) synthesis, in which it is joined with glycerol-3-phosphate by glycerol phosphate acyltransferase (GPAT) to make lysophosphatidic acid. Acyl-glycerol-3-phosphate acyltransferase adds another acyl group to lysophosphatidic acid to make phosphatidic acid. Phosphatidic acid is then dephosphorylated (to free up the glycerol backbone to be able to bind the final acyl group) by phosphatidic acid phosphatase (PAP) to make diacylglycerol. The third fatty-acyl group is then attached to diacylglycerol by diacylglycerol acyltransferase (DGAT) to make TAG. At this

point, the fatty acyl-CoA is esterified and transferred to a lipid droplet for storage. Perilipin 3 is a lipid droplet associated protein that plays a critical role in the formation of lipid droplets (Nose *et al.*, 2013) and perilipin 5 aids in lipid droplet interactions with mitochondria (Wang *et al.*, 2011).

Organ Specific Differences

While fatty acid metabolism occurs in many tissue types, liver, skeletal muscle, adipose tissue and heart are among the tissues with the highest rates of fatty acid consumption in adults. Isoforms of key components are expressed differently in different tissues. CD36 is highly expressed in myocardium, skeletal muscle and adipose tissue in adult mice (Coburn *et al.*, 2001); mouse studies have shown that knocking out CD36 results in defective uptake and oxidation of long chain fatty acids in these three tissues (Coburn *et al.*, 2000). Of the other sarcolemmal fatty acid transport family (FATP), distribution of the 6 isoforms varies across tissues, with FATP6 being principally expressed in the heart (Gimeno *et al.*, 2003), though FATP1 is also found in the heart (Stahl, 2004).

Regulation of Lipid Metabolism

Regulation by Hormones

In adults, cortisol stimulates adipose tissue lipolysis, thereby increasing circulating fatty acid substrates (Djurhuus *et al.*, 2002) while thyroid hormone has been shown to stimulate lipid metabolism through PGC1-α activation (O'Brien *et al.*, 1993; Wulf *et al.*, 2008; Lewandowski *et al.*, 2011). Thyroid hormone has also been shown to

stimulate oxidative metabolism in skeletal muscle in adults (Sayre & Lechleiter, 2012) and also before birth (Davies *et al.*, 2020) suggesting that thyroid hormone plays a critical role in normal metabolic development. In addition to cortisol and thyroid hormone other hormones and paracrine factors may play roles in the regulation of fatty acid metabolic metabolism in the heart. It is possible that these hormones participate in metabolic maturation of cardiomyocytes near term as they have been shown to stimulate lipid metabolism in other tissues.

Regulation by Nutrient Availability

Substrate availability can also influence upregulation of metabolic machinery. *In vitro,* palmitate exposure induces upregulation of fatty acid oxidation machinery in pancreatic β-islet cells (Xiao *et al.*, 2001) and H9c2 ventricular cardiomyoblasts (Cetrullo *et al.*, 2020). Increased lipid substrate availability with suckling in the newborn may similarly contribute to an upregulation of fatty acid oxidation genes in the newborn heart.

Regulation by Oxygen

Since oxygen is required for mitochondrial oxidative phosphorylation, it makes sense that metabolic pathways are influenced by oxygen availability. Hypoxia inducible factor-1 α (HIF-1α) is a master transcriptional regulator of cellular responsible to hypoxia. It induces Hand1 expression, which then represses key regulatory genes involved in lipid metabolism including CPT1a (Breckenridge *et al.*, 2013). At birth,

Hand1 decreases as the newborn is exposed to higher levels of oxygen (Breckenridge *et al.*, 2013).

Adult Cardiomyocytes: Normal and Abnormal Metabolism

The heart and kidneys have the highest energy demands of all the organs in the body, with both requiring 440 kcal/kg/day in the adult (Wang *et al.*, 2010b). Fat is the most energy efficient substrate, yielding 9 calories per gram of fat compared to 4 calories per gram from carbohydrate or protein. This makes it an ideal fuel to provide a high density of energy for storage to provide the relentless heart with a continuous supply of nutrition. Adult myocardium, regardless of the species, utilizes fatty acids for energy. However, the heart is also omnivorous and will utilize other substrates in the absence of fatty acids or in the case of insufficient oxygenation (Su *et al.*, 2021). The diseased adult heart will go so far as to revert to a fetal metabolic phenotype, including an upregulation of CPT1a (the fetal CPT isoform) and reversion to carbohydrate metabolism (Razeghi *et al.*, 2001; Taegtmeyer *et al.*, 2010). This may ensure survival but is a less efficient method of ATP generation than fatty acid oxidation. People with heart failure often have elevated circulating acylcarnitines, indicative of impaired fatty acid oxidation (Ruiz *et al.*, 2017). In addition, lipid droplet stores are larger in these hearts compared to healthy hearts (Schulze *et al.*, 2016).

Cardiac Metabolism in Development

Perinatal Substrate Availability and Utilization

Substrate availability changes drastically between fetal life and postnatal life. In fetal life, the heart utilizes lactate and glucose as fuel, but transitions to primarily fatty acid metabolism postnatally. Circulating substrates in the fetus are utilized both for energy production and to build the rapidly growing fetus. The placenta produces high concentrations of lactate that enter the fetal circulation and are readily available to be oxidized. In a normal fetus, circulating glucose (sheep = 1 mM, human = 4.5 mM) and lactate (sheep = 2 mM, human = 2.5 mM) are readily available while free fatty acids are less readily available (sheep = 0.04 mM, human = 0.1 mM) (Girard *et al.*, 1979). Postnatally, there is a shift in substrate availability with fatty acids becoming more readily available (sheep = 0.3 mM, human = 0.2 mM) (Girard *et al.*, 1979). Higher circulating lipids in newborn mammals can be attributed to suckling of mother's milk. Palmitate (C16:0) and oleate (C18:1) dominate the lipid content of both human and sheep milk (Zou *et al.*, 2013), while a unique feature of sheep milk is the presence of short chain fatty acid (SCFA), butyrate (C4:0) produced *de novo* within ruminant mammary epithelial cells. Weaning is a critical time with regard to lipid metabolism and has been shown to mark the shift from CPT1a predominance to CPT1b predominance in the developing heart (Brown *et al.*, 1995).

Substrate availability and type aside, tissue requirements differ greatly in the fetus and neonate which contributes to different energy needs. For example, skeletal muscle is not under load nor is there much need for locomotion *in utero*, but demands energy

after birth. The heart, however is unique in that it beats throughout fetal and postnatal life, but the work expended by the left ventricle is greater postnatally than before birth, necessitating a smooth transition of augmented energy production at birth.

Perinatal Cardiac Metabolic Maturation and Substrate Utilization

Birth is a transformative event accompanied by dynamic environmental changes that stimulate maturation of multiple systems. These alterations to the physiological environment affect myocardial metabolism and function. Among them, increases in PaO_2 and arterial pressure, changes in blood flow patterns including closure of four major shunts, (the ductus arteriosus, ductus venosus, foramen ovale and umbilical circulation) and reliance on milk as a fuel source all influence myocardial fuel switching. These circulatory changes lead to an increase in left ventricular work due to increased preload and afterload concomitant with a relative unloading of right ventricular work (Dawes *et al.*, 1954).

Table 1-1 Myocardial substrate preferences throughout life in different species.

	Primary substrate for energy production			
	Fetus	Newborn	Adult	References
Mouse	Lactate/Glucose	Lactate/Glucose	Fatty Acids	(Lalowski *et al.*, 2018)
Rat	Lactate/Glucose	Lactate/Glucose	Fatty Acids	(Mdaki *et al.*, 2016b) (Glatz & Veerkamp, 1982)

Rabbit	Lactate/Glucose	Lactate/Glucose	Fatty Acids	(Werner *et al.*, 1982; Lopaschuk *et al.*, 1991)
Guinea Pig	Lactate/ Glucose	-	-	(Rolph & Jones, 1983)
Cow	Lactate/Glucose	Fatty Acids	-	(Brosnan & Fritz, 1971)
Pig	Lactate/Glucose	Fatty Acids	-	(Werner & Sicard, 1987; Ascuitto *et al.*, 1989)
Sheep	Lactate/Glucose	Fatty Acids	Fatty Acids	(Fisher *et al.*, 1980, 1981; Bartelds *et al.*, 2000)

Our limited understanding of the heart's metabolic maturation comes from several species (Table 1-1) with the key feature being the timing of the metabolic switch from using carbohydrates to fatty acids varies depending on the precocity of the species.

It is important to keep in mind that in healthy fetuses, there is a low concentration of circulating free fatty acids (Van Duyne *et al.*, 1960) whereas lactate and glucose are readily available as substrates, hence their preference as substrates. The hearts of altricial species are less capable of fatty acid oxidation *in utero* (Glatz & Veerkamp, 1982), but in contrast precocial species are more able to oxidize fatty acids when it is available: late gestation fetal cow, pig, and sheep hearts are capable of oxidizing fatty acyl-CoA (Brosnan & Fritz, 1971; Werner *et al.*, 1989; Bartelds *et al.*, 2000). These data indicate that fatty acid oxidation systems are at least partially functional *in utero* in precocial species, even though circulating fatty acids remain low.

The prenatal maturation of numerous features of fetal sheep hearts has been extensively studied. Compared to rats whose cardiomyocytes remain proliferative and largely mononucleated for the first week after birth (Clubb & Bishop, 1984), hyperplastic growth significantly decreases before birth in the sheep, and cardiomyocytes are largely terminally differentiate by birth (Jonker *et al.*, 2007). Mitochondria in the sheep myocardium are disorganized at 115d GA, but by 7d PN are neatly organized in rows, sandwiched between myofibrils (Smolich, 1995). Myocardial oxidative capacity in fetal and newborn lambs is higher than in adult sheep (Wells *et al.*, 1972), at least when succinate or glutamate are the primary substrates: oxygen consumption was 87% and 81% higher in fetus and newborn compared to adult and cytochrome c oxidase (Complex IV of the electron transport chain) activity was 56% and 65% higher in fetal and newborn hearts compared to adult. Fetal sheep hearts at 127-134d GA are capable of fatty acid uptake and oxidation prior to birth during a palmitate infusion (Bartelds *et al.*, 2000) though not to the same degree as a newborn (Figure 1-2).

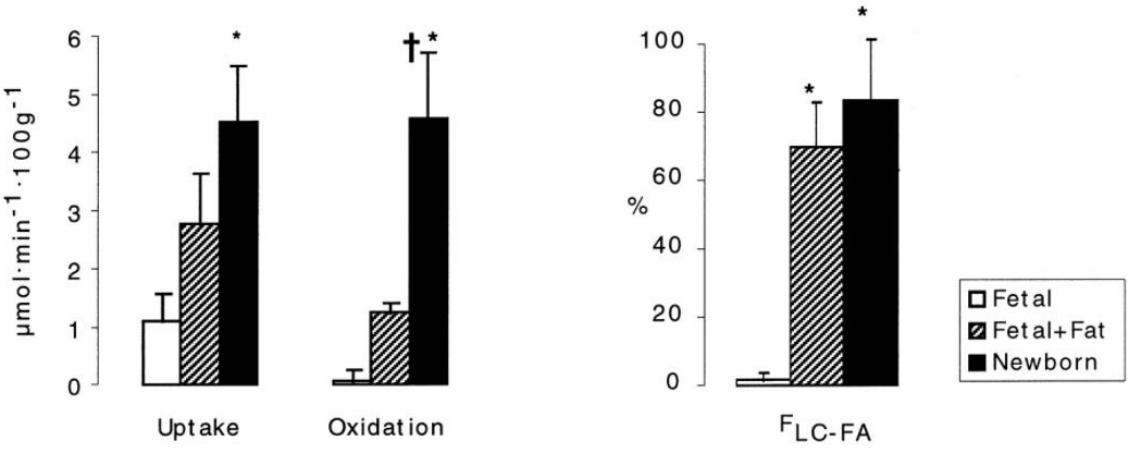

Figure 1-2 Late gestation fetal sheep myocardium is capable of fatty acid uptake and oxidation.

Fetal (127-134d GA, n = 5), Fetal + Fat (palmitate infusion, 0.081g/kg/min for 45 minutes, n = 7) and Newborn (3-15d PN, n = 12) fat uptake, oxidation and % contribution to oxidation of long chain fatty acid to LV oxygen consumption. From (Bartelds *et al.*, 2000).

Although substrates change abruptly as mammals begin suckling, the heart's substrate preference may transition more gradually. In rabbits, even a week after birth, over half of the ATP is still generated from carbohydrates rather than fatty acids (Figure 1-3, Lopaschuk & Jaswal, 2010). Rats have a similarly gradual postnatal transition to fatty acid oxidation; homogenates from 1 day old rat hearts are less than 50% capable of palmitate oxidation compared to 21 day hearts (Mdaki *et al.*, 2016b). However, the regulation of the transporters and enzymes that traffic fatty acids from the circulation to the mitochondrion, and the timing of their maturation relative to birth or the timing

of the metabolic switch have not been explored in depth in altricial or precocial species.

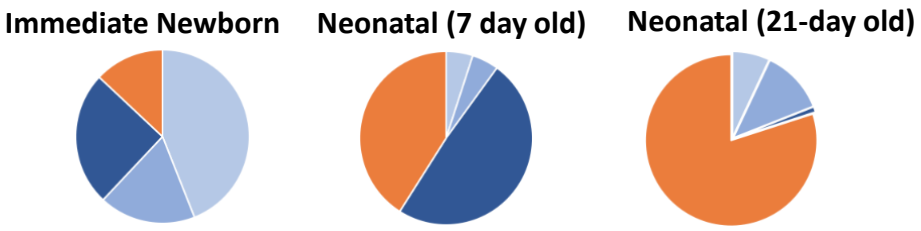

Figure 1-3 Heart metabolic profile changes with development in rabbits.

Predominant source of ATP production by color: **Glycolysis, Glucose Oxidation, Lactate Oxidation, Fatty Acid Oxidation.** Modified from (Lopaschuk & Jaswal, 2010).

Neonatal Nutrition

Controversy of Neonatal Nutrition (Preterm/ IUGR)

Body weight is often used as a measure to guide nutritional intake in the vulnerable newborn. For premature infants, fetal growth curves for normally growing fetuses are often used as a reference since prior to birth, but it is important to keep in mind that growth restricted infants are 2.5 times more likely to be born preterm, so use of these curves may not be appropriate. High levels of carbohydrates and lipids are supplied to preterm infants based on the assumption that this is necessary to promote protein growth, though this tends to produce increased fat deposition (Hay, 2008). Intravenous fat emulsion (IVFE) was originally formulated to provide essential fatty acids and a

calorically dense substrate to minimize volume required for patients on parenteral nutrition (Spray, 2016). Current neonatal intensive care unit (NICU) nutrition support recommends up to 3 grams per kilogram of intravenous lipid (Salama *et al.*, 2015).

Lipids are a critical component of parenteral nutrition for vulnerable infants not capable of enteral feedings. They provide a vital source of energy and prevent essential fatty acid (Ω-3 and Ω-6 fatty acid) deficiencies. Currently, the only intravenous lipid emulsion approved for use in newborns is Intralipid, an emulsion of soybean oil composed of ~44-62% linoleic (C18:2), ~19-30% oleic (C18:1), ~7-14% palmitic (C16) and ~1.4-5.5% stearic acid (C18). In adults, multiple alternative IVLEs are licensed for use including Omegaven (fish oil) and SMOFlipid (soy, medium-chain triacylglycerols, olive and fish oil) but are not routinely used with infants in the United States. A randomized controlled trial conducted in the Netherlands compared a multicomponent IVLE to the conventional soybean oil IVLE in very low birthweight infants (Vlaardingerbroek *et al.*, 2014). They found that SMOFlipid was better tolerated, had better growth outcomes and higher plasma Ω-3 fatty acid (eicosapentaenoic acid, EPA and docosahexaenoic acid, DHA) fatty acid profiles compared to Intralipid. Additionally, infants given Intralipid had higher circulating phytosterols. Phytosterols in plants are comparable to cholesterol in humans in that they affect membrane fluidity and are critical components of the plant cell membrane. In fact, such plant based sterols have been used to treat dyslipidemic patients in combination with other therapies (Gupta *et al.*, 2011). In infants, these phytosterols are thought to be the culprit for intestinal failure associated liver disease (IFALD)—

which involves a spectrum of hepatic steatosis, cholestasis, cholelithiasis and hepatic fibrosis—and develops in 40-60% of infants requiring long term total parental nutrition (Kelly, 2006). Multicomponent lipid emulsions containing a more heterogeneous mixture of lipids (soy, medium chain triglycerides, olive oil, fish oil and coconut oil) might reduce cholestasis.

There are also concerns of predisposition of these already vulnerable infants for life long cardiovascular disease. Intralipid use in premature infants is associated with increased abdominal aortic stiffness as measured by aortic pulse wave velocity and a reduction in peak systolic circumferential strain at age 23-28 (Lewandowski *et al.*, 2011). It stands to reason that these immature infants may not yet be equipped to handle lipids to the same degree as a term infant. As with any substrate, high concentrations of lipids have the potential to become toxic. Lipotoxicity is used to describe deleterious effects of lipid accumulation in non-adipose tissue (Schulze *et al.*, 2016). However, the concentration threshold for lipotoxicity in the immature heart is not known. This suggests the need for further investigation on the capacity of preterm (*in utero* or *ex utero)* hearts to appropriately metabolize lipids and determining the timing of metabolic maturation relative to gestational age as well as the impact of birth itself. Filling part of this knowledge gap will help guide and optimize nutrition protocols for vulnerable infants that may minimize some of the short- and long term consequences of lipid-rich parenteral feeding.

Developmental Origins of Adult Disease

The quality of the perinatal environment, encompassing the periconceptional period all the way through early infancy has a strong influence on an individual's lifelong health. The "first 1000 days" marks a critical period for determining that individual's risk for chronic disease in adulthood. Low birth weight is an indicator of a suboptimal intrauterine environment, though not all prenatal stressors are reflected in altered birth weight. Slow growth before birth is an indicator that the fetus is making tradeoffs (such as compromised organ maturation and alterations in metabolic pathways) to ensure survival in the short term. These modifications may become problematic long term and can detrimentally influence lifelong cardiovascular and metabolic health. The current field of medical science termed Developmental Origins of Health and Disease (DOHaD) gained traction in the early 1990s thanks to the work of David Barker and colleagues (Barker *et al.*, 1989), as mentioned above. However, even then the idea that early life nutrition is crucial to normal development was not completely new, as similar observations were documented by Elsie Widdowson and Robert McCance decades before David Barker devised and articulated his hypothesis (Widdowson & McCance, 1963).

Developmental studies also reveal an individual's susceptibility to obesity and abnormal appetite regulation indicating that systemic lipid handling is also altered by suboptimal intrauterine conditions (Benyshek, 2007; Schulz, 2010). However, of note, the effect of the intrauterine environment on lipid metabolism in the fetal heart has not been investigated. The accommodations of the fetus to an adverse nutritional

environment would have both short term and long term impacts. Immediate effects would be evident as soon as the fetus is born if the heart is unable to transition to fatty acid metabolism. This could have persisting effects over the life of offspring.

Intrauterine Growth Restriction

Intrauterine growth restriction (IUGR) is defined as a reduction in the normal physiological growth rate (Thureen & Hay, 2006; Kesavan & Devaskar, 2019). IUGR infants are usually small for gestational age (SGA), which by definition have a birth weight below the 10^{th} percentile for gestational age (Kesavan & Devaskar, 2019). This definition differs from low birth weight which is defined as 2500 g or under (Peleg *et al.*, 1998). Intrauterine growth restriction or the equivalent "fetal growth restriction" can be further divided into either asymmetric or symmetric body mass distribution and the ponderal index can be used to quantify this. In asymmetric growth (ponderal index > 2), growth of the head is relatively spared and the abdomen is wasted, indicative of late gestation growth restriction and blood flow being diverted to the brain at the expense of abdominal organs. In symmetric growth (ponderal index < 2), all growth parameters are affected similarly and is consistent with growth restriction throughout gestation.

IUGR can be attributed to a variety of etiologies including both genetic and environmental factors. While the etiology of IUGR varies, in most cases it stems from placental insufficiency which is a condition in which the robust transfer of oxygen and nutrients from the mother to the fetus is compromised; it is characterized by

hypoxemia, hypoglucosemia, hypercortisolemia and low IGF-1 (Economides *et al.*, 1988; Nicolaides *et al.*, 1989; Leger *et al.*, 1996).

IUGR affects between 5 and 10% of pregnancies worldwide (Nardozza *et al.*, 2017). IUGR infants can suffer from increased neonatal mortality or morbidities including pulmonary, gastrointestinal, thermoregulatory, metabolic, hematologic, renal and immunological abnormalities (Kesavan & Devaskar, 2019). Since IUGR newborns are at an increased risk of necrotizing enterocolitis—which can be exacerbated by enteral feeding—many IUGR infants are given total parenteral nutrition. Total parenteral nutrition is composed of protein, carbohydrates, electrolytes, minerals and fat (usually Intralipid). Understanding the impact of IUGR on normal metabolic maturation is prerequisite to optimizing lipid supplementation in the immediate postnatal period. IUGR infants have higher circulating levels of acylcarnitines postnatally, indicative of suboptimal fatty acid oxidation (Liu *et al.*, 2016), but the source of these acylcarnitines is unknown.

Numerous studies have shown using ultrasound that IUGR fetuses have altered cardiovascular function (Rasanen *et al.*, 1997; Mayhew *et al.*, 1999; Bahtiyar & Copel, 2008). Few studies have described how the heart is structurally altered by IUGR (Mayhew *et al.*, 1999) and even fewer have looked at how heart metabolism is impacted. The bulk of our knowledge of the effects of IUGR comes from animal studies.

Animal Models of IUGR

Animal models have been used to recapitulate features of IUGR and further our understanding of fetal adaptions to IUGR. Rather than reviewing the differences between all these models or discussing a general overview of what these models have taught us about IUGR, the following section will focus on summarizing what these animal models reveal about alterations to the heart or metabolism in general. While the causes of human IUGR can be varied, it can be caused by prenatal hypoxemia, undernutrition, and hypercortisolemia. Regardless of the model, there are common biological mechanisms that underlie the growth restricted condition, indicative of conserved mechanisms for certain physiological responses to IUGR. The feto-placental unit is dynamic and can make adaptations to its environment, including redistribution of cardiac output to "protect" essential organs such as the brain, heart, and adrenals (Cohn *et al.*, 1974; Giussani, 2016) at the expense of those that are less critical to fetal survival including the liver and skeletal muscle. That being so, these so-called "essential" organs are not entirely protected by changes in blood flow distribution (Mallard *et al.*, 1998; Louey *et al.*, 2007; Roberts *et al.*, 2012; Lo *et al.*, 2018).

A hallmark feature of IUGR in animal models is a slowing of heart growth through reduced proliferation of cardiomyocytes and/or delayed maturation – this has been demonstrated in rat undernutrition models (Corstius *et al.*, 2005), sheep placental insufficiency models including umbilicoplacental embolization, caruncletomy, and heat stress (Cock *et al.*, 2001; Bubb *et al.*, 2007; Louey *et al.*, 2007; Morrison *et al.*,

2007; Jonker *et al.*, 2018). While these adaptations lead to fewer cardiomyocytes in the fetal heart, it is not known whether cell number or maturation catches up in the neonatal period. Several of these models have allowed the IUGR fetuses to be born (Louey *et al.*, 2000; Cock *et al.*, 2001; Louey *et al.*, 2005; De Blasio *et al.*, 2007; Owens *et al.*, 2007; Rueda-Clausen *et al.*, 2011a), proving that these adaptations are not dire enough to impact immediate survival.

Prenatal insults can have persistent effects on cardiac health and function, extending into adulthood. Rats whose dams were made hypoxic (10-11% vs 21% oxygen) in the last 6 days of pregnancy (term 21 days) are more vulnerable to cardiac ischemia/reperfusion injury as a result of persistent impairments to cardioprotective heat shock proteins (Li *et al.*, 2004) and impaired cardiac efficiency due to a myocardial glycolysis/ glucose oxidation mismatch (Rueda-Clausen *et al.*, 2011b). Long term vulnerability to ischemia-reperfusion injury in adulthood has also been shown in a sheep model of prenatal anemia (Yang *et al.*, 2008); this study did not assess cardiac metabolism. To date, there have been no studies specifically investigating the impact of prenatal stress on cardiac fatty acid metabolism.

Changes to metabolic pathways have been demonstrated in other organ systems in response to placental insufficiency as well. The pancreas responds by decreasing ß-cell mass, suppressing insulin secretion and suppressing glucose oxidation (Limesand *et al.*, 2006; Boehmer *et al.*, 2017). IUGR induced changes to triglyceride content and fatty acid binding protein mRNA levels in skeletal muscle and adipose tissue in pigs

(Williams *et al.*, 2009). Hence, these data might not be directly translatable to the heart, nor can they predict how fatty acid pathways might be affected, but they do indicate that metabolic pathways are sensitive to prenatal insults.

Compared to the glucose and insulin metabolic pathways, little attention has been paid to the pathways that regulate fatty acid metabolism in IUGR. Prenatal protein restriction in rats upregulates liver fatty acid synthase and suppresses CPT1b in offspring at 90d PN, suggesting enhanced lipid storage and suppressed oxidation in the liver (de Oliveira Lira *et al.*, 2020). This same model leads to a suppression of PDK4, CS and CPT1b mRNA levels in adipose tissue at 30d PN (de Oliveira Lira *et al.*, 2020). In skeletal muscle, PDK4 gene and protein expression are suppressed at 90d PN (de Brito Alves *et al.*, 2017). Placental insufficiency induced by bilateral uterine artery ligation in rats revealed impairments in skeletal muscle oxidative phosphorylation in offspring postnatally, but only with pyruvate, glutamate, α-ketoglutarate and succinate as substrates, not fatty acids (Selak *et al.*, 2003).

A few studies have investigated the effect of IUGR on cardiac metabolism. Myocardial GLUT4 and insulin receptor protein levels are increased in fetal sheep rendered IUGR through heat-stress-induced placental insufficiency (Barry *et al.*, 2006) such that the degree of insulin stimulated glucose delivery and uptake was greater in IUGR hearts (Barry *et al.*, 2016). Uteroplacental artery ligation in rabbits leads to growth restricted offspring, and alterations in cardiac cytoarchitecture characterized by increased cytosolic space between mitochondria and myofilaments despite no difference

between mitochondrial area or number, and deficiency in mitochondrial respiratory chain complex I gene expression (Gonzalez-Tendero *et al.*, 2013). To date, there has only been one study investigating the long term effects of IUGR on cardiac fatty acid oxidation in IUGR fetuses. This paper (Beauchamp *et al.*, 2015) showed impaired cardiac fatty acid oxidation and elevated plasma short chain acylcarnitines in adult mice whose dams were undernourished during pregnancy. Whether this metabolic aberration was evident *in utero* remains to be determined.

Rationale for Using Sheep as a Model for Current Studies

Since sheep have a similar organ maturation timeline to humans, they provide an excellent model to study the development of metabolic systems in the perinatal period. Their long gestation (147 days), fetal size, fetal number (usually 1-2 per pregnancy) and tolerance to fetal instrumentation makes them ideal to study *in utero* physiology. Data from fetal sheep models have provided critical information about normal fetal human development and have informed clinical practices. Sheep have been used extensively to understand metabolic maturation in the developing myocardium (Fisher *et al.*, 1980, 1981; Bartelds *et al.*, 2000; Bartelds *et al.*, 2004; Lindgren *et al.*, 2019).

Dietary sources of lipid in mature sheep and humans are drastically different, with humans regularly consuming fat through dairy, meat, oils and other sources while sheep are herbivores and consume primarily plant material. The four compartment stomach of the sheep gastrointestinal system allows microbes to ferment and enzymatically digest the fibrous plant material into carbohydrate and fatty acid

metabolites which include three main groups of short chain or volatile fatty acids (SCFA): acetate, propionate and butyrate (Bergman, 1990). SCFAs from fermentation are rapidly absorbed through the rumen wall, metabolized by ruminal or large intestine epithelium and then enter the portal vein. SCFAs are thought to be responsible for ~70% of the caloric requirements of the adult ruminant (Bergman, 1990). Acetate is converted into acetyl-CoA, which is converted into a malonyl-CoA, the first committed step of fatty acid synthesis and substrate for fatty acid synthase (Bortz *et al.*, 1962). C_{14}-acetate and has been shown to be readily incorporated into fatty acids in liver and adipose tissue in the ruminant (Hanson & Ballard, 1967). However, despite these digestion differences between sheep and humans, it appears that processing of fatty acids in the myocardium is comparable between the two species (Bartelds *et al.*, 2004).

Rationale for Using Umbilicoplacental Embolization as a Model of IUGR for the Studies Described in this Thesis

Umbilicoplacental embolization provides a well-controlled model of placental insufficiency and has been used to investigate the effects of IUGR on an array of systems including lung, kidney, brain, retina, blood vessels, hypothalamic-pituitary-adrenal axis and the heart (Gagnon *et al.*, 1994; Cock & Harding, 1997; Murotsuki *et al.*, 1997; Louey *et al.*, 2000; Cock *et al.*, 2001; Joyce *et al.*, 2001; Loeliger *et al.*, 2003; Cock *et al.*, 2004; Duncan *et al.*, 2004; Maritz *et al.*, 2004; Mitchell *et al.*, 2004; Loeliger *et al.*, 2005; Louey *et al.*, 2005; Bubb *et al.*, 2007; Louey *et al.*, 2007; Thompson *et al.*, 2011). This model involves daily injections of microspheres that

effectively block placental area for substrate exchange; daily injections are required due to placental compensation and reserve but the need for daily injections diminishes over time. Fetuses with placental insufficiency are hypoxemic, hypoglycemic and have increased cortisol, mirroring what happens in human intrauterine growth restriction. The magnitude of IUGR (20-50% reduction in body weight) depends on the gestational age, duration and severity of embolizing. Lambs from umbilicoplacental fetuses are viable at birth and they exhibit increased adiposity at maturity, hinting at long term metabolic perturbations (Louey *et al.*, 2005).

Aims and Hypotheses

It is clear that there are specific knowledge gaps in terms of how the prenatal heart prepares for the transition to utilizing fatty acids as its primary energy source after birth. We do not know whether the machinery required to metabolize fatty acids is upregulated prior to birth or if the fetal heart differs in its lipid storage strategies compared to the newborn hear. This thesis addresses some of these deficits. The overarching aim of this thesis was to determine the readiness of key components in the cardiac fatty acid metabolic pathway in late gestation in a precocial species, the sheep.

Specific Aim 1 (Chapter II): To characterize of the normal developmental profile of key components in fatty acid metabolic pathway in the fetal and neonatal heart. This study involved lipid uptake studies in freshly isolated cardiomyocytes from fetal (125d GA) and newborn (8d PN) hearts, and measurement of gene and

protein expression levels of key components involved the fatty acid transport, esterification, and metabolism in fetal (94d, 135d GA) and newborn (5d PNA) hearts.

- **Hypothesis 1:** Both fetal and newborn cardiomyocytes will be capable of fatty acid uptake, and fetal cardiomyocytes will form larger lipid droplets compared to newborn.
- **Hypothesis 2:** All fatty acid metabolism genes and proteins will be upregulated between 94d GA and 135d GA and have even greater expression in newborn myocardium.

Specific Aim 2 (Chapter III): To determine the effect of IUGR on key components of the fetal cardiac fatty acid metabolic pathway. This study involved lipid uptake studies in freshly isolated cardiomyocytes from IUGR fetuses that had been subject to 10 days of placental insufficiency induced by umbilicoplacental embolization, and age-matched controls (125d GA). Gene and protein expression levels of key components involved the fatty acid transport, esterification, and metabolism were also measured in these hearts.

- **Hypothesis 1:** IUGR cardiomyocytes will produce larger lipid droplets compared to control and IUGR fetuses will have higher levels of circulating long chain acylcarnitines compared to control.
- **Hypothesis 2:** Fatty acid metabolism genes and proteins will be suppressed in IUGR fetal myocardium compared to control.

Among the many physiological questions needing resolution in order to improve neonatal care is a better understanding of the metabolic needs of the developing myocardium and how it prepares for birth. Thus far, scientific efforts have only scratched the surface of understanding the regulation of genes responsible for fatty acid metabolism during prenatal and early postnatal life. This thesis will tackle two elements aimed at (1) furthering our understanding of fatty acid metabolic maturation in the perinatal heart and (2) how this maturational process is affected by intrauterine growth restriction.

Chapter 2. Lipid Metabolism Gene Expression Pattern Prepares for Birth in the Ovine Heart

Introduction

One of the curious features of adult-onset cardiac pathology is the reversion of specific proteins to fetal isoforms that promote aerobic glycolysis (Rajabi *et al.*, 2007; Taegtmeyer *et al.*, 2010). While the primary triggers for this isoform switching are not known, metabolic stress has been suggested to play a key role (Taegtmeyer *et al.*, 2010). Many studies are investigating whether this return to a fetal, glycolytic metabolic profile may reflect an adaptation or maladaptation in disease state, but few studies are focusing on the normal metabolic switch that occurs around the time of birth. Understanding the normal ontogeny of the metabolic gene expression patterns in the maturing myocardium will broaden our understanding of the fuel requirements at different stages of development and may shine light on the processes underlying the reversion of adult genes to their immature expression patterns.

It is well established that in several mammalian species, the fetal heart utilizes aerobic glycolysis with glucose and lactate (Fisher *et al.*, 1980, 1981; Rolph & Jones, 1983; Werner & Sicard, 1987; Lopaschuk & Jaswal, 2010) as primary fuels while the adult heart prefers oxidative phosphorylation using long chain fatty acids (Most *et al.*, 1969;

Neely *et al.*, 1972; Neely & Morgan, 1974). Although it is known that the shift from carbohydrate oxidation in immature cardiomyocytes to fatty acid oxidation in more mature myocardium occurs soon after birth (Lopaschuk *et al.*, 1992; Lopaschuk & Jaswal, 2010), the expression patterns of genes and proteins involved in the fuel preference shift around the time of birth has not been studied in depth.

The fetus is hypoxemic relative to the adult and has readily available lactate generated by the placenta and low levels of circulating fatty acids, conditions that favor carbohydrate oxidation (Fisher *et al.*, 1980; Piquereau & Ventura-Clapier, 2018). These conditions theoretically favor carbohydrate oxidation of fatty acid oxidation due to substrate and oxygen availability. There is a postnatal increase in the work required of the heart with increasing systolic load. This increased energy demand is met with increased oxygen availability and elevated circulating fatty acid concentrations that favor a switch to fatty acid utilization. It has been previously reported that there is an increase in *CPT1* gene expression during the transition from fetus to newborn (Bartelds *et al.*, 2004), but it is not known whether this increase begins prior to birth, or is primarily stimulated by the birth process or postnatal suckling. Because fuel substrates, metabolic demands and arterial pressure (Dawes *et al.*, 1980) all change within minutes at birth, the machinery required to convert fatty acids found in milk to ATP must be ready to function at the time of birth in both altricial and precocial species. Relatively little is known about the developmental maturation of additional biochemical machinery responsible for augmenting the use of lipids in the postnatal period in a precocial species such as sheep, whose cardiac developmental timeline

relative to birth is more similar to humans than rodents and other altricial species. Figure 2-1 shows the pathways that underlie fatty acid metabolism in myocardium.

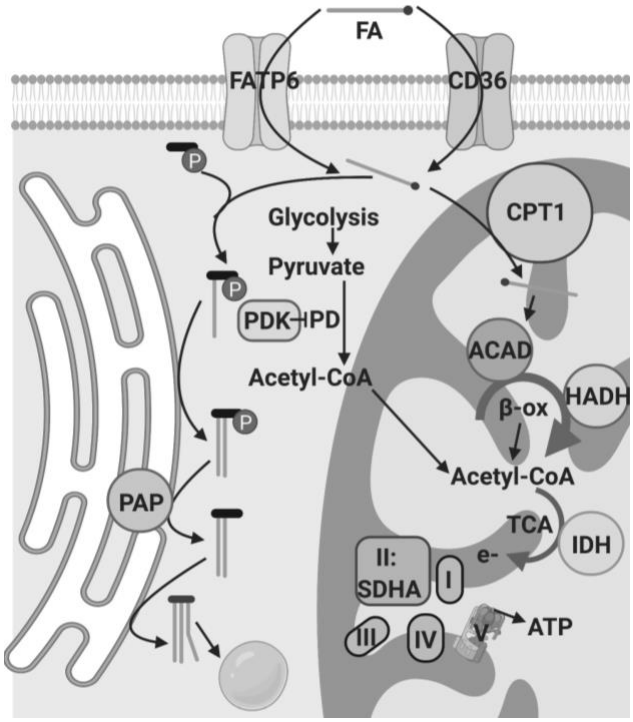

Figure 2-1 Schematic of fatty acid uptake, activation, oxidation, ATP production and esterification highlighting the genes and proteins under investigation.

FA: fatty acid, FATP6: fatty acid transport protein 6, CD36: fatty acid translocase, ACSL1/3: acyl-CoA synthetase long chain, PDK4: pyruvate dehydrogenase kinase, PD: pyruvate dehydrogenase, CPT1: carnitine palmitoyltransferase 1, VLCAD/LCAD: very long/long chain acyl-CoA dehydrogenase, HADH: hydroxyacyl-coenzyme A dehydrogenase, ACAT: acetyl-CoA acetyltransferase, CS: citrate synthase, IDH: isocitrate dehydrogenase, SDHB: succinate dehydrogenase, GPAT: glycerol phosphate acyltransferase, PAP: phosphatidic acid phosphatase, DGAT: diacylglycerol acyltransferase.

Under normal conditions, the late gestation fetal sheep heart does not oxidize fatty acids to an appreciable degree (Bartelds *et al.*, 2000), presumably because substrate availability is low (Noble *et al.*, 1982). However, when a fetal heart is exposed to infused exogenous palmitate, it can both take up and oxidize the substrate, though not to the same degree as a newborn lamb (Bartelds *et al.*, 2000). This demonstrates a limited capacity of the immature myocardium to process lipids *in utero*. Thus, the systems that transport and metabolize fatty acids must have undergone some degree of maturation even before birth.

The timeline underlying the regulation of lipid transport and metabolism systems in the developing heart remains poorly understood. In addition to filling current knowledge gaps concerning the metabolic features of the immature myocardium during the perinatal period, studies of metabolic maturation could inform nutrition protocols in preterm infants and provide insight as to whether immature hearts are able to fully metabolize exogenous lipid substrates. A thorough knowledge of the regulation of the expression of the proteins that constitute the immature state will eventually shed light on the processes in failing adult hearts that revert to a fetal metabolic profile. We hypothesized that the expression of genes that underlie fatty acid metabolism occurs gradually so that by the time of birth, the system is prepared to metabolize free fatty acids acquired from mother's milk.

The goal of this study was to determine the normal maturation of the machinery responsible for lipid metabolism in the developing sheep heart. Therefore, we measured gene and protein expression for fatty acid transporters and enzymes in myocardium at two fetal ages (94 and 135 day gestation) and one newborn age (5 day). To test whether fetal cardiomyocytes are capable of fatty acid uptake and storage in a lipid droplet, we incubated isolated cardiomyocytes from fetal (125 day gestation) and newborn (8 day) animals with a fluorescent tagged long chain fatty acid molecule, BODIPY-C_{12}.

Materials and Methods

Animals

Animal work was conducted with approval of the Institutional Animal Care and Use Committee and Oregon Health and Science University (Portland OR, USA). All sheep were of mixed western breeds, were healthy and within normal flock range for body weight at time of collection. The study group included a balance of males and females in each age group. Animals were used for imaging studies only (125 days gestation, dGA and 8 days postnatal, dPN) or for gene and protein expression analysis only (94 dGA, 135 dGA, 5 dPN; term = 147d GA).

Pregnant ewes were euthanized as previously described (Lindgren *et al.*, 2019) via intravenous injection of sodium pentobarbital (SomnaSol, 80mg/kg, Henry Schein Animal Health, OH, USA). Fetuses were accessed through hysterotomy and umbilical vein injected with 10,000U of heparin (Baxter, IL, USA) followed by 10mL saturated

potassium chloride to arrest the heart in diastole. Fetal weight was recorded, the heart extracted, trimmed in a standardized method and weighed. Hearts were collected in one of two ways; flash frozen in liquid nitrogen (for tissue analysis) or dissociated (for imaging studies). Only control hearts were included in the present study.

Lambs were euthanized in a similar fashion. In short, they were given 10,000U heparin injection, i.v. and then SomnaSol. Lamb weight was recorded, the heart extracted, trimmed in a standardized method and weighed. Hearts were collected in one of two ways, flash frozen in liquid nitrogen (for tissue analysis) or dissociated (for imaging studies). Only control hearts were included in the present study.

For imaging studies, twelve 125 ± 1 dGA fetuses were included. 1 fetus per ewe was collected from the following: 1 ewe carrying a singleton, 10 ewes carrying twins, and 1 ewe carrying triplets; fetuses used had been surgically instrumented to serve as controls for a separate study (not described in the current paper). Eight 8 ± 1 dPN lambs were included: 5 ewes produced 8 lambs, 4 fetuses from 2 ewes with triplet pregnancies where 2 of the 3 fetuses were used, 2 ewes with triplet pregnancies where only 1 of the 3 fetuses was used (and 1 ewe with a twin pregnancy (both fetuses included)).

For tissue analysis, eight (gene studies) or six (protein studies) 94 ± 2 dGA and 135 ± 5 dGA fetuses were included and seven (gene studies) or 6 (protein studies) 5 ± 4 dPN lambs were included. The 94 ± 2 dGA group was comprised of fetuses from 5 ewes

carrying twins where only 1 twin of each pair was included, and 1 ewe carrying triplets where all 3 fetuses were included. The studies at 94 ± 2 dGA included the same 5 fetuses from twin pregnancies and only 1 fetus from the triplet ewe. Eight 135 ± 5 dGA fetuses were included from 8 ewes carrying twins; only 1 twin of each pair was included. Fetuses were uninstrumented control twins of experimental fetuses (not in the present study), or fetuses not subjected to a surgical procedure. Seven (gene studies) or six (protein studies) 5 ± 4 dPN lambs were obtained from 4 ewes carrying triplets where only 1 lamb was used per ewe, 1 ewe carrying twins where both lambs were included, and 1 lamb where information was not available; this last lamb was omitted for protein studies. Lambs were uninstrumented or served as controls to experimental siblings. All groups included a balance of males and females (Table 2-1).

Table 2-1 Experimental workflow, sex distribution and sample size at different age groups.

dGA = days gestational age (Term ~147dGA), dPN = days postnatal.

Experimental Workflow:

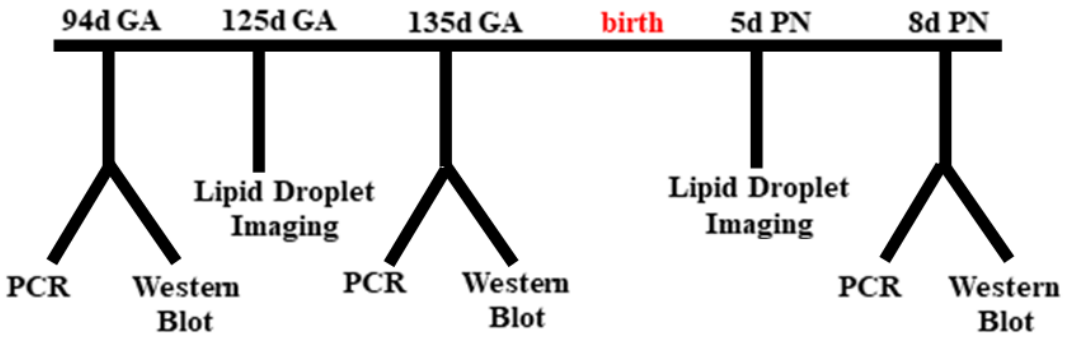

Sex Distribution and Sample Size:

	Fetal			Postnatal	
Age	94 ± 2 dGA	125 ± 1 dGA	135 ± 5 dGA	5 ± 4 dPN	8 ± 1 dPN
qPCR	Male (3) Female (5)		Male (4) Female (4)	Male (5) Female (2)	
Western Blot	Male (3) Female (3)		Male (3) Female (3)	Male (3) Female (3)	
Lipid Droplet Imaging		Male (8) Female (4)			Male (4) Female (4)

Cardiomyocyte Isolation

Cardiomyocytes were enzymatically dissociated using retrograde perfusion as previously described (Jonker *et al.*, 2007). Hearts were cannulated though the ascending aorta and retrograde-perfused with a series of warmed (39°C) and 95% oxygen/5% CO_2 gassed solutions in the following sequence: 1) Tyrode's buffer (Ca^{2+} free, 140mM NaCl, 5mM KCl, 1mM $MgCl_2.6H_2O$, 10mM glucose, 10mM HEPES – pH 7.35) to clear the vasculature of blood, 2) Tyrode's buffer with enzymes (160 U/mL type II collagenase (Worthington) and 0.78 U/mL type XIV protease (Sigma) for disaggregation and 3) KB solution (Kraftbrühe: 74uM glutamic acid, 30uM KCl, 30uM KH_2PO_4, 20uM Taurine, 2mM $MgSO_4$, 0.5mM EGTA, 10mM HEPES and 10mM glucose – pH 7.37) to clear enzymes and further relax cardiomyocytes. Left and right ventricular free walls, and the intraventricular septum were separated for gentle agitation in KB solution for cardiomyocyte release into solution. Following

cardiomyocyte isolation, cells rested in KB solution (room temperature, 30 minutes). A 140µL aliquot of left ventricular cells (~250k cells/mL) were taken for live imaging.

BODIPY-C_{12} Fluorescent Fatty Acid Live Imaging

A protocol, established in our lab for studying placental explants (Kolahi *et al.*, 2016), was adapted for fetal cardiomyocytes to track the incorporation of an exogenous long chain saturated fatty acid into lipid droplets. BODIPY FL-C_{12} (Molecular Probes, cat#D3822) is a 12-carbon chain length saturated fatty acid linked to the fluorophore BODIPY (4,4-difluoro-3a,4a-diaza-s-indacene) (Stahl *et al.*, 1999; Wang *et al.*, 2010a; Kassan *et al.*, 2013; Rambold *et al.*, 2015; Kolahi *et al.*, 2016).

The BODIPY-C_{12} conjugate biologically resembles an 18-carbon saturated fatty acid and permits tracking of exogenous supplied fatty acid via the BODIPY fluorophore which is an intensely fluorescent, intrinsically lipophilic molecule. 10 µM solutions of BODIPY-FL C_{12} were prepared by diluting a 2.5mM stock solution in DMSO 1:250 in fetal or newborn KB solution (KB supplemented with 2mM glutamine, 200 µM sodium pyruvate, 2 or 1mM lactate (fetal vs. newborn respectively), 1 or 5mM glucose (fetal vs. newborn respectively)) supplemented with 0.1% fatty acid free bovine serum albumin and incubated for 30 minutes (37°C, in the dark) to allow fatty acid: BSA conjugation.

Cells were incubated in fetal or newborn KB in 8 well µ-slides (Ibidi, cat#80821) with 2µM of BODIPY-C_{12} for 60 minutes (39°C or 37°C, for fetal vs. newborn cells

respectively) and imaged using the 63x oil lens on the Zeiss 880 LSM with Airyscan. Z-stack images were collected after 60 minutes. BODIPY was imaged with 488 laser (intensity 0.6, gain 825, digital gain 1.0). 90-130 slices, 0.2 µm thick were acquired per frame (18-26 µm thickness, 3-12 frames per animal).

Image Analysis

Z-stacks were processed (Airyscan) and maximum intensity projections performed in ZEN Black Software (Zeiss). Fiji software was used to analyze all images obtained. Images were enhanced using Enhance Local Contrast (CLAHE: blocksize=9, histogram=256, maximum=4), despeckled, and background subtracted (rolling=5). Lipid droplet particles were analyzed by filtering for the following parameters: circularity (0.8-1), size (0.0314 <minimal detectable size for LSM880> to 3<exceeds the maximum non adipocyte lipid droplet size (Suzuki *et al.*, 2011)>), AutoThreshold (Intermodes dark) and images were converted to a mask for lipid droplets and entire cells. For each animal, 10-30 cells were measured in an average of 5 frames (range of 3-8 frames) dependent on number of cells. The mean area of individual lipid droplets in the present study was 0.19µm^2 with a range of 0.036 µm^2 to 1.18µm^2. Masks were manually verified to ensure the parameters did not accidentally exclude viable or include non-viable cells.

RNA isolation and gene expression

RNA was isolated as previously described (Lindgren *et al.*, 2019) from 40-50µg of left ventricular myocardium using Trizol, a steel bead and TissueLyser LT (Qiagen,

Germantown, MD, USA), 50 oscillations/sec for 3 minutes. Isolates were further purified using RNeasy Mini Columns (Qiagen). Reverse transcription on 1µg RNA was conducted to synthesize cDNA using the High-Capacity cDNA Reverse Transcription Kit (ABI) and diluted 1:20 prior to PCR. Quantitative PCR was carried out using SYBR Green in the Stratagene Mx3005. Primers are listed in Table 2-2. Gene expression was analyzed using the ΔC_t method. Genes of interest were normalized to housekeeping gene RPL37a, which was not altered by age.

Table 2-2 Primer Sequences.

Gene ID	Forward	Reverse
RPL37a housekeeper	ACCAAGAAGGTCGGAATCGT	GGCACCACCAGCTACTGTTT
CD36	CTGGTGGAAATGGTCTTGCT	ATGTGCTGCTGCTTATGGGT
FATP6	TTGGAAATGGAGCACGCAGTGA	CTCCCGACTGATCCAATTTTCCCA
ACSL1	GAGCAGAGGTTCTCAGTGAAGCAA	CGGCTGTCCATCCAGGATTCAATA
ACSL3	GACAGATGCCTTCAAGCTGAAACG	GGAATGGACTCTGCCTCACAGTTT
CPT1	GGATGTTTGAGATGCACGGC	GCCAGCGTCTCCATTCGATA
PDK4	CCTGTGATGGATAATTCCCG	TTGGTTCCTTGCTTGGGATA
IDH	CTGTGTTTGAGACGGCTACAAGGA	CGTAGCTGTGGGATTGGCAATGTT
LCAD	TGAAAGCCGCATTGCCATTGAG	ACTTGGATGGCCCGGTCAATAA
VLCAD	AAGATCCCTGAGTGAAGGCCA	TAGAACCAGGATGGGCAGAAA
HADH	AGAAAACCCCAAGGGTGCTGAT	GCCTCTTGAACAGCTCGTTCTT
ACAT1	CTGGGTGCAGGCTTACCTATTTCT	CATAGGGGACATTGGACATGCTCT
GPAT	GAAGTGGCTGGTGAGTTAAACCCT	CAGTCTGATCATTGCCGGTGAAAC
PAP	AGAATGAAGGGAGACTGGGCAAGA	GCAACCAGAGCTCCTTGAATGAGT
DGAT	AGACACTTCTACAAGCCCATGCTC	AGTGCACTGACCTCATGGAAGA

Western Blotting

Protein was isolated as previously described (Lindgren *et al.*, 2019). In brief, 20-30µg of left ventricular myocardium was homogenized in RIPA lysis buffer (MilliporeSigma) with a Complete Mini Protease 227 Inhibitor tablet (MilliporeSigma) and phosphatase inhibitor cocktails I and II (MilliporeSigma). Tissue was added to chilled lysis buffer in 2mL tubes containing a stainless-steel bead and lysed (4 minutes, 50Hz TissueLyser LT). Protein was quantified by a standard

bicinchoninic acid assay as routinely performed in our lab (Jonker *et al.*, 2015) (Pierce BCA Protein Assay Kit) and diluted to a uniform concentration across all groups (2µg/µL). Gels were made using Invitrogen SureCast Stacking Buffer (4% acrylamide) and Resolving Buffer (12% acrylamide) along with SureCast system. 15µg protein was loaded with 6x dye (10% betamercaptoethanol) and separated by SDS-PAGE (90 minutes, 100mV, BioRad system) with running buffer (24.8 mM Tris, 191.8 mM glycine, 3.5 mM SDS). Protein was transferred to PVDF membranes with transfer buffer (24.8 mM Tris, 191.8 mM glycine) and blocked (5% milk in TBST (Tris-buffered saline + 0.01% Tween 20), 1 hour, room temperature). Primary antibody incubation (4°C, overnight) was followed by TBST rinses (3 x 10 minutes) and subsequent secondary incubation (room temperature, 1 hour). Primary antibody dilutions and sources are listed in Table 2-3. For ACADL, which was close in molecular weight to the housekeeper, blots were stripped with Restore Western Blot Stripping Buffer (Thermo Fisher Scientific) and probed again with GAPDH. Ponceau S was used to stain for total protein following wet transfer prior to OXPHOS primary antibody incubation for normalization of OXPHOS expression.

SuperSignal West Dura chemiluminscence substrate was used to visualize membranes (Thermo Fisher Scientific). GBOX (SynGene) and GeneSys software (version 4.3.7.0) were used to image and analyze the blots. CPT1a blots were developed on film (GeneMate Blue Autoradiography Film cat#490001) in a dark room (15 minute exposure). Band intensities were expressed as area under the curve, normalized against α -tubulin or GAPDH which did not have different expression between ages.

Table 2-3 Antibodies used.

Protein	Dilution	Cat #	Vendor	RRID or reference
CD36	1:1000	133625	abcam	RRID:AB_2716564
ACSL1	1:1000	177958	abcam	(Li *et al.*, 2020)
CPT1a	1:500	12252	Cell Signaling	RRID:AB_2797857
CPT1b	1:1000	22170	ProteinTech	(Abudurexiti *et al.*, 2020)
ACADL	1:1000	17526	ProteinTech	(Huang *et al.*, 2014)
CS	1:1000	14309	Cell Signaling	RRID:AB_2665545
OXPHOS cocktail containing: NDUFB8, SDHB, UQCRC2, MTCO1, ATP5A	1:500	110413	abcam	RRID:AB_2629281
GAPDH (housekeeper)	1:5000	47339	Novus Biologicals	RRID:AB_10010294
α-tubulin (housekeeper)	1:5000	2125	Cell Signaling	RRID:AB_2619646
anti-Rabbit HRP (secondary antibody)	1:5000	7074	Cell Signaling	RRID:AB_2099233
anti-Mouse HRP (secondary antibody)	1:5000	7076	Cell Signaling	RRID:AB_330924

Statistics

BODIPY-C_{12} lipid droplet volume, area and droplet number were analyzed by unpaired t-test. One-way ANOVA, followed by Tukey's multiple comparison test was

used to test for differences in gene and protein expression. All data were analyzed using GraphPad Prism 6 and are presented as mean ± SD unless noted otherwise. P-values < 0.05 were considered statistically significant.

Results

BODIPY-C_{12} Lipid Droplet Formation

The 12 carbon fluorescently tagged saturated free fatty acid was used to determine the capacity of the immature cardiomyocyte for lipid uptake and storage. BODIPY-C_{12} lipid droplets in fetal cardiomyocytes were significantly larger than those in newborn cardiomyocytes (Figure 2-2A). There was no difference in the droplet area or number of droplets relative to cell area (Figure 2-2B and C).

Figure 2-2 Lipid droplet accumulation in fetal and newborn cardiomyocytes.

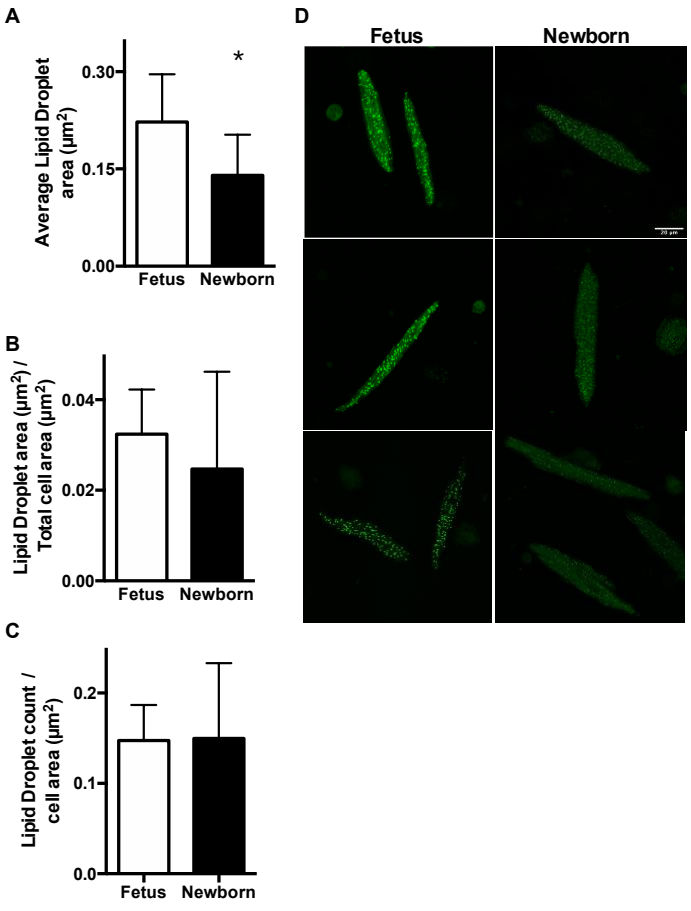

A. Average lipid droplet area (µm^2). B. Lipid droplet area normalized to cell area. C. Number of lipid droplets normalized to cell area. D. Representative images of BODIPY-C_{12} (green) lipid droplet accumulation in fetal and newborn cardiomyocytes. Data are mean ± SD, *p < 0.05. Fetus: white: 125±1 dGA, n=12, Lamb: black: 8±1 dPN, n=8.

Sarcolemmal Fatty Acid Transporter Expression

CD36 and FATP6 are responsible for fatty acid transport into the cardiomyocyte (Coburn et al., 2000; Gimeno et al., 2003). The mRNA levels for CD36 showed progressive increases with advancing age (Figure 2-3A), and this was also reflected in the protein expression (Figure 2-3C). In contrast, FATP6 gene expression was low throughout gestation but was high after birth (Figure 2-3B).

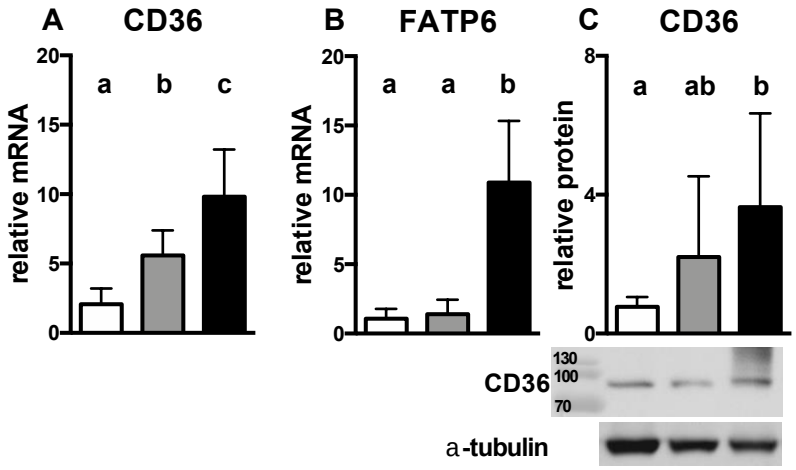

Figure 2-3 Developmental myocardial gene and protein expression of sarcolemmal fatty acid transporters.

Expression is in left ventricular (LV) tissue of 94 ± 2 dGA (white: n=8 gene, n=6 protein), 135 ± 5 dGA (grey: n=8 gene, n=6 protein) and 5 ± 4 dPN (black: n=7 gene, n=6 protein) myocardium. Gene expression relative to RPL37a, protein expression relative to α-tubulin. Data are mean ± SD, non-shared letters indicate statistically significant differences, $p < 0.05$.

Fatty Acid Acylation Enzyme Expression

Acyl CoA Synthetase long chain (ACSL) is responsible for the acylation and activation of fatty acids upon entry to the cell (Chang et al., 2011; Ellis et al., 2011). ACSL1 had stepwise increases in gene expression with age (Figure 2-4A) and protein levels followed the gene expression pattern (Figure 2-4C). In contrast, ACSL3 gene levels were low in the fetal heart and high postnatally (Figure 2-4B).

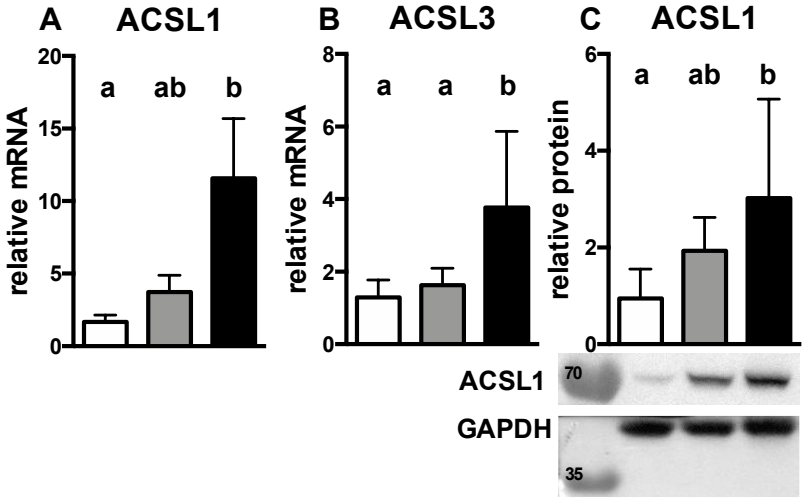

Figure 2-4 Developmental myocardial gene and protein expression of fatty acid acylation enzymes.

Expression is in left ventricular (LV) tissue of 94 ± 2 dGA (white: n=8 gene, n=6 protein), 135 ± 5 dGA (grey: n=8 gene, n=6 protein) and 5 ± 4 dPN (black: n=7 gene, n=6 protein) myocardium. Gene expression relative to RPL37a, protein expression relative to GAPDH. Data are mean ± SD, non-shared letters indicate statistically significant differences, $p < 0.05$.

Mitochondrial Fatty Acid Transporter Expression

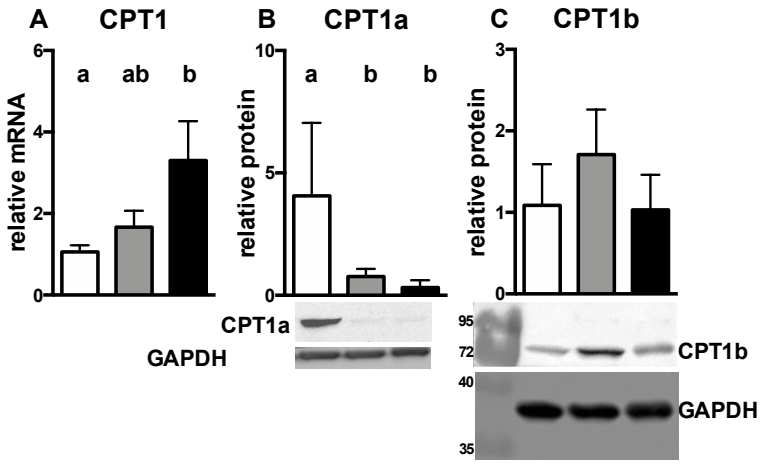

Figure 2-5 Developmental myocardial gene and protein expression of mitochondrial fatty acid transporters.

Expression is in left ventricular (LV) tissue of 94 ± 2 dGA (white: n=8 gene, n=6 protein), 135 ± 5 dGA (grey: n=8 gene, n=6 protein) and 5 ± 4 dPN (black: n=7 gene, n=6 protein) myocardium. Gene expression relative to RPL37a, protein expression relative to GAPDH. Data are mean ± SD, non-shared letters indicate statistically significant differences, $p < 0.05$. CPT1a protein ladder not present due to use of film exposure (15 minutes), which did not transfer protein ladder.

Carnitine palmitoyltransferase 1 (CPT1) is the rate limiting enzyme for fatty acid utilization by the mitochondrion (Schlaepfer & Joshi, 2020) and is found in three isoforms designated as the liver isoform (CPT1a or CPT1-L) which is also expressed in the fetal heart, the muscle isoform (CPT1b or CPT1-M) which is most highly expressed in the adult heart, and the brain isoform (CPT1c). Cardiomyocytes express both CPT1a and CPT1b isoforms (Cook et al., 2001) and in rat cardiomyocytes the shift from CPT1a (fetal) to CPT1b (adult) occurs at weaning (Brown et al., 1995).

While the mRNA levels for all CPT1 isoforms increase with age in the sheep heart (Figure 2-5A), this pattern is not mirrored in protein expression of the isoforms. Protein levels of CPT1a (the fetal isoform) decrease from 94d to 135d gestation and remain low in the newborn myocardium (Figure 2-5B). Adult isoform (CPT1b) protein expression appears to be constitutively expressed, consistent with the findings of Bartelds *et al.* (Bartelds *et al.*, 2004) (Figure 2-5C).

Fatty Acid β-Oxidation Expression

The first step in fatty acid β-oxidation is catalyzed by long chain or very long chain fatty acyl CoA dehydrogenase, LCAD and VLCAD respectively. LCAD and VLCAD gene expression levels are low throughout fetal life and increase more than twofold postnatally (Figure 2-6A, B); interestingly, LCAD protein concentration did not follow gene expression levels but rather increased during fetal life and was not different postnatally (Figure 2-6E). Short/medium chain fatty acid β-oxidation pathway enzyme hydroxyacyl CoA dehydrogenase (HADH) displayed a stepwise increase in expression throughout development (Figure 2-6C), while ketone metabolic enzyme acetyl-CoA acetyltransferase (ACAT1) gene expression increased with advancing gestation but wasn't higher after birth. (Figure 2-6D).

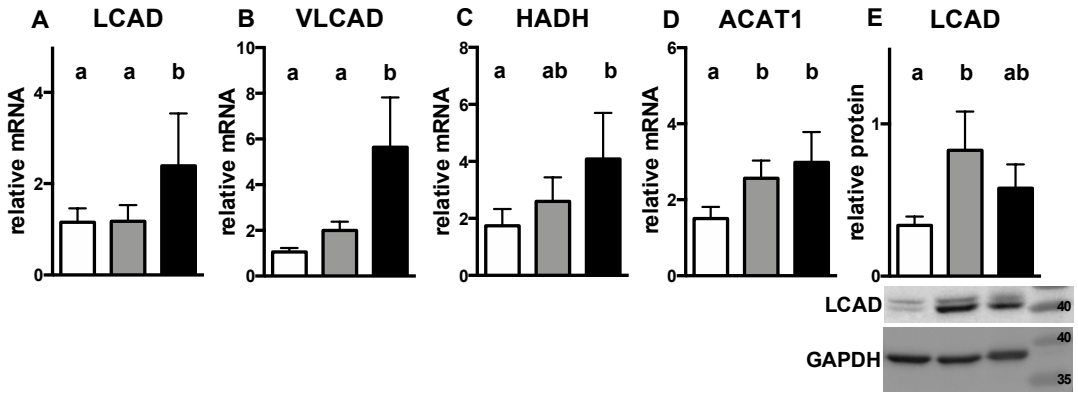

Figure 2-6 Developmental myocardial gene and protein expression of fatty acid ß-oxidation enzymes.

Expression is in left ventricular (LV) tissue of 94 ± 2 dGA (white: n=8 gene, n=6 protein), 135 ± 5 dGA (grey: n=8 gene, n=6 protein) and 5 ± 4 dPN (black: n=7 gene, n=6 protein) myocardium. Gene expression relative to RPL37a, protein expression relative to GAPDH. Data are mean ± SD, non-shared letters indicate statistically significant differences, $p < 0.05$.

Glycolysis/ β-Oxidation Regulator Expression

The relative contributions to oxidative metabolism from glycolysis versus fatty acid β-oxidation is heavily regulated by pyruvate dehydrogenase kinase (PDK4). This protein deactivates the final step of glycolysis via phosphorylation and subsequent deactivation of pyruvate dehydrogenase which would normally yield acetyl CoA. Inhibition of acetyl-CoA production permits increased carbon flux through the β-oxidation of fatty acids, which also yields acetyl-CoA. Gene expression of PDK4 was low throughout gestation and was higher in the newborn myocardium (Figure 2-7).

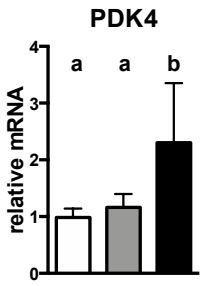

Figure 2-7 Developmental myocardial gene expression of glycolysis/ß-oxidation regulator pyruvate dehydrogenase kinase 4 (PDK4).

Expression (relative to RPL37a) is in left ventricular (LV) tissue of 94 ± 2 dGA (white: n=8), 135 ± 5 dGA (grey: n=8) and 5 ± 4 dPN (black: n=7) myocardium. Data are mean ± SD, non-shared letters indicate statistically significant differences, $p < 0.05$.

Tricarboxylic Acid Cycle (TCA) Expression

Isocitrate dehydrogenase (IDH) produces the first reducing equivalent (NADH) for supplying electrons to Complex I of the electron transport chain. Expression of the IDH gene increases toward term and into postnatal life (Figure 2-8A). The first step in the TCA cycle joins oxaloacetate and Acetyl-CoA and is catalyzed by citrate synthase (*CS*). CS protein expression was not different between ages (Figure 2-8B).

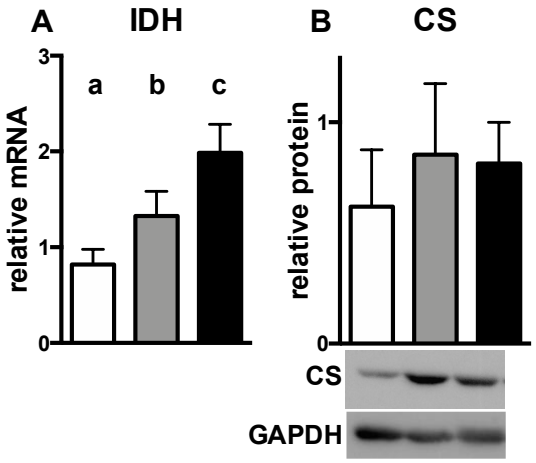

Figure 2-8 Developmental myocardial gene and protein expression of TCA cycle enzymes.

Expression is in left ventricular (LV) tissue of 94 ± 2 dGA (white: n=8 gene, n=6 protein), 135 ± 5 dGA (grey: n=8 gene, n=6 protein) and 5 ± 4 dPN (black: n=7 gene, n=6 protein) myocardium. Gene expression relative to RPL37a, protein expression relative to GAPDH. Data are mean ± SD, non-shared letters indicate statistically significant differences, $p < 0.05$. The CS protein band was confirmed to be the correct size in a separate blot; protein ladder did not show up for this particular blot.

Electron Transport Chain Expression

Complex I subunit NDUFB8 protein expression was low in fetuses and had significantly higher expression in the newborn (Figure 2-9A). Electron transport chain subunit protein expression from complex II (SDHB), complex III (UQCRC2), and complex IV (MTCO1) were not different between ages (Figure 2-9B, C and D). ATP synthase (complex V) subunit ATP5A protein levels had a similar pattern to NDUFB8,

with low levels in the fetal ages and higher expression in newborn myocardium (Figure 2-9E).

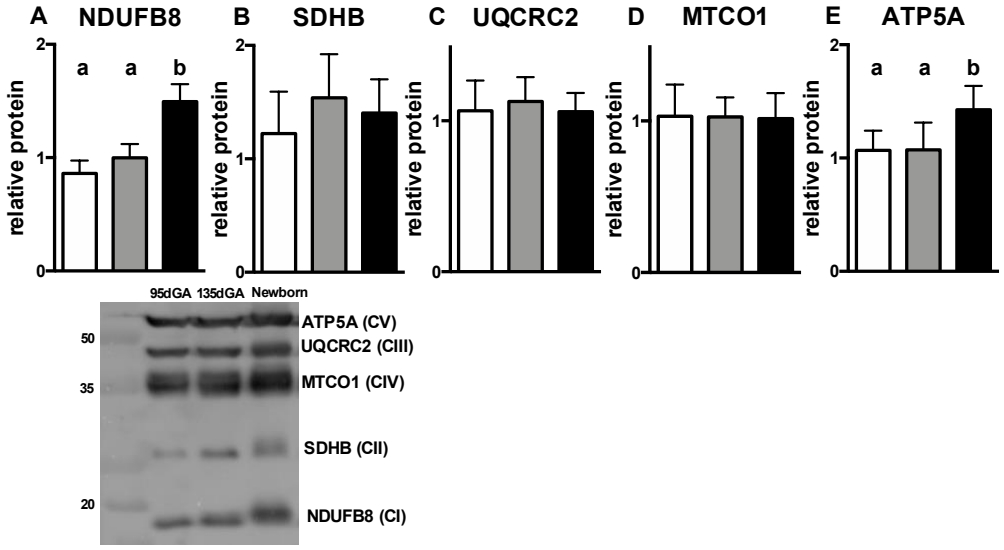

Figure 2-9 Developmental myocardial gene and protein expression of electron transport chain subunits.

Expression is in left ventricular (LV) tissue of 94 ± 2 dGA (white: n=8 gene, n=6 protein), 135 ± 5 dGA (grey: n=8 gene, n=6 protein) and 5 ± 4 dPN (black: n=7 gene, n=6 protein) myocardium. Gene expression relative to RPL37a, protein expression relative to total protein. Data are mean ± SD, non-shared letters indicate statistically significant differences, $p < 0.05$.

Fatty Acid Esterification Pathway Expression

GPAT catalyzes the joining of a glycerol-3-phosphate with fatty acyl-CoA to form lysophosphatidic acid, the rate limiting step in *de novo* glycerolipid synthesis (Wendel *et al.*, 2009). GPAT gene expression had a stepwise increase with age (Figure 2-10A).

Phosphatidic acid phosphatase (PAP) catalyzes the production of diacylglycerol (DAG) by dephosphorylation of phosphatidate. Diacylglycerol acyl transferase (DGAT) adds the final fatty acyl-CoA to DAG to produce triacylglycerol. Both *PAP* and DGAT had low gene expression in both 94d and 135d fetal myocardium with higher expression in newborns (Figure 2-10B and C).

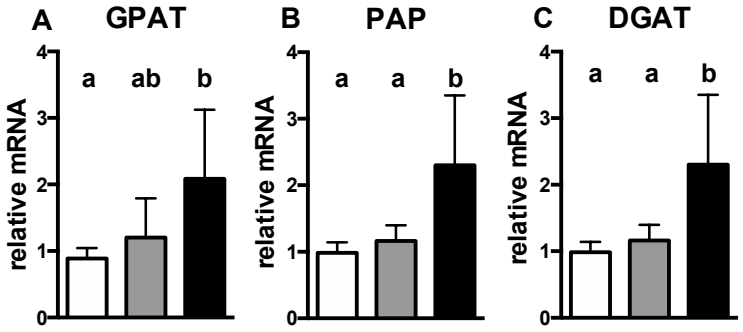

Figure 2-10 Developmental myocardial gene expression of fatty acid esterification enzymes.

Expression (relative to RPL37a) is in left ventricular (LV) tissue of 94 ± 2 dGA (white: n=8 gene, n=6 protein), 135 ± 5 dGA (grey: n=8 gene, n=6 protein) and 5 ± 4 dPN (black: n=7 gene, n=6 protein) myocardium. Data are mean ± SD, non-shared letters indicate statistically significant differences, $p < 0.05$.

Discussion

Fatty acid concentrations are low in the fetal circulation but sharply increase with suckling after birth. Thus, if the myocardium of the neonate is to take advantage of a new lipid fuel supply, the systems required to transport, oxidize and esterify fatty acids

must have gone through their maturation phases before birth. This process has been recently reviewed by Piquereau *et al.* (Piquereau & Ventura-Clapier, 2018). The aim of this study was to determine the maturation of gene expression patterns that determine the components of the lipid metabolism system in the sheep heart during the perinatal period. The developing sheep heart has been found to have many similarities with the human heart both in size and in function.

Several critical components of the metabolic pathways studied exhibited progressive upregulation of gene expression prior to birth including CD36, ACSL1, CPT1, HADH, ACAT1, IDH and GPAT while some metabolic genes, including FATP6, ACSL3, LCAD, VLCAD, PDK4, NDUFB8, ATP5A, PAP and DGAT, had low expression throughout fetal life and higher expression in the postnatal period. This gives new insights on the temporal maturation of metabolic systems as term approaches.

A previous study has shown that some components of the fatty acid metabolism pathway appear in human hearts at 10-18 weeks gestation (Iruretagoyena *et al.*, 2014). The focus of the present study was limited to the perinatal period which is a pivotal period of nutritional and metabolic transition. CD36, ACSL1 and GPAT gene upregulation would presumably augment fatty acid transport into the cell, acetylation and esterification within the fetal cardiomyocyte, respectively. Fatty acids acetylated by ACSL1 are preferentially destined for storage in a lipid droplet (Sandoval *et al.*, 2008). ACSL1 gene and protein expression increases with age along with GPAT gene

expression while PAP and DGAT are only higher in the newborn. Thus, some but not all of the enzymes required for fatty acid esterification are fully mature prior to birth. It stands to reason that newborn myocardium would have the highest need for esterification enzymes due to drastic increases in circulating lipids at the time of the first feed. The prenatal maturation of these elements could enable storage of fatty acids in immature cardiomyocytes to some degree, especially if the mitochondrial elements needed to metabolize the lipids to energy are not yet mature, but the implications of exposure to high concentrations of exogenous lipids coupled with this immature esterification system remain unclear.

In adults, intracellular lipid droplet size is indicative of metabolic status, with larger and more abundant droplets being observed in heart failure, diabetes and metabolic disease (Goldberg *et al.*, 2018). Prior to this study, it was unclear whether the esterification and subsequent storage of exogenously supplied fatty acids was the same in fetal and newborn hearts or whether the esterification pathway undergoes a maturational process. We showed that the size of lipid droplets containing exogenous BODIPY-C_{12} were significantly larger in fetal cardiomyocytes compared to newborn. In other circumstances, enlarged lipid droplets are associated with mitochondrial dysfunction (Lee *et al.*, 2013). Lipid droplet accumulation may also be important in the context of intravenous lipid support in premature infants whose capacity to metabolize lipids may be more similar to a fetus than a term-born newborn.

A randomized controlled trial of short-term exposure to exogenous lipids in premature infants led to a reduction in myocardial left ventricular peak systolic apical circumferential strain at age 23 to 28 (Lewandowski *et al.*, 2011), suggesting impaired myocardial function in young adults who were born prematurely. The infants in this randomized controlled trial were born at 28 weeks gestational age (~70% developed) and the fetuses used for the imaging studies in the present study were ~85% developed (125 dGA, term ≈147 dGA), so presumably the ability of prematurely born babies to handle exogenous lipids is on par or less able than those cardiomyocytes used in our present study. Exposing immature cardiomyocytes to lipids may lead to a permanent dysregulation of β-oxidation that in the short term is revealed as abnormally large lipid droplets but in the longer term may impair contractile function in the adult heart.

Larger lipid droplets in fetal cardiomyocytes suggest a propensity to storage of exogenous lipids rather than metabolic use, as supported by the low fetal gene expression of LCAD and VLCAD, the first step of ß-oxidation. It is possible that fatty acyl CoA substrate would then accumulate in the mitochondrial matrix rather than effectively cycle through ß-oxidation. Low expression of LCAD and VCAD might account for the differences in fatty acid oxidation in fetuses infused with palmitate compared to newborn lambs (Bartelds *et al.*, 2000). The ability for uptake and oxidation in palmitate infused fetuses suggests that components of the transport pathways are mature enough to allow entry of fatty acids to the mitochondrial matrix. Furthermore, developmental upregulation of CPT1 as well as downstream mitochondrial ß-oxidation enzymes HADH and ACAT1 and TCA cycle enzyme IDH

suggest there is at least some capacity for the fetal myocardium to oxidize exogenously supplied fatty acids *in utero*.

It would be advantageous for clinicians to be cognizant of the metabolic state and needs of the myocardium in preterm infants to ensure that substrate support is appropriate. Lipid exposure *in utero* has been shown to cause metabolic stress and impaired cardiac function along with increased lipid peroxidation in rat offspring (Mdaki *et al.*, 2016a). This increased lipid peroxidation, indicative of increased oxidative stress could lead to underlying lipid-induced cardiotoxicity. The near term ovine fetal heart does appear to have some antioxidative mechanisms in place (von Bergen *et al.*, 2009), but the degree to which they are able to mitigate higher levels of oxidative stress from premature exposure to lipid remains to be determined. While several studies have investigated the impact of hypoxia on antioxidant responses in fetal sheep (Giussani *et al.*, 2012; Giussani *et al.*, 2014), the role of lipid exposure on the cardiac antioxidant response has not been studied. Future studies should measure antioxidant activity and lipid peroxidation in lipid infused fetuses or a model of preterm birth to determine the viability of this hypothesis.

For most genes in this study, mRNA and protein concentrations were in concordance. However, gene expression for CPT1 (non-specific to isoform a or b) increased with age while CPT1a protein expression dropped off during fetal life and CPT1b, the adult/muscle isoform was notably similar between ages. Bartelds *et al.* previously reported CPT1b (CPT1-M) protein expression during development in sheep

myocardium and concluded that it was constitutively expressed over the latter half of gestation (Bartelds *et al.*, 2004). CPT1a and b activities were not measured in this study, so we cannot conclude that their constitutive protein expression levels were indicative of constitutive function. CPT1a has been shown to be upregulated in rats by epigenetic mechanisms including increased methylation of histone protein H3K4 and reduced DNA methylation in the promoter region under conditions of a high fat diet (Moody *et al.*, 2019), which would similarly be encountered with suckling, this could explain the higher CPT1 gene expression postnatally. Additionally, LCAD gene expression did not match the appearance of protein. These discrepancies could be due to differential regulation at the translational level. It is also possible that LCAD is not the primary acyl-coA dehydrogenase involved in energy production of the sheep heart. In humans, VLCAD is the primary acyl-CoA dehydrogenase involved in fatty acid oxidation and LCAD is thought to be of little consequence for energy production. More recently, ACAD9 has been shown to play a role in fatty acid oxidation in various tissues (Schiff et al., 2015). Sheep may rely primarily on VLCAD for cardiac fatty acid oxidation similar to humans (Yamaguchi *et al.*, 1993) while mouse models have suggested both enzymes are active in cardiomyocytes (Yamaguchi *et al.*, 1993; Kurtz *et al.*, 1998; Cox *et al.*, 2009).

One of the most important adaptations to adult heart failure is a reversion to a fetal metabolic phenotype including CPT1 isoform switching and a shift towards augmented glucose metabolism (Rajabi et al., 2007). At the same time, fatty acid oxidation enzyme gene expression, including LCAD expression is downregulated in

the failing heart (Sack et al., 1996). However, whether other components critical to this metabolic pathway are affected in heart failure remains to be determined. This study helps identify other candidate genes that may be responsible for metabolic changes in adult heart failure.

Conclusion

In conclusion, critical components of the lipid metabolism pathway including a sarcolemmal fatty acid transporter (CD36), cytosolic fatty acid activation enzyme (ACSL1), mitochondrial transporter (CPT1), ß-oxidation enzymes (HADH and ACAT1), TCA cycle enzyme (IDH) and esterification enzyme (GPAT) are upregulated prior to birth. These transporters and enzymes presumably enable the fetal heart to oxidize and esterify fatty acids to some degree in preparation for postnatal life and to be functional by birth. Interestingly however, not all genes of interest showed this prenatal maturation, though further studies are required to elucidate whether these will mature in the immediate pre-partum period or in response to the initiation of enteral feeding and high circulating lipid levels. These findings increase our understanding of prenatal metabolic abilities, an important consideration in devising lipid nutrition strategies in preterm infants. Fetal cardiomyocytes also store exogenous long chain fatty acids in larger droplets relative to newborn, suggesting a different strategy for fatty acid storage and utilization in fetal life compared to postnatal life. One possibility is that the fetal heart is less able to properly esterify and package fatty acids, resulting in a haphazard storage mechanism in the form of larger lipid droplets. This study has demonstrated the ontological pattern for a group of genes that appear

to be reversed under pathological conditions. These observations offer novel insights into the metabolic maturation of fatty acid metabolism in cardiomyocytes in the perinatal period.

Chapter 3. Intrauterine Growth Restriction Elevates Circulating Acylcarnitines and Suppresses Fatty-Acid Metabolism Genes in the Fetal Sheep Heart

Introduction

Placental Insufficiency suppresses fetal growth, causing intrauterine growth restriction (IUGR) and is the second most common cause of perinatal mortality (Nardozza *et al.*, 2017). In addition to being a common and complex perinatal problem, IUGR predisposes the fetus to a myriad of adult-onset diseases including cardiovascular and metabolic disease (Hoffman *et al.*, 2017).

Various animal models have been used to investigate molecular responses to IUGR in the fetus. Sheep models are particularly advantageous as sheep are born precocial and have a similar organ development timeline (relative to gestational age) to humans. Several sheep models of IUGR reveal physiological insights regarding the fetal cardiac response to placental insufficiency. The models consistently report decreased cell cycle activity and binucleation, indicators of cell cycle activity and maturation (Bubb *et al.*, 2007; Louey *et al.*, 2007; Morrison *et al.*, 2007; Jonker *et al.*, 2018). The fetal heart is relatively protected from the detrimental effects of chronic hypoxia

because of its powerful vasodilatory capacity leading to a redistribution of cardiac output to the heart (Block *et al.*, 1990; Gagnon *et al.*, 1996) and preservation of blood flow to the myocardium (Kiserud *et al.*, 2000). Despite this preservation of blood supply to the heart, the impairment of cardiomyocyte proliferation and maturation reveal that the heart is not completely spared from the effects of fetal hypoxemia and restricted growth.

The mammalian fetal heart utilizes primarily lactate and glucose (Fisher *et al.*, 1980; Werner & Sicard, 1987; Lopaschuk & Jaswal, 2010) as fuels for energy production and the newborn heart utilizes primarily fatty acids (Werner *et al.*, 1989; Bartelds *et al.*, 2000; Bartelds *et al.*, 2004). This dramatic switch is made around the time of birth. Presumably, the expression of the genes that code for the proteins required for fatty acid metabolism should be elevated in the fetal myocardium in preparation for augmented postnatal fatty acid oxidation when fat-laden milk becomes available. However, the temporal regulation of the genes required for the switch that regulates fatty acid metabolism in normal development is poorly understood. Even less is known about whether suboptimal intrauterine conditions like those encountered in IUGR affect metabolic maturation in the heart.

Few studies have investigated oxidative metabolism in the fetal heart in response to IUGR. In one model of IUGR, pregnant ewes exposed to elevated ambient temperatures develop placental insufficiency and impaired oxidative metabolism in fetal skeletal muscle and liver (Brown *et al.*, 2015). However, since blood flow to fetal

skeletal muscle and liver is known to be compromised in IUGR compared to the heart, it is uncertain whether this metabolic alteration occurs in myocardium. (Barry *et al.*, 2016) found that the myocardium in fetuses compromised by IUGR is more sensitive to insulin, suggesting that placental insufficiency can modify metabolic processes in the fetal heart. Hypoxemia is a hallmark of IUGR and has been shown to inhibit fatty acid ß-oxidation and induce lipid droplet accumulation in hepatocellular carcinoma cells (Mylonis *et al.*, 2019). However, the metabolic responses of cardiomyocytes to conditions of chronic hypoxemia have been understudied.

The aim of this study was to determine the effect of placental insufficiency on fatty acid metabolism in the near term fetal heart. We measured circulating acylcarnitines (a marker for impaired fatty acid oxidation), lipid droplet formation and storage using a fluorescent tagged fatty acid molecule, BODIPY-C12, and the expression levels of genes and proteins required for the switch from glycolysis to β-oxidation in the myocardium of IUGR fetuses. We hypothesized that circulating acylcarnitines would be elevated, lipid droplets would be larger and gene and protein expression of fatty acid metabolic machinery would be suppressed in IUGR myocardium.

Methods

Animals

Twenty time-bred ewes of mixed Western breeds were purchased from a commercial supplier and brought to the laboratory 4-7 days before surgery for acclimatization. All protocols were approved by the Institutional Animal Care and Use Committee. A total

of 38 fetuses were studied, included were 34 twins (from 17 pregnancies), 2 triplets from the same pregnancy and 2 singletons. The study groups included a balance of males and females, see

Table 3-1 for details.

Table 3-1 Experimental workflow, sample size and sex distribution.

Experimental Workflow:

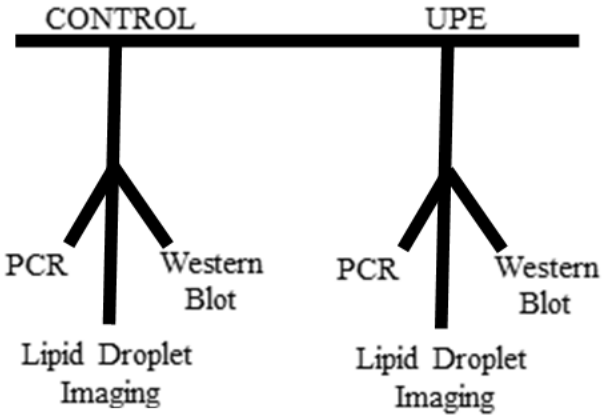

Sample size and sex distribution:

	Plasma Acylcarnitines	Lipid Droplet Imaging	qPCR	Western blotting
Age	126 ± 1 day	125 ± 1 day	126 ± 1 day	126 ± 1 day
Control	n=12 (7 male, 5 female)	n=12 (8 male, 4 female)	n=6 (3 male, 3 female)	n=11 (6 male, 5 female)
IUGR	n=12 (5 male, 7 female)	n=12 (6 male, 6 female)	n=6 (3 male, 3 female)	n=12 (6 male, 6 female)

Surgery

Ewes were fasted for 24 h prior to surgery, with water ad libitum. Induction of anesthesia was with intravenous diazepam (10 mg) and ketamine (400 mg) followed by immediate intubation. Anesthesia was maintained with 1-2% isoflurane in a 70:30 mixture of oxygen: nitrous oxide during mechanical ventilation. Sterile surgery was performed at 110 ± 2d GA days gestational age (d GA, term ≈ 147d GA), as previously described (Louey *et al.,* 2007). In brief, a midline incision through the ewe's linea alba to access the uterus and the fetal rump exteriorized though a uterine incision. A catheter (1.8 mm o.d. polyvinyl; Scientific Commodities, V-8, Lake Havasu City, AZ, USA) was inserted 7 cm into the fetal femoral artery for blood pressure measurements, sampling and microsphere injections. Catheter tip position was 1-2 cm below the renal arteries and above the umbilical arteries, confirmed at autopsy. Prior to returning the fetus to the uterus, a catheter (1.8 mm o.d.) was sutured to the rump for delivery of antibiotics and measurement of amniotic pressure. The uterus was sutured securely to prevent fluid loss. Following instrumentation of the first fetus, its twin was exposed through a second incision in the uterus and catheterized in the aforementioned manner. Penicillin G (1,000,000 units per fetus; Bristol-Myers Squibb, Princeton, NJ, USA) and ciprofloxacin (2mg/ fetus) was injected into the amniotic space of each fetus through their respective amniotic catheters. All catheters were then flushed with heparinized saline. The exteriorized ends of the catheters were securely tied off, exteriorized through a flank incision in the ewe and finally secured to a pouch sutured to the ewe's flank. The midline was closed in anatomic layers. Following surgery, isoflurane administration was stopped and the endotracheal tube removed once the

ewe had autonomous respiratory drive. Ewes were given 0.3 mg Buprenex (bupreneorphine HCl), and 0.05 mg/kg sustained release buprenorphine (ZooPharm, CO) subcutaneously at the conclusion of surgery, returned to a clean pen and monitored. A minimum of 3 days recovery period was given to ewes prior to commencing experiments.

Experimental Protocol

Two groups of fetuses were studied: one group was subjected to 10 days of umbilicoplacental embolization (UPE; this is the IUGR group) and the other was their age-matched controls. For fetuses in the IUGR groups, 20-50 μm (mean ± S.D. diameter, 35 ± 9 μm) non-radioactive, non-soluble microspheres (Sephadex Superfine G-25; Amersham, Sweden; 1% w/v suspended in heparinized saline with 0.02% Tween 80) were injected into the fetal femoral artery catheter to reduce P_{aO2} by approximately 8 mmHg from baseline values on study day 1 as previously reported (Cock & Harding, 1997; Louey *et al.*, 2000; Louey *et al.*, 2007).

Studies for all fetuses commenced at 114-117d GA and were terminated at 124-127d GA. Included in the study were 17 ewes carrying twins; both twins were included, 1 ewe carrying triplets; two fetuses were included, and 2 singletons. Fetuses were randomly assigned to each experimental group; 1 control and 1 experimental fetus per ewe if the ewe was carrying multiple fetuses. During the experimental time period, ewes were kept in individual stanchions with water and food ad libitum. Arterial blood

samples were taken from all fetuses to assess pH, glucose, blood gas status using a blood gas analyzer (Radiometer ABL825, OH).

Plasma acylcarnitine assays

Arterial blood samples were collected on the final day of the study (following 10 days of UPE) at 126 ± 1 d GA from a subset of fetuses (n=12 controls, n=12 IUGR). Samples were heparinized and centrifuged for 10 minutes, 2500g at 4°C and plasma stored at -20°C and analyzed for acylcarnitines by electrospray tandem mass spectrometry (Applied Biosystems/MDS SCIEX API 3000) at the Biochemical Genetics Laboratory, Mayo Clinic (Smith & Matern, 2010). Samples were compared to known internal standards and were identified by characteristic mass to charge ratios.

Tissue Collection

Ewes were euthanized with an intravenous overdose of sodium phenobarbital (SomnaSol, 80mg/kg, Covetrus, OH, USA). As a result, the fetuses were deeply anesthetized, exteriorized and given 10 000 units of heparin though the umbilical vein followed by 10 mL of saturated KCl to arrest the heart in diastole. The fetus was then removed from the uterus and weighed. The heart was excised, trimmed in a standardized manner and weighed. Brain and liver weights were documented.

14 fetal hearts (7 control, 7 experimental) were separated into left ventricle, right ventricle and septum, and each wall was snap frozen in liquid nitrogen; only left ventricular tissue was used in this study. Of these hearts, 12 were used for qPCR (6

control, 6 experimental). Western blotting was conducted on all 14 (7 control, 7 experimental) animals plus an additional 9 animals (4 control, 5 experimental) that each had a $5mm^3$ section of mid-wall left ventricle (LV) flash frozen before dissociation to isolate cardiomyocytes for live imaging studies; the cut edges of the left ventricle were sealed with SuperGlue and cardiomyocyte isolation was not compromised.

Cardiomyocyte Isolation

24 hearts total were dissociated for imaging (12 control, 12 IUGR). Of these, 9 hearts (4 control, 5 experimental) were also used for western blotting (see above). The aorta was perfused in a retrograde fashion using established methods in the laboratory (Louey *et al.*, 2007). In brief, the heart was perfused with a warmed (39°C) and 95% oxygen/5% CO_2 gassed solutions in the following order: 1) Ca^{2+}-free Tyrodes buffer (140mM NaCl, 5mM KCl, 1mM $MgCl_2$ • 6H2O, 10mM glucose, 10mM HEPES; pH 7.35 with NaOH) for ~5-10 min, until the tissue was washed-out, 2) Tyrodes buffer with enzymes (160 U/mL Type II Collagenase (Worthington), 0.78 U/mL Type XIV protease) (Sigma) until the heart was sufficiently digested (~5-10 min), 3) KB solution (74 mM glutamic acid, 30mM KCl, 30 mM KH_2PO_4, 20mM taurine, 3mM $MgSO_4$, 0.5mM EGTA, 10mM HEPES, 10mM glucose; pH 7.37 with KOH). Following the KB perfusate rinse, the left ventricular free wall was dissected and gently agitated in a conical containing KB solution to release cardiomyocytes. The cell slurry was left to rest at room temperature for 30-45 minutes before imaging. A 140µL aliquot of left ventricular cells (~250k cell/mL) were used for live imaging.

BODIPY-C_{12} Fluorescent Fatty Acid Live Imaging

A protocol, established in our lab for studying placental explants (Kolahi *et al.*, 2016), was adapted for fetal cardiomyocytes to track the incorporation of an exogenous long chain saturated fatty acid into lipid droplets. BODIPY FL-C_{12} (Molecular Probes, cat#D3822) is a 12-carbon chain length saturated fatty acid linked to the fluorophore BODIPY (4,4-difluoro-3a,4a-diaza-s-indacene) (Stahl *et al.*, 1999; Wang *et al.*, 2010a; Kassan *et al.*, 2013; Rambold *et al.*, 2015; Kolahi *et al.*, 2016).

The BODIPY-C_{12} conjugate biologically resembles an 18-carbon saturated fatty acid and permits tracking of exogenous supplied fatty acid via the BODIPY fluorophore which is an intensely fluorescent, intrinsically lipophilic molecule. 10 µM solutions of BODIPY-FL C_{12} were prepared by diluting a 2.5mM stock solution in DMSO 1:250 in fetal or newborn KB solution (KB supplemented with 2mM glutamine, 200 µM sodium pyruvate, 2 or 1mM lactate (fetal vs. newborn respectively), 1 or 5mM glucose (fetal vs. newborn respectively)) supplemented with 0.1% fatty acid free bovine serum albumin and incubated for 30 minutes (37°C, in the dark) to allow fatty acid: BSA conjugation.

Cells were incubated in fetal KB in 8 well µ-slides (Idibi, cat#80821) with 2µM of BODIPY-C_{12} for 60 minutes (39°C) and imaged using the 63x oil lens on the Zeiss 880 LSM with Airyscan. Z-stack images were collected after 60 minutes. BODIPY

was imaged with 488 laser (intensity 0.6, gain 825, digital gain 1.0). 90-130 slices, 0.2 µm thick were acquired per frame (18-26 µm thickness, 3-18 frames per animal).

Image Analysis

Z-stacks were processed (Airyscan) and maximum intensity projections performed in ZEN Black Software (Zeiss). Fiji software was used to analyze all images obtained. Images were enhanced using Enhance Local Contrast (CLAHE: blocksize=9, histogram=256, maximum=4), despeckled, and background subtracted (rolling=5). Lipid droplet particles were analyzed by filtering for the following parameters: circularity (0.8-1), size (0.0314 <minimal detectable size for LSM880> to 3<maximum intracardiomyocyte lipid droplet size (Wang *et al.*, 2013)>, AutoThreshold (Intermodes dark) and images were converted to a mask for lipid droplets and entire cells.

We measured average individual lipid droplet size (lipid droplet area, μm^2), the area occupied by lipid droplets relative to total cell area (Lipid droplet area/ total cell area), and number of lipid droplets relative to cell area (lipid droplet number / total cell area). For each animal, 13-56 cells were measured in 4-12 frames. Masks were manually verified to ensure the parameters did not accidentally exclude or include an unintentional measurement from a non-viable cell.

RNA isolation and gene expression

RNA was isolated as previously described (Lindgren *et al.*, 2019) from 40-50µg of left ventricular myocardium using Trizol, a steel bead and TissueLyser LT (Qiagen, Germantown, MD, USA), 50 oscillations/sec for 3 minutes. Isolates were further purified using RNeasy Mini Columns (Qiagen). Reverse transcription on 1µg RNA was conducted to synthesize cDNA using the High-Capacity cDNA Reverse Transcription Kit (ABI) and diluted 1:20 prior to PCR. Quantitative PCR was carried out using SYBR Green in the Stratagene Mx3005. Primers are listed in Table 3-2. Gene expression was analyzed using the ΔC_t method. Genes of interest were normalized to housekeeping gene ribosomal protein L37a (RPL37a), which was not altered by umbilicoplacental embolization.

Table 3-2 Primer sequences.

	Sequence 5' – 3'		
Gene ID	Forward	Reverse	Accession #
RPL37a housekeeper	ACCAAGAAGGTCGGAATCGT	GGCACCACCAGCTACTGTTT	XM_027965159.1
CD36	CTGGTGGAAATGGTCTTGCT	ATGTGCTGCTGCTTATGGGT	XM_027968558.1
FATP6	TTGGAAATGGAGCACGCAGTGA	CTCCCGACTGATCCAATTTTCCCA	KP735933.1
ACSL1	GAGCAGAGGTTCTCAGTGAAGCAA	CGGCTGTCCATCCAGGATTCAATA	XM_015104563.2
ACSL3	GACAGATGCCTTCAAGCTGAAACG	GGAATGGACTCTGCCTCACAGTTT	XM_034955270.1
CPT1	GGATGTTTGAGATGCACGGC	GCCAGCGTCTCCATTCGATA	XM_027965744.1
IDH	CTGTGTTTGAGACGGCTACAAGGA	CGTAGCTGTGGGATTGGCAATGTT	XM_027963525.1
LCAD	TGAAAGCCGCATTGCCATTGAG	ACTTGGATGGCCCGGTCAATAA	XM_004003336.4
VLCAD	AAGATCCCTGAGTGAAGGCCA	TAGAACCAGGATGGGCAGAAA	XM_004012636.3
HADH	AGAAAACCCCAAGGGTGCTGAT	GCCTCTTGAACAGCTCGTTCTT	XM_004009637.4
ACAT1	CTGGGTGCAGGCTTACCTATTTCT	CATAGGGGACATTGGACATGCTCT	XM_027979167.1
GPAT	GAAGTGGCTGGTGAGTTAAACCCT	CAGTCTGATCATTGCCGGTGAAAC	XM_012102930.2
PAP	AGAATGAAGGGAGACTGGGCAAGA	GCAACCAGAGCTCCTTGAATGAGT	XM_004016984.4
DGAT	AGACACTTCTACAAGCCCATGCTC	AGTGCACTGACCTCATGGAAGA	XM_027972747.1
BSCL2	CTGCCTCCCTGACTCTGAAGT	TGCGGAGGCCAGAATGATG	XM_012102049.3
PDK4	CCTGTGATGGATAATTCCCG	TTGGTTCCTTGCTTGGGATA	NM_002612.4

Western Blotting

We did not have working antibodies for all proteins in sheep. Thus, for several enzymes we have mRNA levels but not protein levels. Protein was isolated as

previously described (Lindgren *et al.*, 2019). In brief, 20-30µg of left ventricular myocardium using RIPA lysis buffer (MilliporeSigma) with a Complete Mini Protease 227 Inhibitor tablet (MilliporeSigma) and phosphatase inhibitor cocktails I and II (MilliporeSigma). Tissue was added to chilled lysis buffer in 2mL tubes containing a stainless-steel bead and lysed (4 minutes, 50Hz TissueLyser LT). Protein was quantified by a standard bicinchoninic acid assay as routinely performed in our lab (Jonker *et al.*, 2015) and diluted to a uniform concentration across all groups (2µg/µL). Gels were poured (Stacking: 4% acrylamide, Resolving: 12% acrylamide) using SureCast Stacking Buffer and Resolving Buffer along with SureCast system (Invitrogen). 15µg protein was loaded with 6x dye (10% betamercaptoethanol) and separated by SDS-PAGE (90 minutes, 100mV, BioRad system) with running buffer (24.8 mM Tris, 191.8 mM glycine, 3.5 mM SDS). Protein was transferred to PVDF membranes (MilliporeSigma) with transfer buffer (24.8 mM Tris, 191.8 mM glycine), and blocked (5% milk in Tris-buffered saline + 0.01% Tween 20 (TBST), 1 hour, room temperature). Antibody incubations took place in the following order: 1) primary antibody (4°C, overnight), 2) TBST rinses (3 x 10 minutes) and 3) secondary antibody (room temperature, 1 hour), all on a rocker. Dilutions and antibodies can be found in Table 3-3.

SuperSignal West Dura chemiluminscence substrate was used to visualize membranes (ThermoFisher Scientific). GBOX (SynGene) and GeneSys software (version 4.3.7.0) were used to image and analyze the blots. Band intensities were expressed as area under the curve, normalized against α-tubulin, GAPDH or total protein (as determined

by Ponceau S staining immediately after protein transfer, prior to primary antibody incubation) which was not affected by IUGR.

Statistics

Unpaired student's t-tests with post hoc Bonferroni correction were used to test for differences between end P_{aO2}, glucose, body weight, heart: body weight, brain: liver, acylcarnitine levels, lipid droplet sizes, gene and protein levels. All generated datasets and analysis for the present study are available from the corresponding author upon request. All data were analyzed using GraphPad Prism 6 and are presented as mean ± SD unless noted otherwise. P-values < 0.05 were considered statistically significant, denoted with asterisk *. A paired statistical test was not appropriate for this study since not all controls and experimental animasl came from the same mother (there were singleton pregnancies included).

Table 3-3 Antibodies used.

Protein	Dilution	Catalog #	Vendor	RRID or reference
CD36	1:1000	133625	abcam	RRID:AB_2716564
ACSL1	1:1000	177958	abcam	(Li *et al.*, 2020)
CPT1a	1:500	12252	Cell Signaling	RRID:AB_2797857
CPT1b	1:1000	22170	ProteinTech	(Abudurexiti *et al.*, 2020)
VDAC	1:1000	12454	Cell Signaling	RRID:AB_2797922
ACADL	1:1000	17526	ProteinTech	(Huang *et al.*, 2014)
CS	1:1000	14309	Cell Signaling	RRID:AB_2665545
OXPHOS cocktail containing: NDUFB8, SDHB, UQCRC2, MTCO1, ATP5A	1:500	110413	abcam	RRID:AB_2629281
GAPDH (housekeeper protein)	1:5000	47339	Novus Biologicals	RRID:AB_10010294
α-tubulin (housekeeper protein)	1:5000	2125	Cell Signaling	RRID:AB_2619646
anti-Rabbit HRP (secondary antibody)	1:5000	7074	Cell Signaling	RRID:AB_2099233
anti-Mouse HRP (secondary antibody)	1:5000	7076	Cell Signaling	RRID:AB_330924

Results

Arterial Blood

IUGR fetuses were hypoxemic (10 day average: IUGR 13.3 ± 0.7 mmHg P_{aO2} vs control 20.8 ± 1.9 mmHg, $p < 0.05$) and hypoglycemic (10 day average: IUGR 0.9 ± 0.1mM vs control 1.1 ± 0.2 mM glucose, $p < 0.05$) during UPE (Figure 3-1A,B). This led to fetuses that were 28% lighter than controls (Figure 3-1C), and although they were asymmetrically growth restricted (Figure 3-1E), heart weight/body weight was not different between groups (Figure 3-1D).

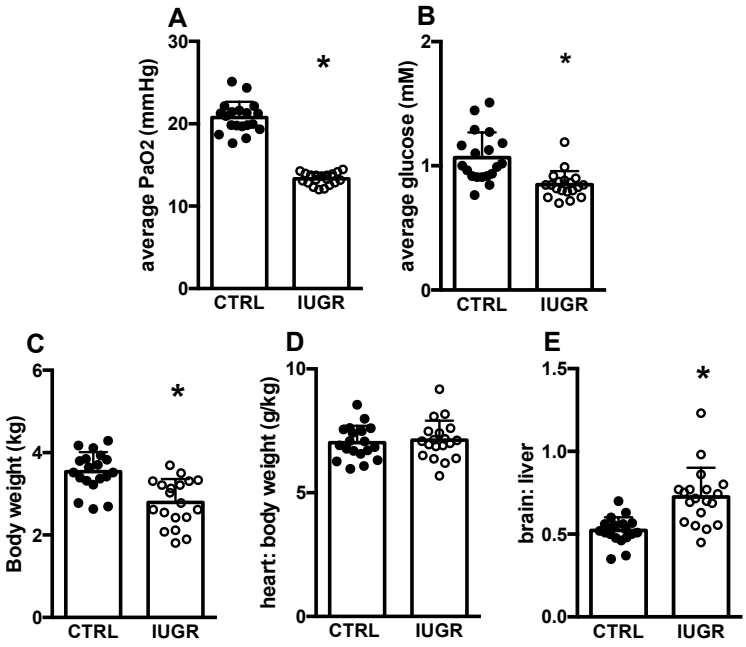

Figure 3-1 Oxygen, glucose, and growth in IUGR fetuses.

Umbilicoplacental embolization induces (A) hypoxemia, (B) hypoglycemia, (C) growth restriction (low body weight), (D) no change in heart to body weight ratio, and (E) asymmetric growth (increased brain to liver ratio). Average P_{aO2} and glucose reflect the 10 day average of each. n=19 control, n=19 IUGR. Mean ± SD, * $p < 0.05$.

Circulating plasma acylcarnitines are higher in intrauterine growth restricted fetuses

Elevated plasma acylcarnitines are indicative of incomplete of partial fatty acid oxidation. In these studies, free carnitine levels were not different between groups (Figure 3-2A). Long chain fatty acid-C14 and -C18 plasma acylcarnitines were elevated in growth restricted fetuses compared to control (Figure 3-2B, D). C16 (palmitate)-acylcarnitine was not different between groups (Figure 3-2C).

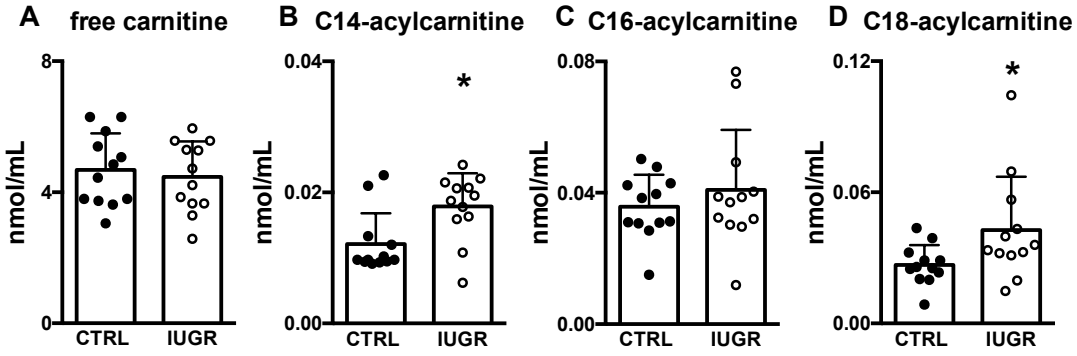

Figure 3-2 Acylcarnitines in IUGR fetuses.

IUGR fetuses have (A) no differences in free carnitine, higher circulating long-chain (B) C14 and (D) C18 fatty-acylcarnitines and no differences in (E) C16 fatty-acylcarnitines. n=12 control, n=12 IUGR. Mean ± SD, * $p < 0.05$

BODIPY-C12 Long Chain Fatty Acid Uptake and Lipid Droplet Formation

Lipid droplet size (Figure 3-3A), area occupied by lipid droplets relative to cell area (Figure 3-3B), and number of lipid droplets (Figure 3-3C) were not different is IUGR cardiomyocytes compared to control. A representative image of BODIPY-C12 lipid droplet formation in control and IUGR cardiomyocytes is shown in Figure 3-3D.

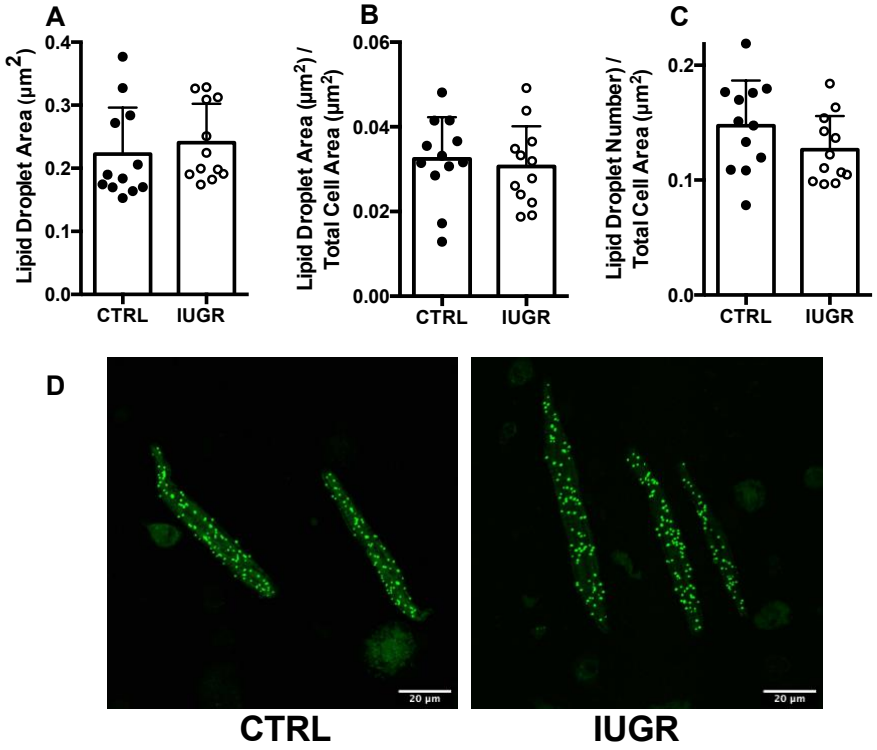

Figure 3-3 Lipid droplets in IUGR fetuses.

IUGR and control cardiomyocytes do not differ in their formation of (A) lipid droplet size, (B) lipid droplet size relative to cell size or (C) number of lipid droplets relative to cell size. n=12 control, n=12 IUGR. Mean ± SD, * $p < 0.05$.

Sarcolemmal Fatty Acid Transporter Expression

Sarcolemmal lipid transporter genes CD36 and FATP6 both had lower mRNA levels in IUGR myocardium compared to controls, with FATP6 expression being especially suppressed (Figure 3-4A, B). CD36 protein levels in IUGR hearts were not different from controls (Figure 3-4C).

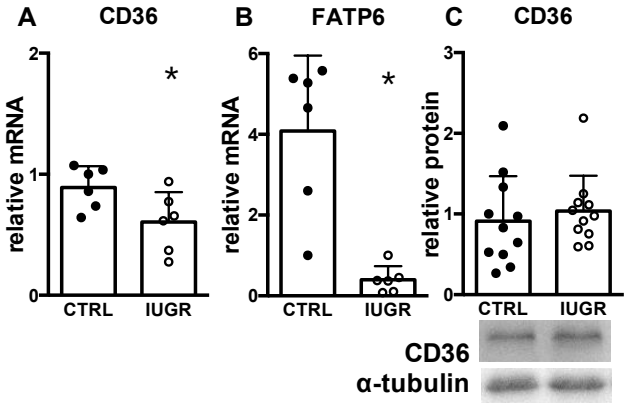

Figure 3-4 Gene and protein expression of sarcolemmal fatty acid transporters in growth restricted LV myocardium.

mRNA: n=6 control, n=6 IUGR, protein: n=11 control, n=11 IUGR. Gene expression relative to RPL37a and protein expression relative to α-tubulin. Mean ± SD, * $p < 0.05$.

Fatty Acid Acylation Enzyme Expression

Acyl-CoA synthetase (ACSL) is responsible for the acylation and activation of fatty acids upon entry to the cell. The ACSL1 isoform gene (Figure 3-5A) and protein

(Figure 3-5C) levels were not different between control and IUGR myocardium, while ACSL3 mRNA was suppressed in IUGR myocardium (Figure 3-5B).

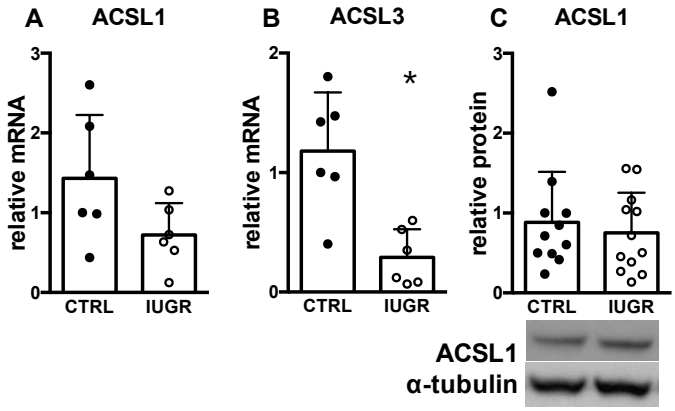

Figure 3-5 Gene and protein expression of fatty acid activation enzymes in growth restricted myocardium.

mRNA: n=6 control, n=6 IUGR, protein: n=11 control, n=12 IUGR. Gene expression relative to RPL37a and protein expression relative to α-tubulin. Mean ± SD, * $p < 0.05$.

Mitochondrial Transporter Expression

The expression of the CPT1 gene, the rate limiting protein in mitochondrial utilization of fatty acids was significantly lower in growth restricted hearts (Figure 3-6A). The myocardium expresses both CPT1a (fetal isoform) and CPT1b (adult isoform) and the protein levels for both were not different between groups (Figure 3-6B, C). Voltage dependent anion channel protein (VDAC), which transports other mitochondrial metabolites was not different between IUGR and control myocardium (Figure 3-6D).

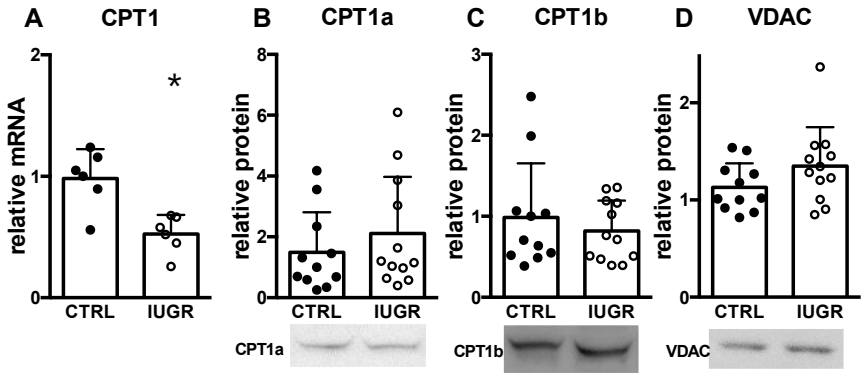

Figure 3-6 Gene and protein expression of mitochondrial transporters in growth restricted myocardium.

mRNA: n=6 control, n=6 IUGR, protein: n=11 control, n=12 IUGR. Gene expression relative to RPL37a and protein expression relative to total protein. Mean ± SD, * $p < 0.05$.

ß-Oxidation Enzyme Expression

mRNA levels of mitochondrial ß-oxidation enzymes LCAD and VLCAD were lower in myocardium from IUGR fetuses relative to controls (Figure 3-7A and B). Short/medium chain oxidation enzyme HADH was lower in IUGR myocardium (Figure 3-7C) as well as ketone metabolism enzyme ACAT1 (Figure 3-7D) Protein levels of LCAD, the only enzyme in this group for which we had a working antibody, were not different between the groups (Figure 3-7E).

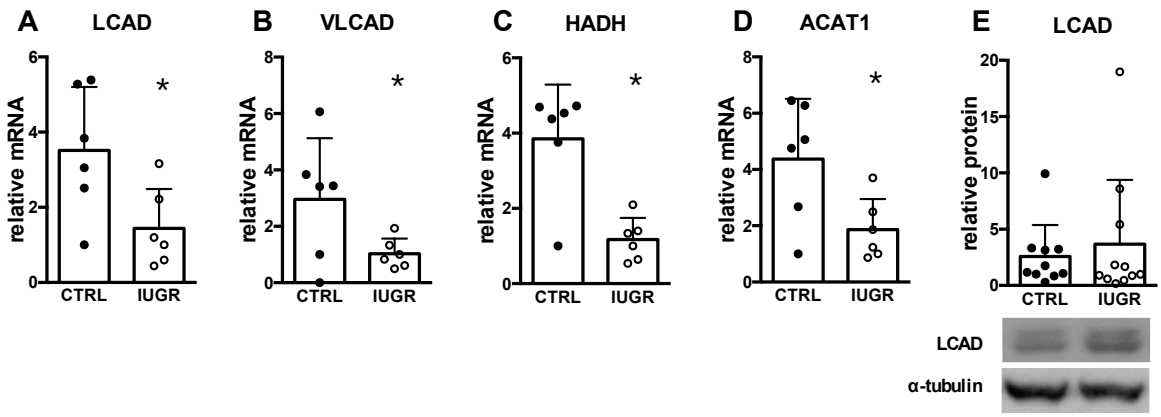

Figure 3-7 Gene and protein expression of mitochondrial ß-oxidation enzymes in growth restricted myocardium.

mRNA: n=6 control, n=6 IUGR, protein: n=10 control, n=11 IUGR. Gene expression relative to RPL37a and protein expression relative to α-tubulin. Mean ± SD, * $p < 0.05$.

Tricarboxylic Acid (TCA) Cycle Enzyme Expression

Myocardial mRNA expression of Isocitrate dehydrogenase (IDH), a TCA cycle enzyme that catalyzes the production of the first reducing equivalent (NADH) was suppressed in IUGR myocardium (Figure 3-8A). The first step of the TCA cycle which joins oxaloacetate and acetyl-CoA to form citrate is performed by citrate synthase; protein levels for citrate synthase were not different between control and IUGR (Figure 3-8B).

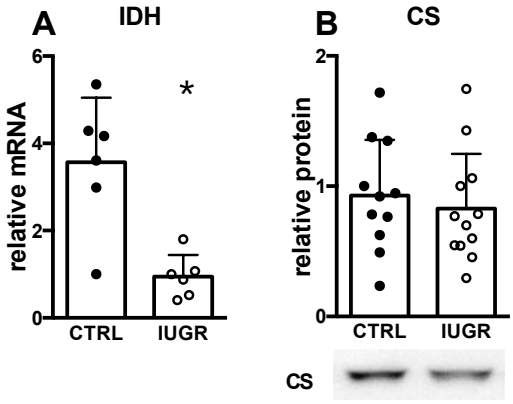

Figure 3-8 Gene and protein expression of TCA cycle enzymes in growth restricted myocardium.

mRNA: n=6 control, n=6 IUGR, protein: n=11 control, n=12 IUGR. Gene expression relative to RPL37a and protein expression relative to total protein. Mean ± SD, * $p < 0.05$.

Electron Transport Chain Subunit Expression

The electron transport chain is composed of 5 complexes, each with several subunits. Protein expression for the 5 subunits (NDUFB8 (CI), SDHB (CII), UQCRC2 (CIII), MTCO1 (CIV) nor ATP5A (CV)) were not different between groups (Figure 3-9). Figure 3-9F shows a representative blot for all complexes included in the antibody cocktail. mRNA levels were not measured.

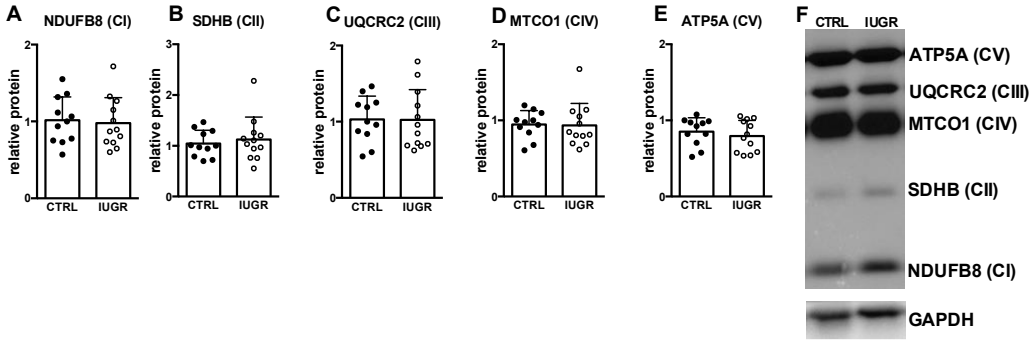

Figure 3-9 Protein expression of electron transport chain subunits in growth restricted myocardium.

n=11 control, n=12 IUGR. Expression relative to GAPDH. Mean ± SD, * $p < 0.05$.

Fatty Acid Esterification Enzyme Expression

Glycerol phosphate acyltransferase (GPAT) catalyzes the first step of fatty-acyl CoA esterification by adding fatty-acyl CoA to glycerol-3-phosphate. Phosphatidic acid phosphatase (PAP) is responsible for converting phosphatidic acid to diacylglycerol (DAG), and diacylglycerol acyltransferase (DGAT) converts DAG into triacylglycerol (TAG) by adding a third fatty-acyl group to the glycerol backbone. BSCL2 (Seipin) is associated with lipid droplet morphogenesis and may aid in anchoring lipid droplets to the endoplasmic reticulum. Gene expression for all except GPAT is suppressed in IUGR myocardium (Figure 3-10).

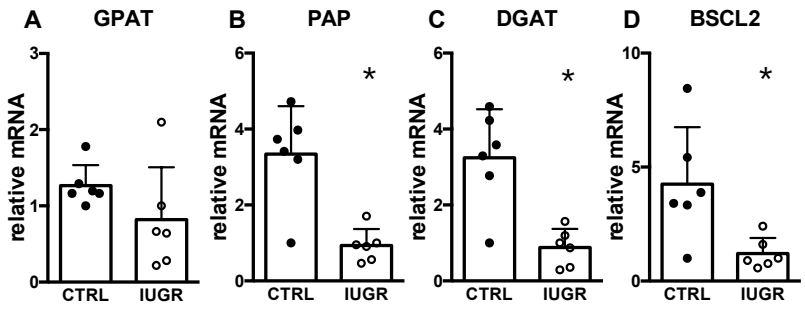

Figure 3-10 Gene expression of fatty acid esterification enzymes in growth restricted myocardium.

n=6 control, n=6 IUGR. Expression relative to RPL37a. Mean ± SD, * $p < 0.05$.

Glycolysis and ß-Oxidation Regulator Expression

Since our gene expression data suggest a suppression of fatty acid transport and oxidation, we sought to determine whether this might lead to increased activity of the glycolytic pathway. Pyruvate dehydrogenase kinase (PDK4) is a well-established gatekeeper of the carbon flux from glycolysis to the TCA cycle. It accomplishes this through phosphorylation and inhibition of pyruvate dehydrogenase, the final step of glycolysis. Amounts of PDK4 gene were not different between IUGR and control (Figure 3-11).

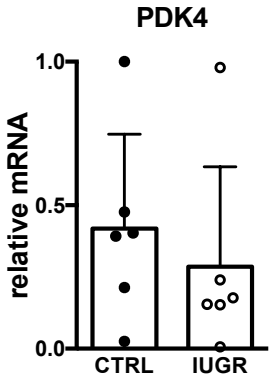

Figure 3-11 Gene expression of glycolysis/ oxidation regulatory enzyme in growth restricted myocardium.

n=6 control, n=6 IUGR. Expression relative to RPL37a. Mean ± SD, * $p < 0.05$.

Discussion

We tested the hypothesis that the metabolic systems responsible for fatty acid handling would be suppressed in IUGR fetal hearts compared to control. We hypothesized that circulating acylcarnitines would be elevated in fetal plasma and that intracellular droplets from exogenous lipids would be larger in cardiomyocytes from growth-restricted fetuses. We found higher levels of circulating long chain fatty acylcarnitines in IUGR fetuses, indicative of global impaired fatty acid oxidation. Fatty acid transporters, esterification and metabolic machinery all had lower gene expression in IUGR myocardium with the exception of acylation enzyme ACSL1 and esterification enzyme GPAT. Despite widespread suppression of mRNA expression, none of the key fatty acid enzyme products were altered in IUGR myocardium. Lipid droplet formation was not different in isolated IUGR cardiomyocytes compared to control.

Elevated long-chain acylcarnitines are indicative of adverse outcomes in chronic heart failure patients (Ahmad *et al.*, 2016). In the perinatal period, it is normal for acylcarnitines to be elevated as newborns transition to a high fat diet (Vieira Neto *et al.*, 2012). However, IUGR infants have even higher circulating long chain acylcarnitines relative to normal birth weight controls (El-Wahed *et al.*, 2017). Consistent with this clinical data, we found elevated long chain circulating acylcarnitines (C14 and C18) in IUGR fetuses. We did not measure the difference in concentrations of acylcarnitines in arterial vs. venous blood in the coronary sinus. Thus we cannot be sure of the degree to which the elevation in acylcarnitines is dominated by the heart. However, because the heart is the organ that is preparing to

use free fatty acids as a fuel, we speculate that it is a major contributor to the circulating concentrations of acylcarnitines under conditions of placental insufficiency. Regardless, elevated acylcarnitines are still indicative of impaired fatty acid metabolism within the fetal compartment and are another indicator of dysregulated metabolism in the stressed fetus. This could impact the transition from a low-lipid environment *in utero* to a lipid-rich environment postnatally. If the metabolic deficiency persists, this could portend problems beyond the suckling period. Additionally, if the fetus is metabolically disadvantaged as it transitions to fatty acid metabolism, it will be ill-equipped to adapt to the increased workload in response to hemodynamic changes at birth.

Our hypothesis that cardiomyocyte lipid droplets would be altered in IUGR fetal cardiomyocytes, as they are in conditions of hypoxia, was not supported by our experimental data. There was no difference in lipid droplet size in IUGR fetal cardiomyocytes compared to control. Lipid droplet size is a downstream measure of fatty acid esterification in the endoplasmic reticulum and relies on GPAT, PAP, and DGAT. This suggests that although there was a significant suppression of genes responsible for fatty acid esterification and lipid droplet formation, this did not translate to a functional difference. It is possible that the suppressed mRNA levels did not translate to a suppression of protein levels for these three molecules. Unfortunately, we did not have antibodies that work in sheep to test this. Another possibility is that esterification enzyme function was not altered in IUGR hearts.

However, additional functional measures including enzyme activity of GPAT, PAP and DGAT would be required to further explore this possibility.

Gene expression of critical components in mitochondrial ß-oxidation and fatty acid esterification was suppressed in IUGR myocardium. ACSL is known to play a role in determining the fate of fatty-acyl CoAs, with ACSL1 and 3 being the predominant isoforms in the heart. ACSL1 colocalizes to mitochondria and when deficient, leads to an impairment of fatty acid oxidation (Ellis *et al.*, 2011). ACSL3 is important for esterification, as its knockdown blocks lipid accumulation when endoplasmic reticulum-stress is present (Chang *et al.*, 2011). Suppression of ACSL3 but not ACSL1 suggests an impairment of fatty acid activation destined for the endoplasmic reticulum but not the mitochondrion. This implies that fatty acid trafficking to the endoplasmic reticulum might be impaired while trafficking to the mitochondrion is maintained. However, in the reported studies, mRNA expression was suppressed for pathways occurring in both of these organelles. Even if distribution of fatty-acyl CoAs to each organelle remained normal, the downstream pathways of esterification and ß-oxidation still have lower gene expression. The global suppression of both fatty acid storage and metabolism genes suggests a general mechanism that may stifle the normal transition to fatty acid metabolism at birth. This may not be critical before birth, but if these changes persist, the newborn heart would be unprepared to handle the high levels of circulating lipids after birth.

We were surprised to find that for all of the genes studied, protein levels were unchanged. This apparent protective mechanism fits with other physiological responses suggesting a favored status for the fetal heart under stressful conditions. For example, under acute reductions in fetal arterial oxygen content, blood flow to the heart, brain and adrenal glands is conserved compared to other organs (Cohn *et al.*, 1974; Giussani, 2016). This leads to asymmetrical growth with an increase in the head to abdomen (or brain to liver) ratio, fetuses facing placental insufficiency in our study showed a similar response. We have previously shown that reduced oxygen content in fetal arterial blood leads to astonishing levels of coronary vasodilation under the influence of nitric oxide and adenosine (Thornburg & Reller, 1999). Additionally, fatty acid oxidation proteins are preferentially preserved in the fetal alligator heart in response to hypoxia (Alderman *et al.*, 2019). Whether this protective mechanism is preserved across species is unknown. Although the expression of genes regulating fatty acid metabolism were considerably suppressed, it is reasonable to suggest that the cellular levels of the protein products of these genes are protected under stressful conditions to maintain an organ vital to the survival of the fetus. While this adaptation may allow the fetus to survive, epidemiological studies in adults born with asymmetrical growth restriction (occurring in response to hypoxic and nutritive deficits) are nevertheless predisposed to detrimental outcomes (Hoffman *et al.*, 2017).

Conclusion

In summary, placental embolization causes IUGR and suppresses myocardial fatty acid transport and metabolism genes. Unexpectedly, lower mRNA levels did not

translate to a corresponding reduction in protein levels and lipid droplet formation was not different. The underlying reason for the mismatch between genes, proteins and function is not known, however the increase in circulating acylcarnitines implies a bourgeoning metabolic dysfunction. Though the fetal heart does not rely on fatty acid metabolism, this metabolic ability is critical postnatally. Whether the observed suppression of fatty acid metabolism genes persists postnatally, or whether this eventually translates to functional protein changes is not known. However, we know that these impairments in gene expression do not impact immediate survival after birth (Louey *et al.*, 2000) or survival to young adulthood under resting conditions (Louey *et al.*, 2005). It remains to be seen whether cardiac function is compromised under a secondary postnatal stress.

Chapter 4. General Discussion

The overarching aim of this work was to determine the maturational trajectory of fatty acid metabolic machinery in the perinatal heart and the effect of intrauterine growth restriction on this maturation.

This was addressed by 2 series of experiments whose specific aims were:

1. To characterize the normal developmental profile of key components in the fatty acid metabolic pathway in the fetal and neonatal heart (Chapter 2).
2. To determine the effect of IUGR on the development of fatty acid metabolic machinery in the fetal heart (Chapter 3).

Preterm Hearts are Poorly Prepared to Metabolize Lipids

Prior to the studies presented in this thesis, none had comprehensively characterized the ontogeny of the fatty acid metabolic pathway in the fetal myocardium. Previous studies looked at changes in fatty acid metabolism between pre- and postnatal time points and consistently reported augmented fatty acid oxidation in animals after birth (Brosnan & Fritz, 1971; Wells *et al.*, 1972; Ascuitto *et al.*, 1989; Bartelds *et al.*, 2000). No previous study has investigated the degree to which machinery of fatty acid oxidation systems are in place at the time of birth in any mammalian species. This deficit in knowledge is especially obvious in precocial species whose prenatal developmental timeline is similar to the human. To fill this gap in knowledge, we considered two prenatal times points at

94d GA and 135d GA (0.64 and 0.91 developed) in addition to one postnatal age (5 days old) in sheep. To put these two fetal time points into the context of a human pregnancy, they equate to 25 weeks and 36 weeks gestational age, respectively. Babies born before 37 weeks are considered preterm, and many require special care for their survival. Babies born at 25 weeks old have a ~75% chance of survival, even with the most sophisticated life support (Chan *et al.*, 2001). There is controversy about how to best care for these vulnerable infants given the drastic physiological between fetal and postnatal life. Current practices for supporting a premature infant are not designed to mimic the fetal life (Partridge *et al.*, 2017) but rather focus on life-sustaining support of crucial individual organ systems. Nutritional supplementation of preterm infants includes administering intravenous lipids despite a poor understanding of the metabolic machinery in any organ, let alone the heart.

We were able to characterize the maturation of metabolic systems in fetal and neonatal myocardium. We found that both gene and protein levels for critical components of the fatty acid metabolism pathway were lower in 94d GA compared to 135d GA, indicating gradual maturation of the fatty acid metabolic pathway. These data also suggest that the very immature myocardium (94d GA) is not yet fully equipped to metabolize fatty acids to the same degree as would a more mature fetal heart (135d GA).

Functional studies could determine whether our findings of lower gene and protein expression translate to a functional difference in fatty acid oxidation at these fetal ages. Fortunately, it is possible to study the metabolic features of isolated cells in culture using

the Bioagilient extracellular flux analyzer (Seahorse). This commercial instrument is designed to measure oxidative capacity *in vitro* and can be used to test the hypothesis that 94d GA fetal cardiomyocytes are less capable of fatty acid oxidation compared to 135d GA fetal cardiomyocytes. Preliminary studies designed to test this hypothesis are found in the appendix (Figure 5-1 through Figure 5-5). The difficulty in conducting and interpreting these pilot studies is related to recapitulating the fetal environment *in vitro*. Most culture studies are done in room air with 21% O_2 and supraphysiological glucose levels. "Hypoxic" studies are usually conducted under conditions using 3% oxygen. For fetuses in utero, normoxia is 3% O_2, therefore to be "physiological" in culture, we should be culturing fetal cells in what is considered severely hypoxic for adult cells. The same reasoning can be applied to glucose: most commercially available basal media has supraphysiological glucose levels compares to the fetus (1 mM).

In order to gain insight regarding the function of isolated fetal cardiomyocytes, cells were studied under a variety of culture conditions to test the degree to which oxygen and glucose levels affect metabolic activity. It is evident that fetal cardiomyocytes are more metabolically active in higher oxygen (Figure 5-2) and glucose (Figure 5-3) even if those levels do not imitate the relatively hypoxic, hypoglycemic conditions found in the normal fetus. Following culture conditions in 21% oxygen and 5.5 mM glucose, oxygen consumption with palmitate at 135d GA was nearly double the oxygen consumption at 94d GA (Figure 5-5), which provides functional support to our finding of upregulated fatty acid metabolism genes and proteins in older fetuses.

Prepartum Regulation of Lipid Metabolism: Still a lot of Unknowns

Many myocardial fatty acid metabolism genes and their associated proteins increased expression between 135d GA and postnatal day 5. This was not surprising considering previous reports of fatty acid metabolic maturation in the heart in the peripartum period (Brosnan & Fritz, 1971; Bartelds *et al.*, 2004). The studies reported here show more precisely that there is a 1.2-7.8 fold increase in mRNA production by fatty acid metabolic genes between 135d GA and 5d PN. For the fetus, this 17 day period is met with numerous pre- and postnatal environmental changes, all of which may influence the observed maturation of metabolic systems in the myocardium.

Prenatal Regulators of Lipid Metabolism

The prepartum environment changes across gestation. In later gestation, surges in cortisol and thyroid hormone are amongst the factors that influence cardiomyocyte maturation (Jonker & Louey, 2016). The direct effect of cortisol and thyroid hormone on fatty acid metabolic maturation has not been studied. However, both of these hormones have maturational effects on other fetal systems. Cortisol promotes the expression of iodinases that lead to increased concentrations of tri-iodo-L-thyronine, the active form of thyroid hormone. Thyroid hormone stimulates mitochondrial maturation in fetal skeletal muscle (Davies *et al.*, 2020), though this may not be directly applicable to the heart. Our laboratory has shown thyroid hormone matures the heart by increasing ovine cardiomyocyte binucleation, decreasing proliferation and increasing cellular width (Chattergoon *et al.*, 2012a; Chattergoon *et al.*, 2012b). Our preliminary data show that 5 days of fetal thyroid hormone infusion matures CPT1 and CD36 gene expression in the

late gestation fetal heart (Figure 4-1), implying that the prenatal rise in thyroid hormone likely plays a role in fetal cardiac metabolism.

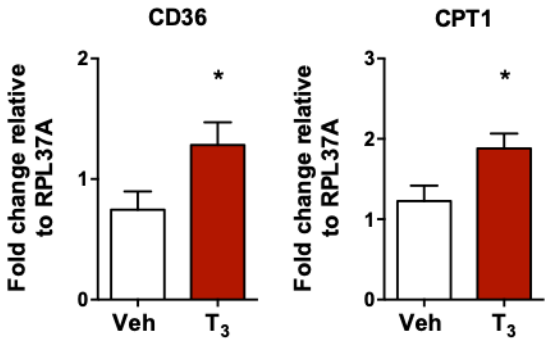

Figure 4-1 Thyroid hormone stimulates cardiac fatty acid transport (CD36) and metabolic (CPT1) gene expression.

T_3 was infused (54 μg/ day) into fetal sheep from 125-130d GA (n=7 vehicle, n=8 T_3). Chattergoon et al. unpublished.

Postnatal Switch to Lipid Metabolism

Around the time of birth, there is a metabolic shift from lactate and glucose oxidation to fatty acid oxidation. Based on early rodent experiments, many investigators surmised that birth itself and initiation of air breathing led to increased arterial oxygen, causing an immediate switch to fatty acid oxidation. This led to the dogma that fatty acid oxidation can only occur after birth. This, however did not consider the possibility of a limited capacity for fatty acid oxidation in the fetus in preparation for a successful switch. A close examination of the literature shows that there may be a more gradual maturation (Bartelds *et al.*, 2000) but despite this, the dogma remains. Our data supports Bartelds in that we

observe prenatal increases in several components of the fatty acid oxidation pathway. This is the first time this has been characterized in a precocial species.

Among the dramatic changes for the heart that occur in the perinatal period are a (1) ~fourfold increase in oxygen availability, (2) increased left ventricular pre- and afterload as left atrial and systemic arterial pressures rise, and (3) increased lipid substrate availability with suckling. Transcription factors including Meis1 and Hand1 play a role in this switch, with downregulation of these transcription factors leading to an upregulation of oxidative metabolism genes (Breckenridge *et al.*, 2013; Lindgren *et al.*, 2019). The physiological signals mediating this downregulation are not fully understood, but low oxygen induced HIF1-α expression has been shown to regulate Hand1 in mice (Breckenridge *et al.*, 2013). Downregulation of both of the transcription factors with development leads to an upregulation of oxidative metabolism genes.

Once born into an oxygen rich world, newborns no longer have the same oxygen limitations as in fetal life. This increased oxygen availability permits more oxidation of lipids which requires more oxygen (2.8 oxygen atoms per carbon) than glucose oxidation (2 oxygen atoms per carbon) (Grynberg & Demaison, 1996). Isolating the influence of oxygen availability on myocardial fatty acid oxidation could be done by ventilating late gestation fetuses. Previous studies have demonstrated feasibility of this study (Willis *et al.*, 1985; Reller *et al.*, 1987).

Functional Testing of Fatty Acid Metabolism in the Perinatal Heart

Newborn mammals begin suckling after birth and this leads to increased circulating lipids, providing the substrate for fatty acid metabolism. However, since there are multiple dynamic changes occurring around this time, it is difficult to discern the influence of fatty acid substrate availability on upregulation of fatty acid oxidation machinery in the newborn heart. In rat pancreatic β-islet cells, palmitate exposure induces upregulation of fatty acid oxidation genes including CPT1 and LCAD *in vitro* (Xiao *et al.*, 2001). It is likely that cardiomyocytes will respond similarly to direct fatty acid exposure; the upregulation of these genes in the newborn lamb myocardium may be due to normal increase due to maturation independent of fatty acid exposure, fatty acid exposure from suckling, or a combination of both. The degree to which fatty acid exposure alone contributes to the observed upregulation in fatty acid oxidation genes in the newborn lamb myocardium remains to be seen.

We demonstrate that increasing age is met with higher levels of fatty acid transporters and enzymes with gene expression for most, highest in the lamb. A remaining question is: how much of this increase is solely due to substrate availability after birth or is part of a normal maturational increase even in the absence of high circulating lipid? The maturation of the machinery may increase in the fetus when circulating lipid levels remain low. Bartelds has shown late gestation (127 – 135d GA) fetal sheep heart has limited uptake and oxidative capacity but these abilities could further increase in the immediate prepartum period (135 – 147d GA). Future experiments assessing the same parameters

(gene and protein expression, BODIPY uptake experiments) described in this thesis, and lipid infusion studies would address this.

Additional lipid infusion studies could also be done in IUGR fetuses. This would assess whether IUGR fetuses have suppressed fatty acid uptake and oxidation, or whether lipid exposure stimulates upregulation of fatty acid metabolic machinery.

Perinatal Cardiomyocyte Lipid Droplet Formation

There are additional fates for fatty acids aside form mitochondrial β-oxidation One such fate is esterification and storage of fatty acids in a lipid droplet. We cannot find data from other laboratories showing quantification of lipid droplet size and number in the fetal or newborn heart of a precocial animal model. Nor are there data in the literature showing how IUGR affects lipid droplet formation in the fetal heart. We took advantage of a commercially available saturated long chain fatty acid with a fluorescent BODIPY tag. BODIPY-C12 is the equivalent size of a C18 fatty acid and was used to measure lipid droplet formation in fetal, newborn and IUGR fetal cardiomyocytes: by necessity, the technique requires the living cell to be able to take up the lipid into the cytoplasm. Our study revealed that fetal cardiomyocytes (control and IUGR) are capable of taking up fatty acids, esterifying them and forming lipid droplets. Thus, sarcolemmal transporters are at least mature enough to transport lipids into the cell and the esterification machinery is at least mature enough to form lipid droplets. A limitation of this technique is that it doesn't assess transport of lipids into mitochondria for oxidation; other techniques, such as the

Seahorse-based studies of glycolysis and β-oxidation would be required for functional assessment of fatty acid metabolism.

In our study, fetal cardiomyocytes produce larger lipid droplets compared to newborn cardiomyocytes. In the diseased adult heart, larger lipid droplets are indicative of hazardous lipid storage or impaired oxidation (Goldberg *et al.*, 2018), however this may not be applicable to the fetal heart. In other organs, such as the liver, IUGR rats had increased hepatic lipid deposition compared to controls in fetal, newborn and adult life (Magee *et al.*, 2008; Yamada *et al.*, 2011). Interestingly, the size of lipid droplets in cardiomyocytes that grew under conditions of placental insufficiency were not different from controls despite a ~22% reduction in somatic and heart growth and nearly universal suppression of genes that regulate fatty acid metabolism. Even though we didn't measure levels of proteins that are key to fatty acid esterification for lack of specific antibodies, all other proteins investigated were not altered in IUGR despite mRNA expression suppression. Preservation of protein expression in combination with no differences in lipid droplet size suggests that certain pathways may be conserved even in the face of severe prenatal stress.

Circulating Acylcarnitines in the Perinatal Period as a Marker of Fatty Acid Oxidation Dysfunction

Circulating levels of acylcarnitines are used as markers for impaired fatty acid oxidation and correlate with severity of heart failure in adults (Ahmad *et al.*, 2016; Ruiz *et al.*, 2017). In healthy newborns, circulating acylcarnitines are elevated as infants are exposed to

higher lipid levels with suckling (Vieira Neto *et al.,* 2012). Though we did not measure acylcarnitines in the ontogeny study, it is likely that circulating acylcarnitines would be low in the fetus and higher postnatally, similar to what is seen in humans (Meyburg *et al.*, 2001). IUGR infants have higher levels of long chain fatty acyl carnitines compared to healthy infants, suggesting an impairment in fatty acid oxidation somewhere in the fetus (El-Wahed *et al.*, 2017). In alignment with human IUGR fetuses, we found higher circulating long chain acylcarnitines in our IUGR study. However, we don't know the origins of the acylcarnitines in these studies as they were measured in the general circulation. To test the hypothesis that the heart is the source of the elevated acylcarnitines, we could measure myocardial arteriovenous differences in IUGR fetal sheep by catheterizing the coronary sinus and aorta to measure inflow and outflow specific to the heart. However, we were not able to include such studies in this project. If the heart is not the major source of the acylcarnitines, the next target would be the liver as we know that the liver is relatively wasted in IUGR fetuses. A study in exercised adult rats, however suggests that the heart is the major source of circulating acylcarnitines and not liver or skeletal muscle (Makrecka-Kuka *et al.*, 2017).

Long Term Metabolic Effects of IUGR

Compromised growth in fetuses programs them for augmented postnatal catch-up growth that is accompanied by long-term outcomes including heart disease, stroke, hypertension and type 2 diabetes. The term "programming" here refers to the changes during development that lead to elevated risk for disease in later life. The risks for such conditions are thought to stem from accommodations made during fetal life that ultimately

prove detrimental by the time a person reaches adulthood. The bulk of these studies have focused on metabolism from the standpoint of diabetes and mismatches in glucose and insulin sensitivity (Barry *et al.*, 2016). Although epidemiologic studies demonstrate the high risk for heart disease based on early life conditions, what we are missing is the underlying precise cardiometabolic changes that may contribute to these outcomes. A baboon study in maternal undernutrition reveal a distinct cardiac lipid phenotype in IUGR fetuses suggesting alterations to lipid metabolism (Muralimanoharan *et al.*, 2017). The mechanisms leading to these lipid differences and whether this persists postnatally is unknown. Additionally, future studies should determine whether our observed downregulation in fatty acid metabolism genes persists postnatally and whether this alters metabolic function. Long-term mouse studies from maternal undernutrition demonstrate impaired fatty acid oxidation in adults that were born IUGR (Beauchamp *et al.*, 2015).

Concluding Remarks

Despite a ubiquitous switch from primarily carbohydrate sources for energy *in utero* to fatty acids after birth, knowledge of the timeline and capacity of the developing myocardium to handle fatty in the lead-up to birth was limited. Clinical use of lipid-rich formulas in preterm and IUGR infants is standard, even without a thorough understanding of the maturity of the myocardium to process these substrates. This body of work provides insight into the maturation of fatty acid oxidation systems in the normal and IUGR myocardium.

We demonstrate a gradual maturation of critical components regulating fatty acid oxidation across late gestation through to the newborn period. This is paired with larger lipid droplets in fetal cardiomyocytes compared to newborn. Whether this is due to increased storage or a limited capacity for β-oxidation in the fetus is unknown. Based on these data, we conclude that immature cardiomyocytes are less capable than the postnatal myocardium to metabolize fatty acids. Out data show that IUGR hearts may be even less able to adequately handle fatty acids, however, whether the mismatch between gene and protein levels is translated to a functional deficit remains to be elucidated. Elevated acylcarnitines in IUGR fetuses indicate an impairment in fatty acid oxidation, consistent with findings in IUGR infants, though the source of the source of the acylcarnitines needs to be determined. Persistence of these mismatches could underlie vulnerability to cardiac metabolic dysfunction leading to disease but long-term studies are required to determine this.

These studies are an important first step in furthering our understanding of myocardial metabolic maturation in immature and growth restricted hearts. This work is foundational for future studies aimed at improving nutritional support for premature and growth restricted infants.

Chapter 5. Appendix

Metabolic Performance of Developing Cardiomyocytes

It should be noted that most studies of fetal cells in the literature are performed in room air and temperature, which is 21% oxygen and a water saturated partial pressure ($P_{atm}O_2$) of 150 mmHg. This quite different from the environment in which fetal cardiac cells grow *in utero* where the partial pressure of oxygen in ovine fetal arterial blood is 20-25mmHg. In addition, fetuses have arterial glucose concentrations around 1mM compared to about 5mM in their mothers. It is very difficult to reproduce all of the important conditions found in the fetus in the laboratory and most investigators are satisfied using standard laboratory conditions in room air. The aim of this study was to systematically test the effect of oxygen and glucose concentration on fetal cardiomyocyte energetics. Below the influence of culture conditions (oxygen and substrate availability) and assay conditions (glucose and palmitate availability) are systematically tested. All assays were conducted in the BioAgilent Extracellular Flux Analyser XF96 (Seahorse) at room air (21% O_2).

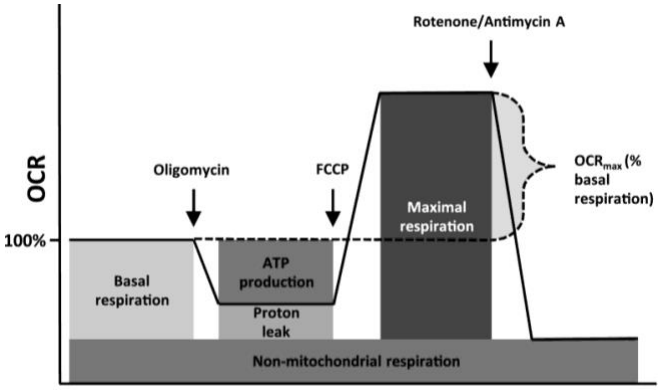

Figure 5-1 Seahorse mitochondrial stress test.

Schematic of seahorse mitochondrial stress test with three injections: (1) ATP synthase inhibitor (oligomycin), (2) uncoupling agent (FCCP) and (3) rotenone/antimycin A (complex I and III inhibitor) injections. From Bioagilent.

Effect of O_2

122d GA fetal sheep cardiomyocytes were plated (20,000 cells/well at a concentration of 500k cells/mL) in serum DMEM (5.5 mM glucose), supplemented with 10% fetal bovine serum (FBS; Gibco), 1 ml/L antibiotic-antimycotic solution (MilliporeSigma, Burlington, MA, USA), and 10 mg/L insulin-transferrin-sodium selenite supplement (MilliporeSigma) for 24 hours at 21% O_2. The cells were either left at 21% O_2 or moved to 3% O_2 (hypoxic conditions achieved using a ROXY-1 hypoxic regulator (Sable Systems) and nitrogen gas). When cells were 80% confluent, media was changed to serum free DMEM 24 hours before the assay.

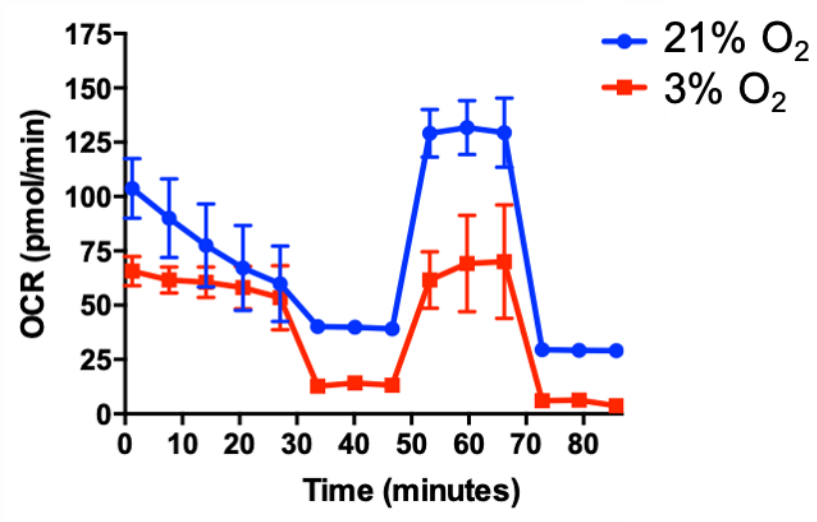

Figure 5-2 Oxygen culture conditions dictate OCR regardless of oxygen level during seahorse experiment.

Culture conditions: 21% O_2 or 3% O_2, regular media

Assay conditions: seahorse media containing 5.5 mM glucose, 1 mM lactate, 2 mM glutamine, 2% FBS. n=3, 122d GA, left ventricular cardiomyocytes.

In order to elicit a maximal response to palmitate, we opted to give the cells the best culture conditions to permit this response and decided to continue with 21% O_2 for the future experiments even though this is hyperoxic to the fetus. Next, we wanted to determine the effect of different substrate availability on palmitate oxidation (200 µM, conjugated to BSA). Regular, fetal and IUGR media were prepared using a minimal base media and adding physiologically relevant substrates at the concentrations below and was not prepared using serum from the actual fetuses used in the study. Regular media was the same as in Figure 5-2 (with 50 µM carnitine supplementation), fetal media contained (1 mM glucose, 1 mM pyruvate, 2 mM lactate and 2 mM glutamine, 50

µM carnitine) and IUGR media was identical to fetal media except it contained 0.5 mM glucose.

Effect of Substrate Availability

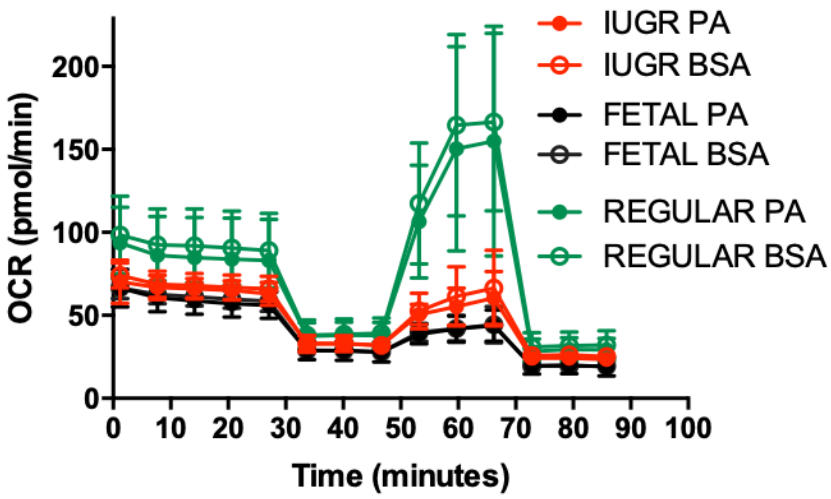

Figure 5-3 Glucose availability *in vitro* dictates OCR regardless of assay substrate availability.

Culture conditions: 21% O_2, 5.5mM glucose (regular), 1mM glucose (fetal), 0.5mM glucose (IUGR). Assay conditions: 21% O_2, KHB media + 200uM palmitate or BSA equivalent (n=3), 122d GA, left ventricular cardiomyocytes.

Effect of Palmitate

Regardless of palmitate availability, fetal cardiomyocytes preferentially oxidized glucose; oxygen consumption rates (OCR) reflected glucose concentration, with regular (5.5mM glucose) media having the highest OCR. Based on this, we opted to continue palmitate studies in a minimal media (KHB) supplemented with carnitine. 5x KHB stock is prepared by adding 32.532 g NaCl (555 mM), 1.752 g KCl (23.5 mM), 1.204g $MgSO_4$ (10 mM) and 0.852g Na_2HPO_4 (9 mM) to 900mL distilled water, the final volume brought to 1L, filtered and stored at 4°C. 1x KHB was prepared with the day before the assay by adding 50 mL 5x stock to 200 mL milliQ water and adding 297.5 mg HEPES. 250 µL of 50mM carnitine was added on the day of the assay.

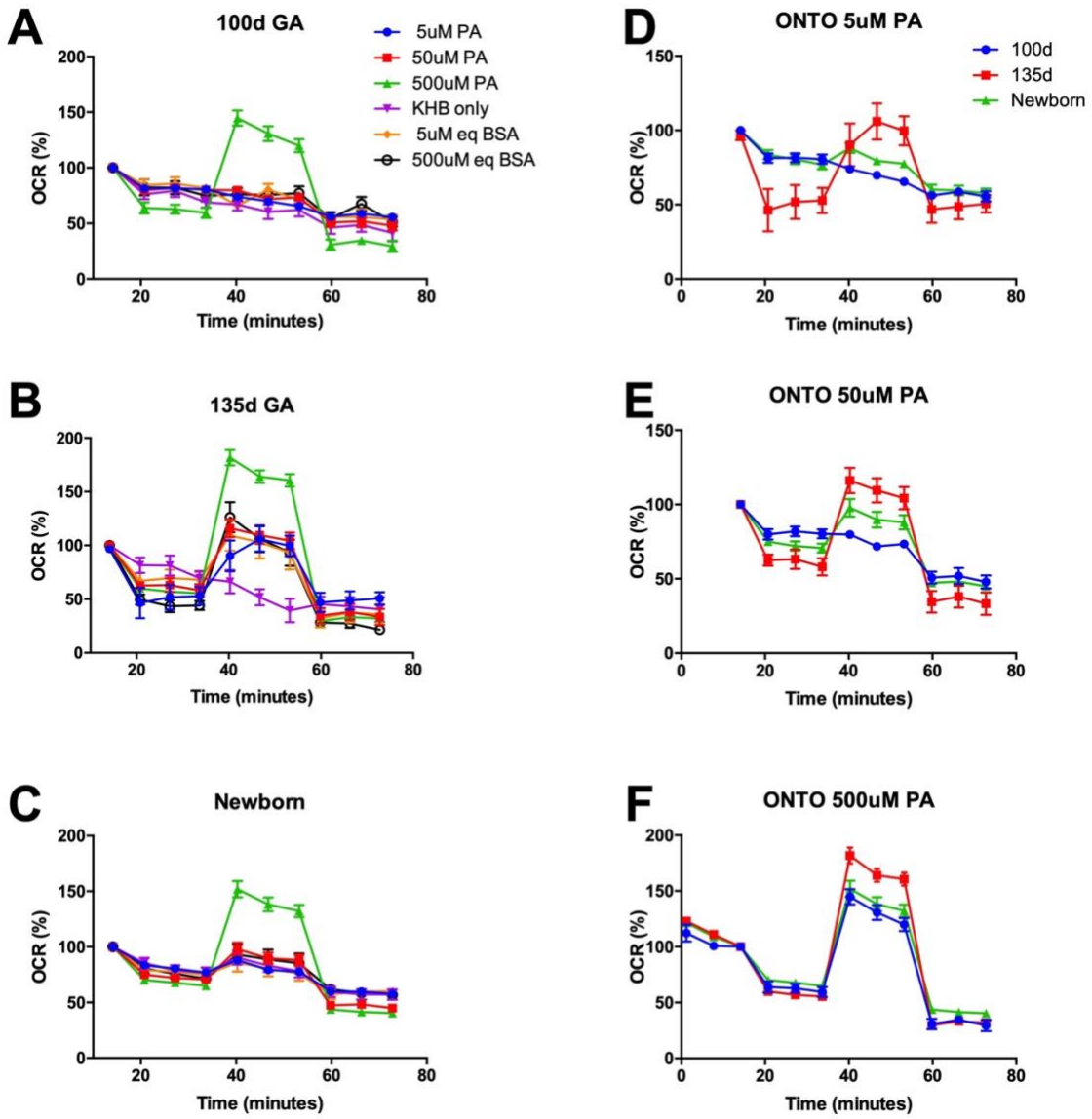

Figure 5-4 100d, 135d GA, Newborn cardiomyocyte palmitate dose response.

A-C: 3 separate age, (A) 100d GA, (B) 135d GA, (C) Newborn (1-2d GA)

D-F: all 3 ages, different concentrations of palmitate (A) 5 µM palmitate, (C) 50 µM palmitate, (C) 500 µM palmitate. Culture conditions: 21% O_2, regular media. Assay conditions: 21% O_2, KHB media (supplemented with carnitine) + 5, 50 or 500 µM palmitate.

Based on these studies, we decided to proceed with a supraphysiological dose of palmitate (500uM PA) as this was the only dose that consistently produced a response in OCR.

Fetal Maturation of Palmitate Oxidation

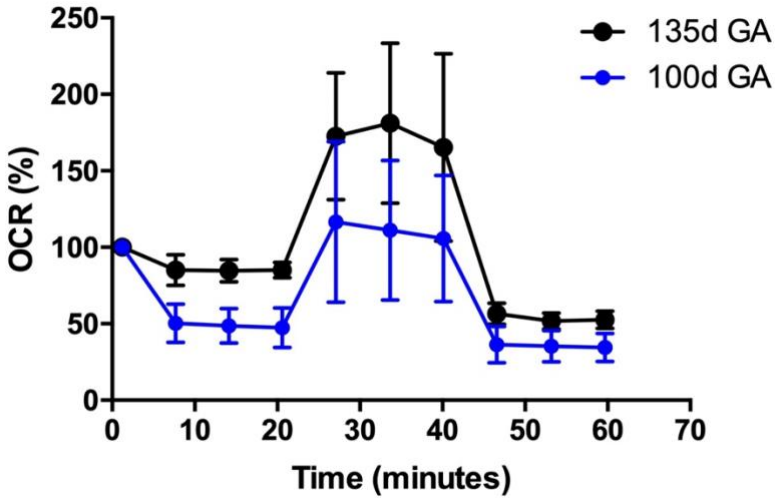

Figure 5-5 Fetal maturation of palmitate oxidation capacity from 94d GA to 135d GA.

Culture conditions: 21% O_2, regular media (5.5 mM glucose), no palmitate. Assay conditions: 21% O_2, no glucose, 500 µM palmitate

Based on these experiments, we conclude that supraphysiologic conditions (21% O_2, regular media: 5.5 mM glucose) are required to see a response to added palmitate.

Outstanding Problems

An additional challenge to interpreting results from these experiments is that it is difficult to normalize the data. Typically, one will normalize each well to protein or DNA with DAPI staining. Protein normalization is suboptimal because the BSA used to conjugate PA likely adheres to the plastic plate, giving falsely high readings for protein content. This can be partially mitigated by rinsing wells twice with HBSS (+Ca, +Mg), though rinsing comes with an added risk of perturbing the cells. The challenge with normalizing to DNA content is that hearts at different ages have variable degrees of mono and binucleated cardiomyocytes. For these reasons, the above data is normalized to baseline, so that measurements following drug injections are relative to the baseline oxygen consumption.

Simulating IUGR in vitro is also challenging due to the heavy influence of culture and assay conditions on experimental outcomes. IUGR conditions would be 1.3% O_2 and 0.5 mM glucose.

Plasma Lipid Assays

The aim of this study was to determine circulating levels of lipids in late gestation, newborn and adult sheep plasma.

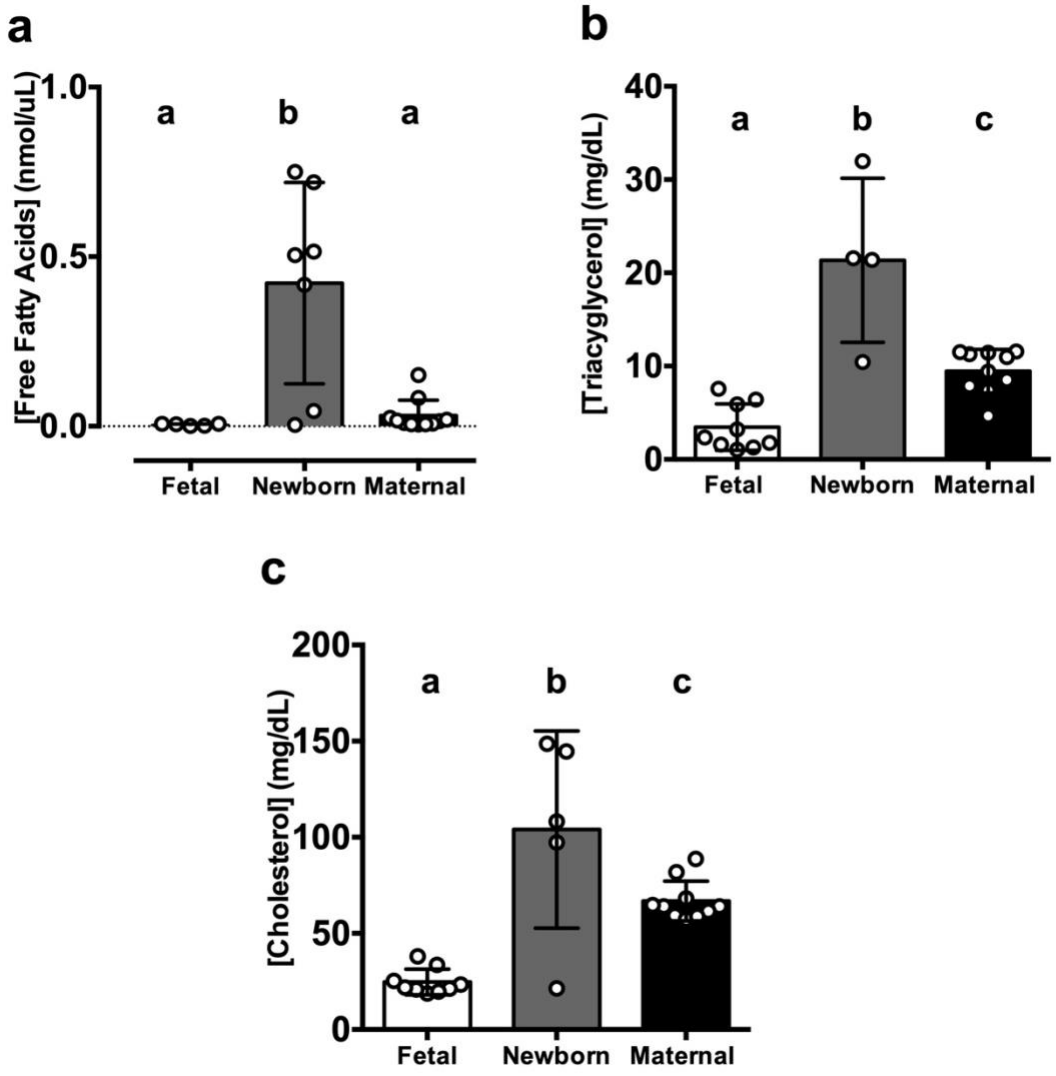

Figure 5-6 Plasma lipid content in fetal, newborn and maternal sheep.

Fetal n = 9, (129-136d GA), Newborn n = 4-7, (2-28d PN) and Maternal n = 10, (included a mix of pregnant and lactating) circulating lipid content. Non-shared letters denote statistical significance, $p < 0.05$.

Cholesterol and TAG assays conducted with kits from Pointe Scientific: Triglyceride reagent set: cat#23-666-410, Triglyceride reagent kit: cat#23-666-412. Cholesterol: cat#23-666-201. Free fatty acid assays conducted with Sigma-Aldrich Free Fatty Acid Quantitation Kit: cat#MAK044-1KT

BODIPY-C16 lipid droplet formation cardiomyocyte uptake *in vitro*

Studies in this dissertation investigated the uptake and incorporation into a lipid droplet for BODIPY-C12, which is equivalent to a long chain (C18) fatty acid (LCFA). We also wanted to test whether fetal and newborn cardiomyocytes were capable of taking up and storing a very long chain fatty acid in a similar manner. To test this we used BODIPY-C16, which is equivalent to a very long chain (C22) fatty acid (VLCFA).

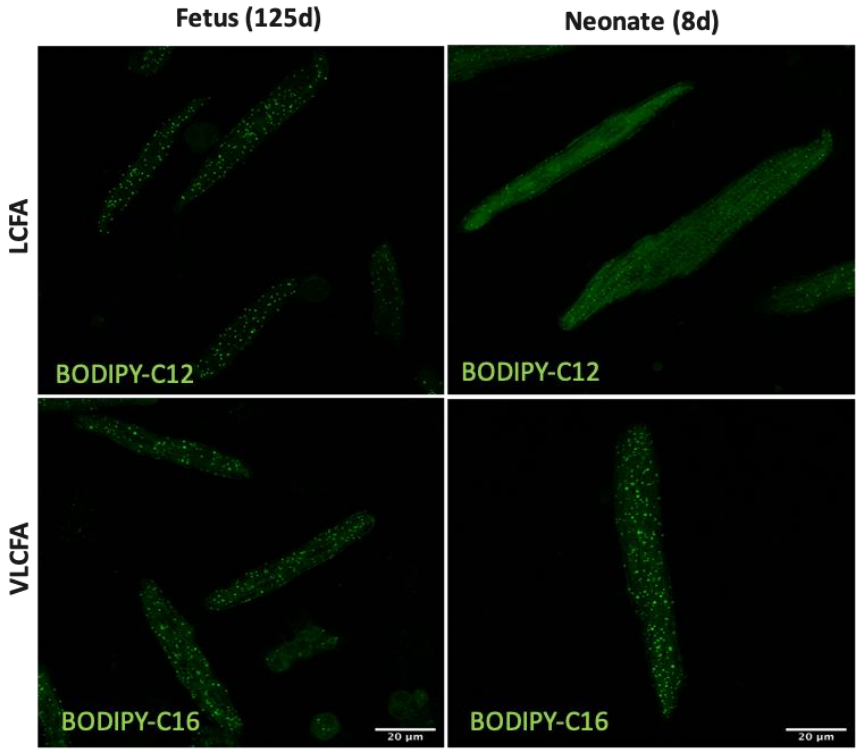

Figure 5-7 BODIPY-C16 uptake and lipid droplet formation in fetal and newborn cardiomyocytes.

Representative images of isolated fetal (125d GA) and neonatal (8d PN) cardiomyocyte lipid droplets following a 60 minute incubation with either 2µM LCFA (BODIPY-C12) or 2µM VLCFA (BODIPY-C16). Images acquired on LSM880 using FastAiry, details can be found in the methods section. Scale bar = 20 µm.

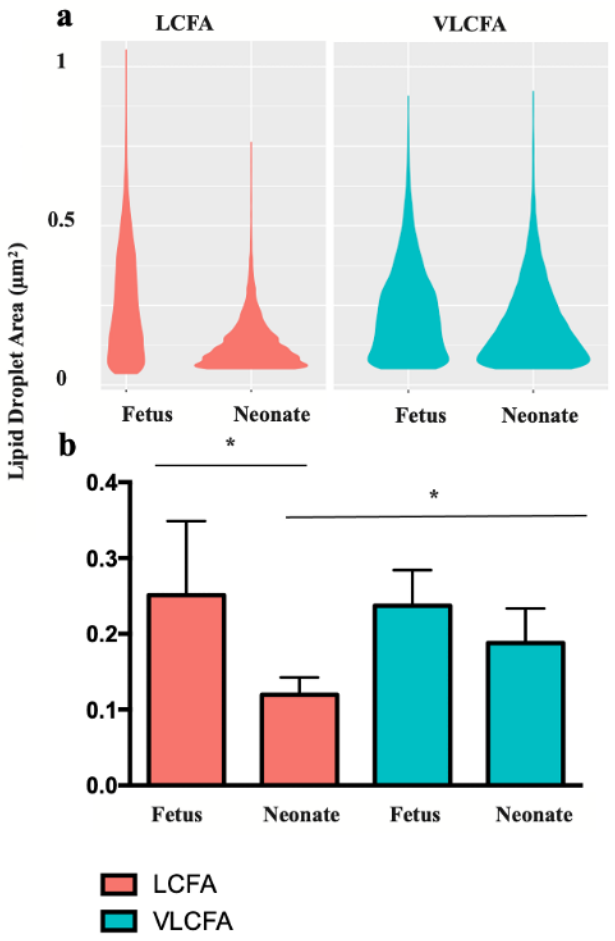

Figure 5-8 Quantification of LCFA and VLCFA lipid droplets in fetal and newborn cardiomyocytes.

(a) Fetal and neonatal cardiomyocytes have distinct lipid droplet size distribution for LCFA and VLCFA. Fetus: n = 6, Newborn: n = 7, 10-30 cells per animal, 50-300 droplets (b) LCFA-containing lipid droplets are smaller in neonatal compared to fetal cardiomyocytes. VLCFAs form larger lipid droplets than LCFAs in neonatal cells. n = 6-7 per age group, mean ± SD, unpaired student's t test compared to neonatal LCFA. * $p < 0.05$

Saturated versus polyunsaturated fatty acid uptake and distribution in newborn cardiomyocytes

We also wanted to test whether newborn cardiomyocytes were capable of taking up polyunsaturated fatty acids and if so, what the cellular distribution would be compared to saturated fatty acids.

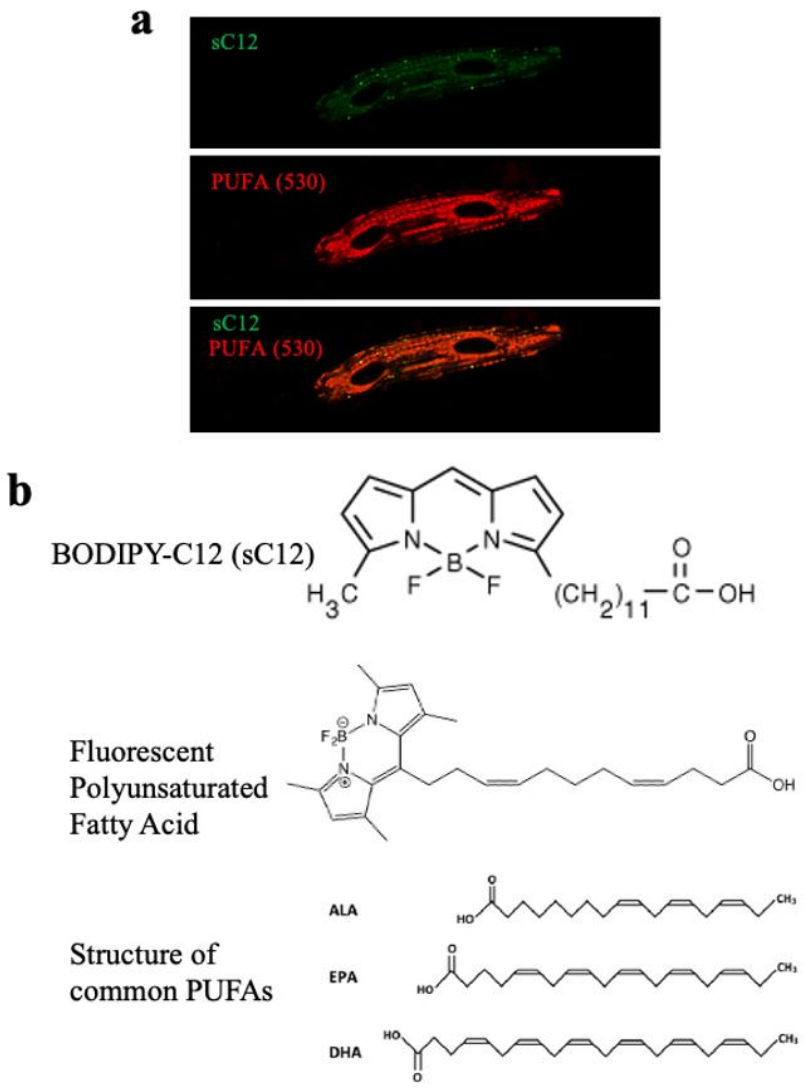

Figure 5-9 Polyunsaturated and saturated fatty acid uptake in newborn cardiomyocytes.

(a) Newborn cardiomyocyte incubated with saturated (sC12) and polyunsaturated fatty acid (PUFA) for 60 minutes. Top: BODIPY-C12 (LCFA, sC12) saturated fatty acid lipid droplets, middle: PUFA distribution, bottom: overlay. (b) top: structure for BODIPY-C12 saturated long chain fatty acid, middle: structure for synthetic fluorescent PUFA, bottom: structure of common PUFAs for comparison.

We concluded that newborn cardiomyocytes were capable of PUFA uptake and that the cellular distribution was more widespread compared to saturated fatty acids.

*Synthetic PUFA provided by Summer Gibbs, PhD. Oregon Health & Science University.

***Ex vivo* administration of BODIPY-C12**

In order to determine whether fetal cardiomyocytes were capable free fatty acid uptake and esterification when the lipid was supplied to the coronary arteries, 2 mL of 10 µM BODIPY-C12 conjugated to BSA in serum free media was injected into the left anterior descending coronary artery. Following injection, we waited 5 minutes and dissociated the heart in a standardized fashion (see methods). Left ventricular cardiomyocytes downstream from injection were imaged as previously described (methods).

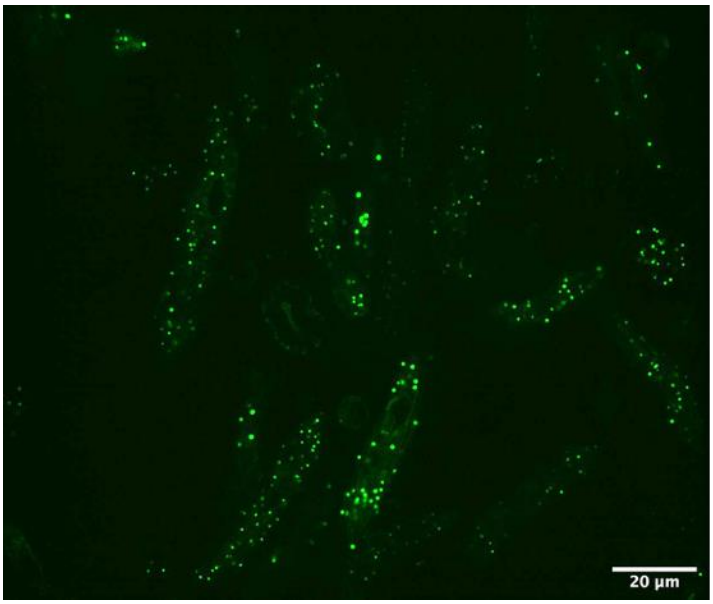

Figure 5-10 Lipid droplet formation following left anterior descending coronary artery injection with BODIPY-C12.

BODIPY-C12 lipid droplet formation in isolated 122d GA fetal cardiomyocytes following 10uM BODIPY-C12: BSA injection into left anterior descending artery. This is a snapshot, not a maximum intensity projection of a z-stack.

Lipidomics in Control and IUGR myocardium

In order to comprehensively determine the lipid species present in IUGR myocardium compared to controls, lipidomics were conducted on myocardium from IUGR (n = 14) and control (n = 14) fetal sheep (125d GA) in collaboration with Fred Stevens and Jaewoo Choi (Oregon State University). IUGR fetuses were generated using umbilicoplacental embolization (10 days from 115 – 125d GA, see Chapter 3). Apical left ventricular (LV) myocardium was excised and flash frozen in liquid nitrogen prior to lipid extraction. Lipid extraction was performed in bullet blender (2 minutes, speed 8) by adding 30-50 mg of frozen LV (control: n=14, IUGR: n=14), zirconium oxide beads (1.4mm) and 10 µL/mg tissue cooled extraction solvent (methylene chloride: isopropanol: methanol (25:10:65; v/v/v) + 0.1% butylated hydroxytoluene cooled to -20°C) to microsolv 2mL mass spectrometry vials (Agilent cat#95025-1WCP). 10 µL/mg solvent was added again, then centrifuged at 13,000 rpm and incubated at 4°C for 10 minutes. Supernatant was transferred to new tubes. A 30uL aliquot was transferred to a 300 µL mass spectrometry vial (Agilent cat#95325-1CP) + 165 µL extraction solvent + 5 µL Lipidomix standards (Avanti Lipids).

Four mobile phase solvents were used, 2 for positive ion mode and 2 for negative ion mode.

Positive ion mode:

1. 60% acetonitrile, 40% H_2O + 10mM ammonium formate + 0.1% formic acid
2. 90% isopropanol, 10% acetonitrile + 10mM ammonium formate + 0.1% formic acid

Negative ion mode:

1. 60% acetonitrile, 40% H_2O + 10mM ammonium acetate
2. 90% isopropanol, 10% acetonitrile + 10mM ammonium acetate

Analysis:

PeakView 1.2.1 software was used to identify peaks at characteristic retention times and mass to charge ratios for precursor ions (MS) and daughter ions (MS2). MultiQuant software (Sciex) was used to quantify intensities following identification.

Triacylglycerols

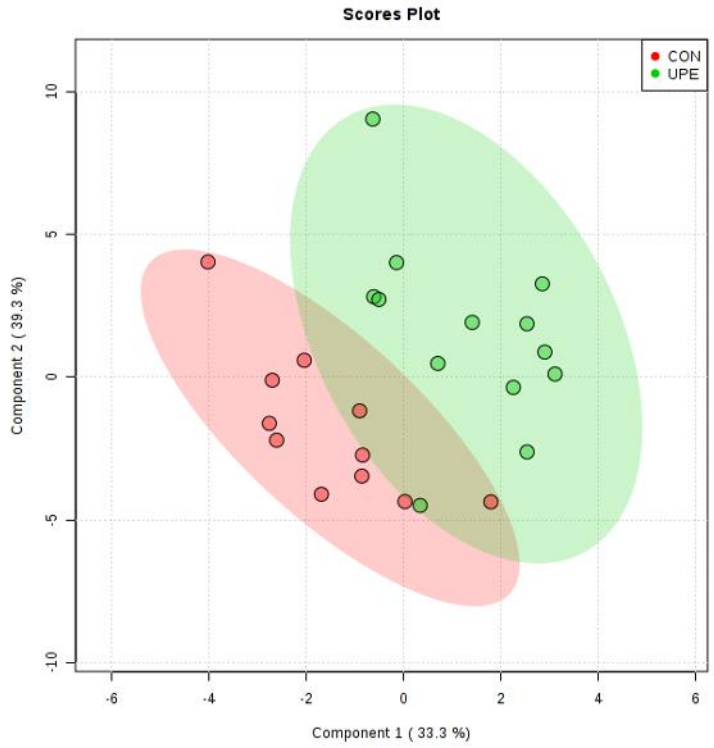

Figure 5-11 Triacylglycerol content of IUGR and control myocardium

(PLS-DA predominance of partial least squares – discriminant analysis)

UPE: umbilicoplacental embolization, IUGR (green), CON: control (red).

In this figure, each symbol represents a fetus; the symbol is representative of the unique TAG fingerprint for that animal. The symbols are clustered by treatment group and this figure demonstrates that the TAG fingerprints from IUGR and control are dissimilar but are not completely distinct. Follow up analysis on the specific TAG species and consultation with lipidomics experts are needed to determine the viability of this finding.

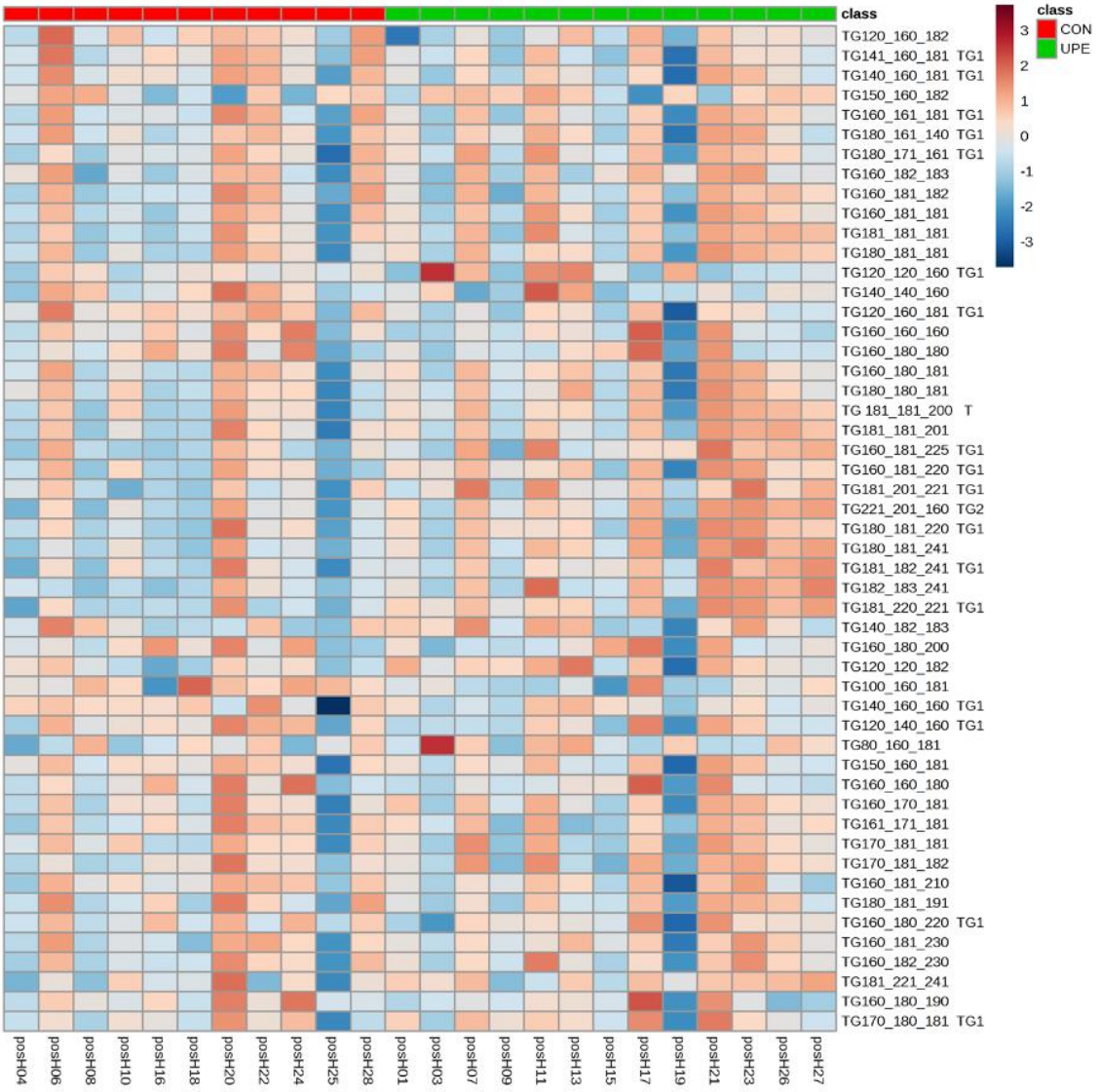

Figure 5-12 Triacylglycerol heat map in IUGR and control myocardium

This heat map was produced using the same data from Figure 5-11 but separates the unique TAG fingerprint from each animal. There is no clear pattern of up or downregulation.

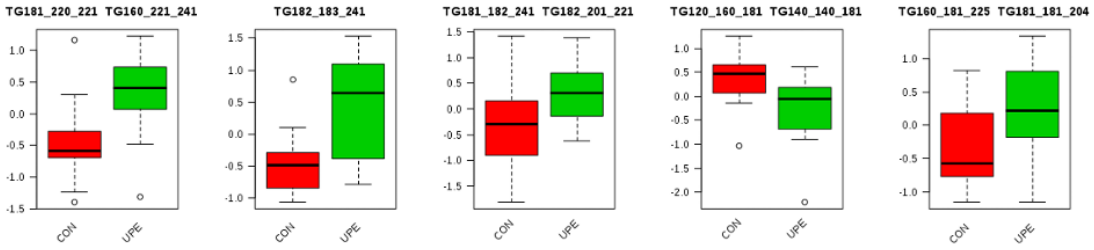

Figure 5-13 Triacylglycerol species differences in IUGR and control myocardium

UPE: umbilicoplacental embolization, IUGR (green), CON: control (red).

The spread in data within an experimental group varies between TAG species. IUGR does not consistently upregulate or downregulate all the species. The challenge of analyzing the data is that these numerous species identified from lipidomics experiments have unknown functions.

Phosphatidylcholine

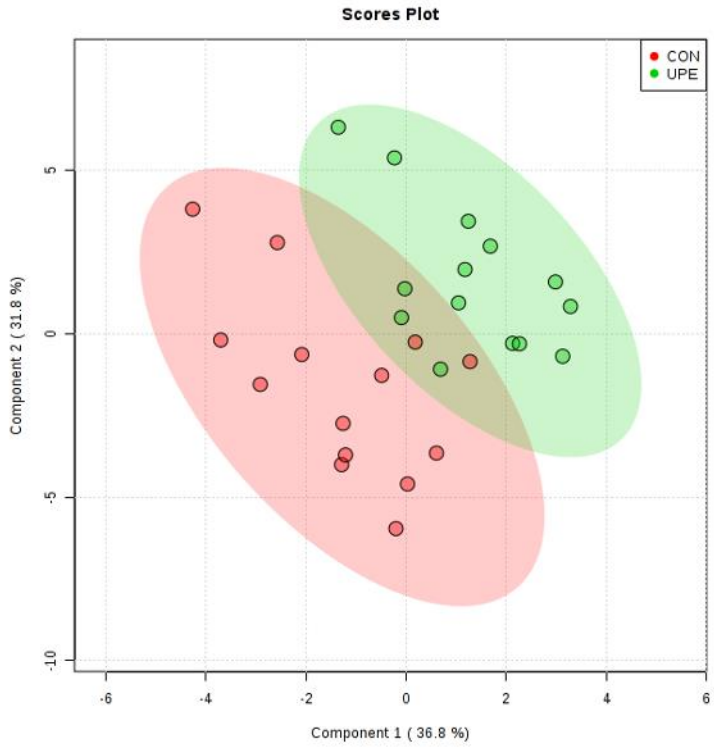

Figure 5-14 Phosphatidylcholine species in IUGR and control myocardium

(PLS-DA predominance of partial least squares – discriminant analysis)

UPE: umbilicoplacental embolization, IUGR (green), CON: control (red).

In this figure, each symbol represents a fetus; the symbol is representative of the unique phosphatidylcholine fingerprint for that animal. The symbols are clustered by treatment group and this figure demonstrates that the phosphatidylcholine fingerprints from IUGR and control are dissimilar but are not completely distinct. Follow up analysis on the specific phosphatidylcholine species and consultation with lipidomics experts are needed to determine the viability of this finding.

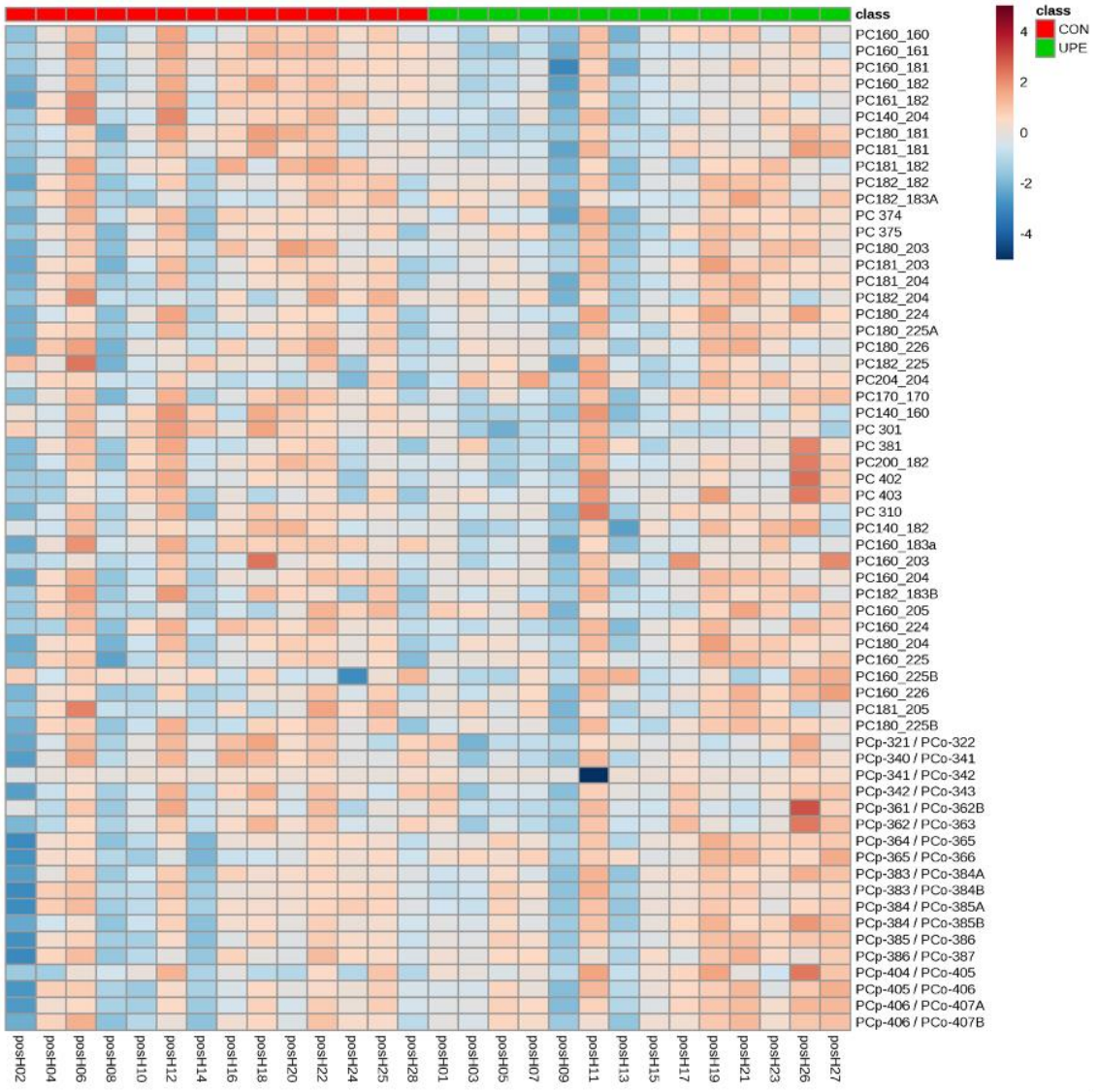

Figure 5-15 Phospatidylcholine heat map in IUGR and control myocardium

This heat map was produced using the same data from Figure 5-14 but separates the unique phosphatidylcholine fingerprint from each animal. There is no clear pattern of up or downregulation.

Phosphatidylethanolamine

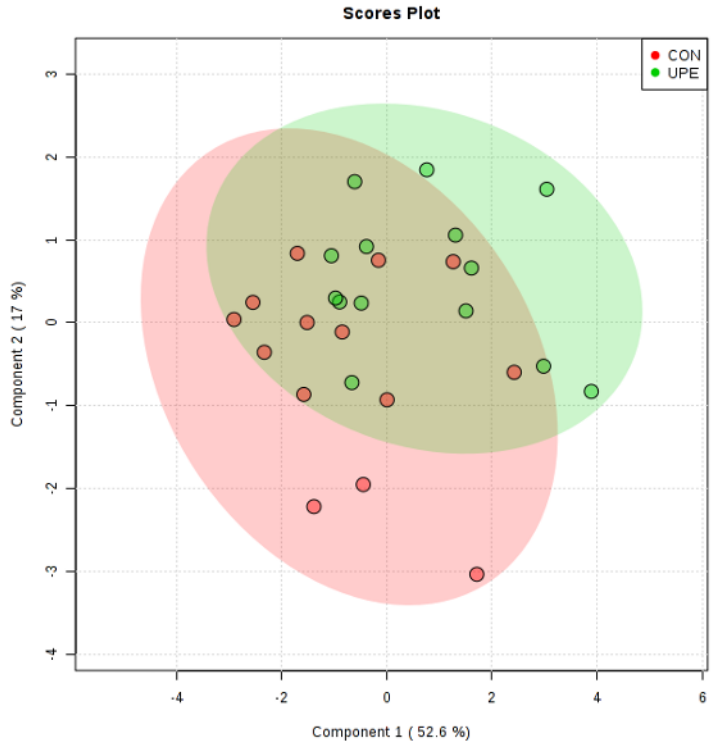

Figure 5-16 Phosphatidylethanolamine species in IUGR and control myocardium

(PLS-DA predominance of partial least squares – discriminant analysis)

In this figure, each symbol represents a fetus; the symbol is representative of the unique phosphatidylethanolamine fingerprint for that animal. The symbols are clustered by treatment group and this figure demonstrates that the phosphatidylethanolamine fingerprints from IUGR and control are dissimilar but are not completely distinct. Follow up analysis on the specific phosphatidylethanolamine species and consultation with lipidomics experts are needed to determine the viability of this finding.

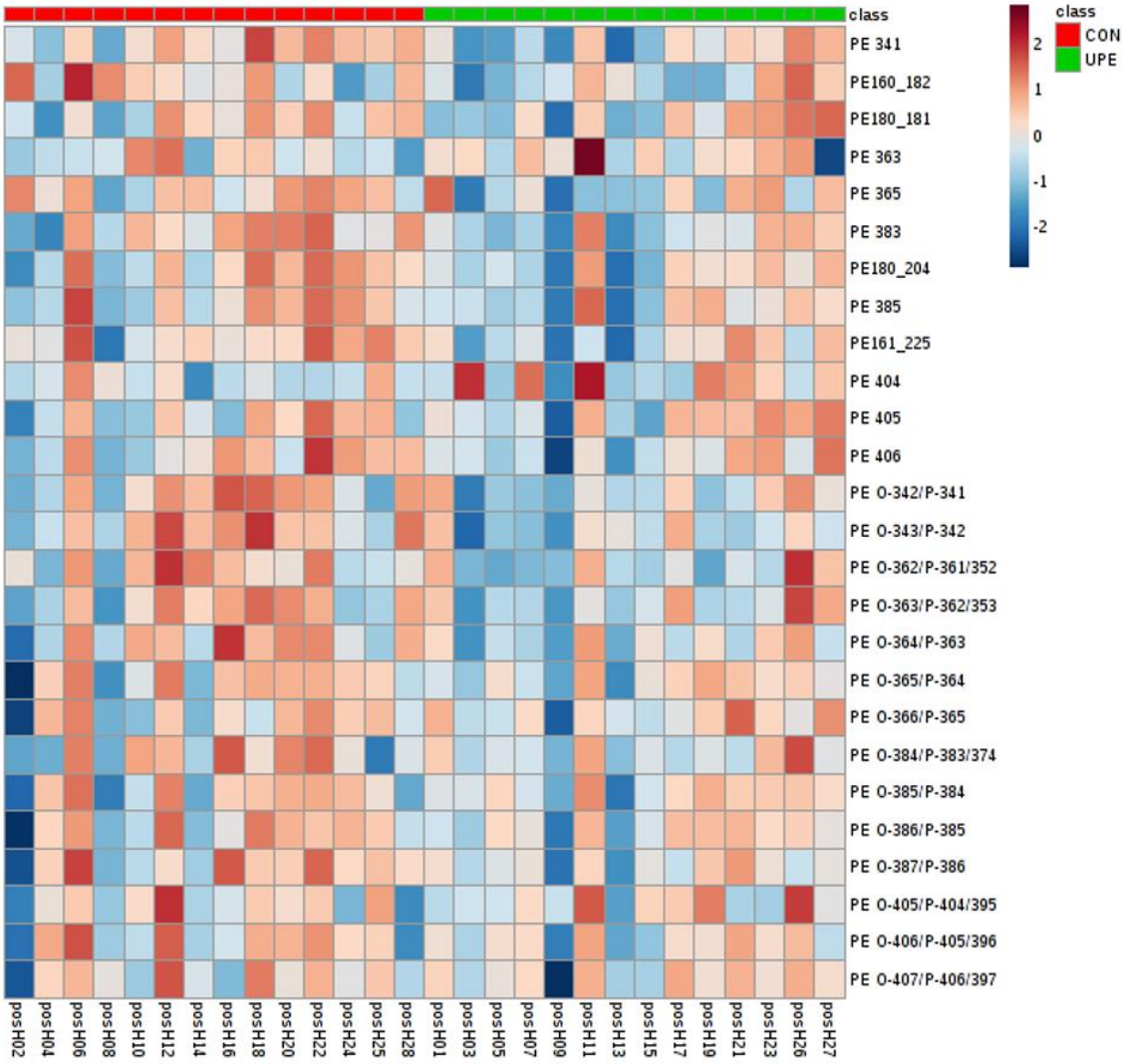

Figure 5-17 Phophatidylethanolamine heat map in IUGR and control myocardium

This heat map was produced using the same data from Figure 5-16 but separates the unique phosphatidylethanolamine fingerprint from each animal. There is no clear pattern of up or downregulation.

Circulating Acylcarnitines in IUGR plasma

Circulating acylcarnitines were measured in IUGR fetal (125d GA) sheep plasma in our model of umbilicoplacental embolization (10 days from 115-125d GA, see Chapter 3). Arterial blood samples were collected on the final day of the study at 126 ± 1 d GA (n=12 controls, n=12 IUGR). Samples were heparinized and centrifuged for 10 minutes, 2500g at 4°C and plasma stored at -20°C and analyzed for acylcarnitines by electrospray tandem mass spectrometry (Applied Biosystems/MDS SCIEX API 3000) at the Biochemical Genetics Laboratory, Mayo Clinic (Smith & Matern, 2010). Samples were compared to known internal standards and were identified by characteristic mass to charge ratios. This was done in collaboration with Melanie Gillingham (Oregon Health and Science University) and Dietrich Matern (Mayo Clinic, Rochester Minnesota). The data is separated in four groups: short, medium, long and other acylcarnitines.

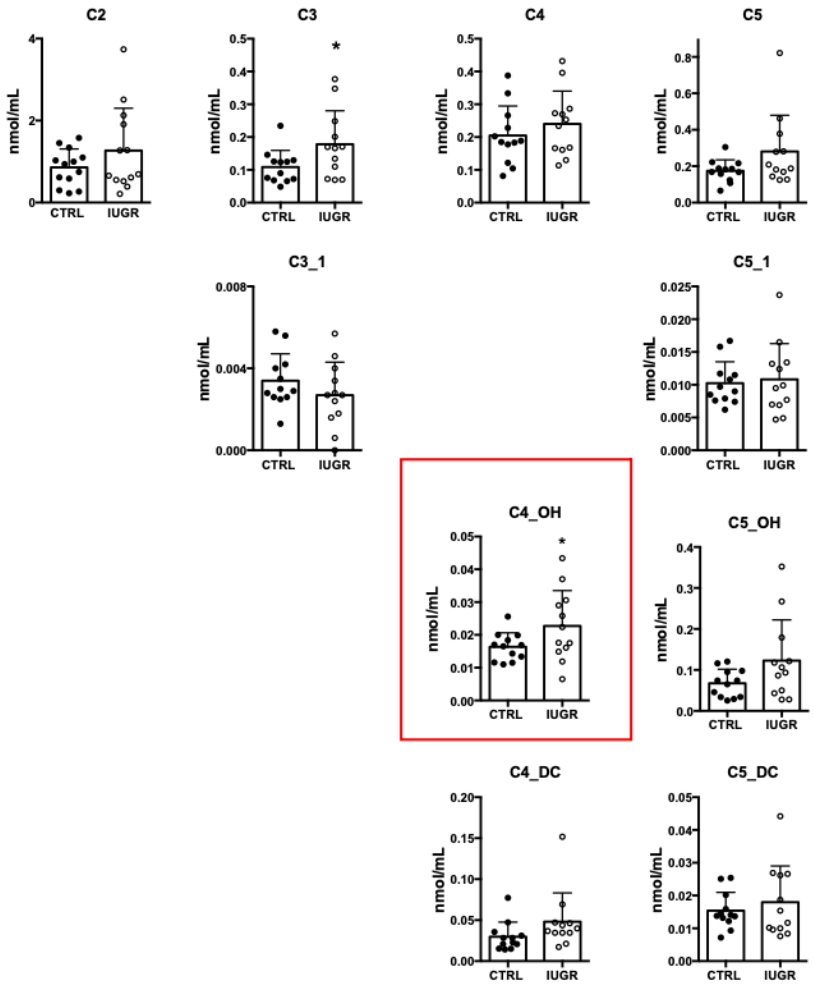

Figure 5-18 Short chain acylcarnitines in IUGR and fetal plasma

CTRL n=12, IUGR n=12. Mean ± SD, unpaired student's t-test. *p <0.05

Each column of graphs is the same chain length, each row has the same modifications and statistically significant differences are boxed in red.

Medium Chain Acylcarnitines

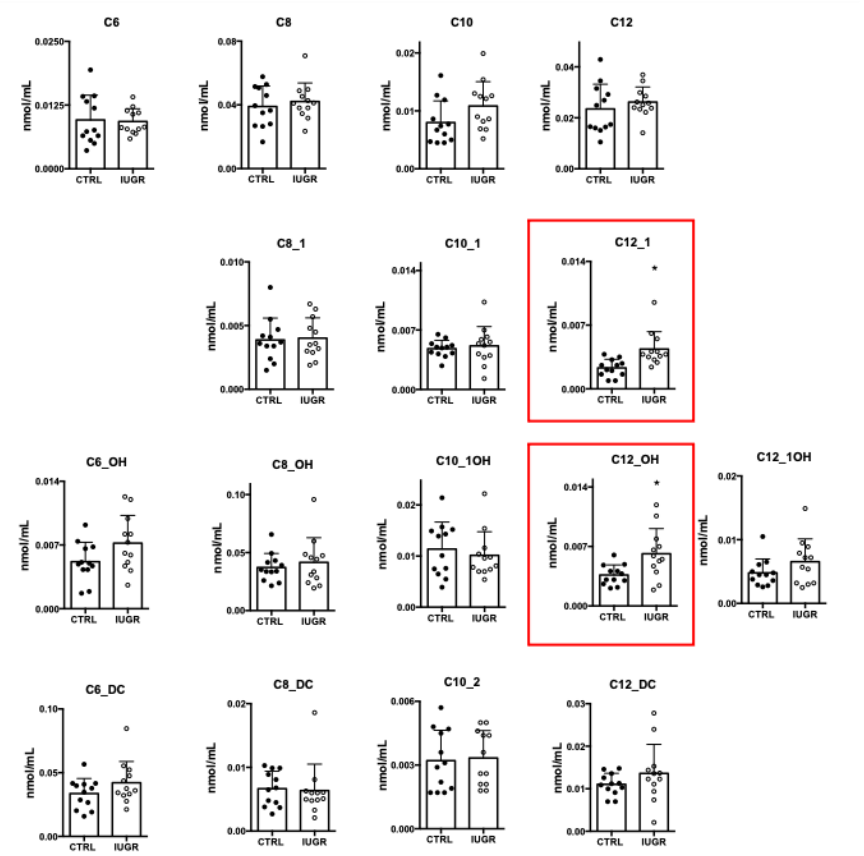

Figure 5-19 Medium chain acylcarnitines in IUGR and control fetal plasma

CTRL n=12, IUGR n=12. Mean ±SD, unpaired student's t-test. *p <0.05

Each column of graphs is the same chain length, each row has the same modifications and statistically significant differences are boxed in red.

Long Chain Acylcarnitines

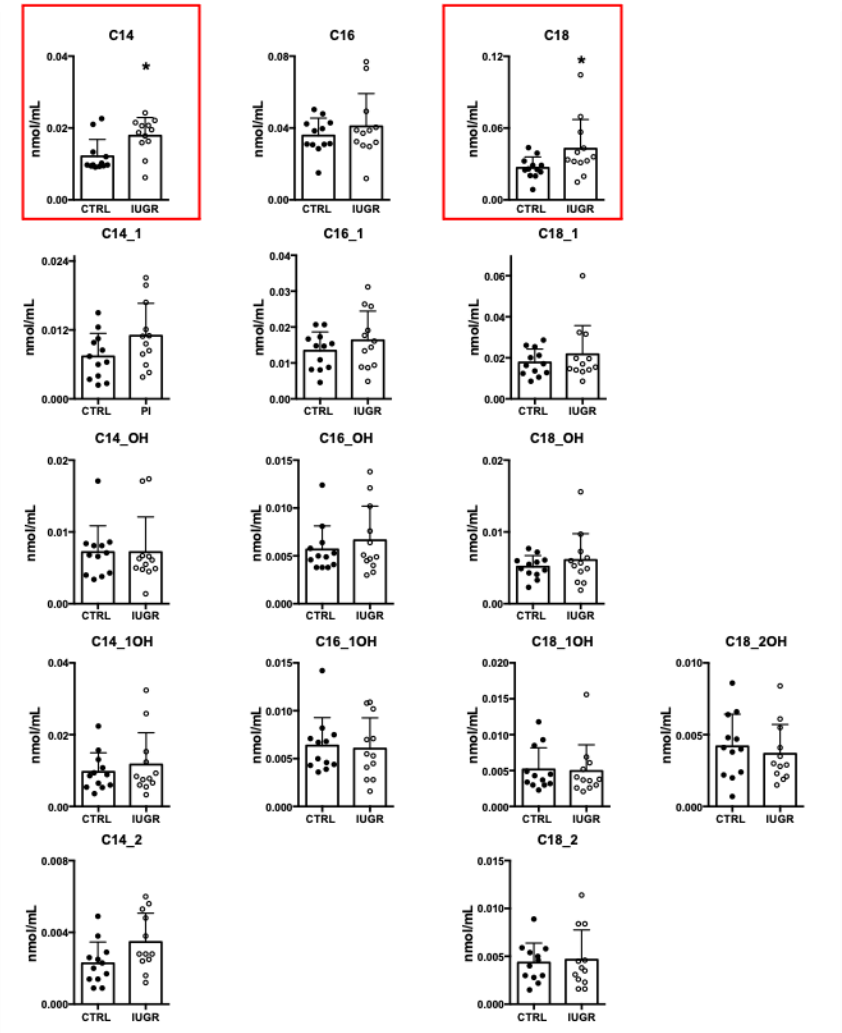

Figure 5-20 Long chain acylcarnitines in IUGR and control fetal plasma

CTRL n=12, IUGR n=12. Mean ±SD, unpaired student's t-test. *p <0.05

Each column of graphs is the same chain length, each row has the same modifications and statistically significant differences are boxed in red.

Additional Acylcarnitines

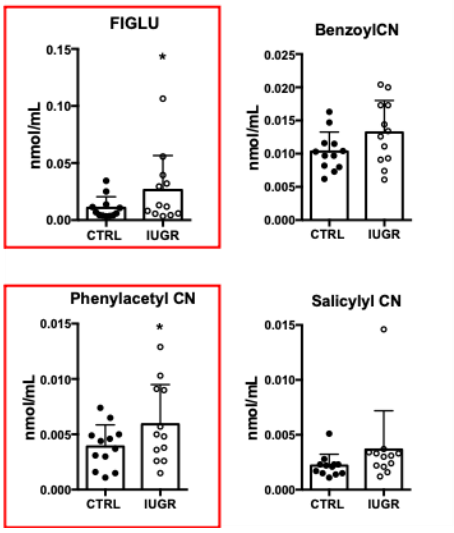

Figure 5-21 Additional acylcarnitines in IUGR and control fetal plasma

CTRL n=12, IUGR n=12. Mean ±SD, unpaired student's t-test. *p <0.05

Each column of graphs is the same chain length, each row has the same modifications and statistically significant differences are boxed in red.

Image analysis code

In order to quantify lipid droplet size (following incubation with BODIPY-C12 or BODIPY-C16) and compare this to cell area, maximum intensity projections of z-stacks were produced and the two codes below were run as macros in Fiji (Image J).

Code used to measure cell area:

```
run("Split Channels");
setAutoThreshold("MinError dark");
//run("Threshold...");
setOption("BlackBackground", false);
run("Convert to Mask");
run("Gaussian Blur...", "sigma=10");
run("Convert to Mask");
run("Erode");
run("Dilate");
run("Analyze Particles...", "size=400-Infinity show=Masks summarize");
```

Code used to measure droplets:

```
run("Split Channels");
green = getImageID();
selectImage(green);
run("Subtract Background...", "rolling=5 stack");
```

```
run("Despeckle", "stack");
run("Enhance Local Contrast (CLAHE)", "blocksize=9 histogram=256 maximum=4 mask=*None*");
run("Make Composite");
setAutoThreshold("Intermodes dark");
//run("Threshold...");
setOption("BlackBackground", false);
run("Convert to Mask");
run("Analyze Particles...", "size=0.0314-3.00 circularity=0.80-1.00 show=Outlines display summarize");
```

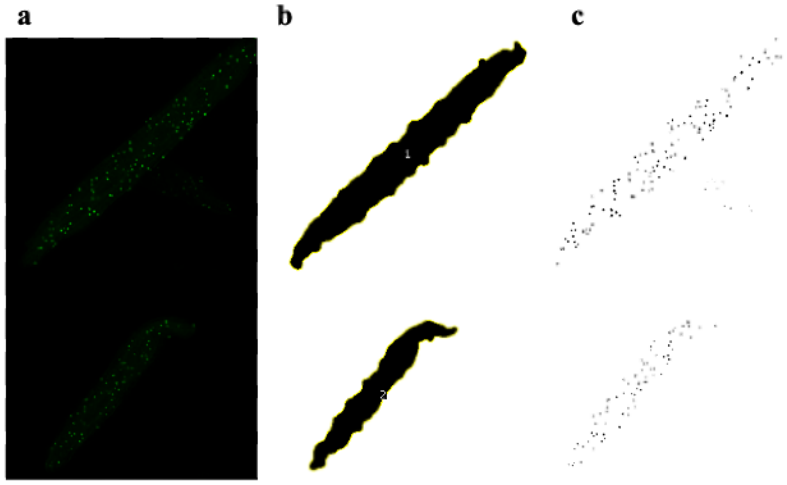

Figure 5-22 Sample of imaging analysis workflow.

(a) original image, (b) cell area mask, (c) lipid droplet mask.

REFERENCES

Abudurexiti M, Zhu W, Wang Y, Wang J, Xu W, Huang Y, Zhu Y, Shi G, Zhang H, Zhu Y, Shen Y, Dai B, Wan F, Lin G & Ye D. (2020). Targeting CPT1B as a potential therapeutic strategy in castration-resistant and enzalutamide-resistant prostate cancer. *Prostate* **80,** 950-961.

Ahmad T, Kelly JP, McGarrah RW, Hellkamp AS, Fiuzat M, Testani JM, Wang TS, Verma A, Samsky MD, Donahue MP, Ilkayeva OR, Bowles DE, Patel CB, Milano CA, Rogers JG, Felker GM, O'Connor CM, Shah SH & Kraus WE. (2016). Prognostic Implications of Long-Chain Acylcarnitines in Heart Failure and Reversibility With Mechanical Circulatory Support. *J Am Coll Cardiol* **67,** 291-299.

Alderman SL, Crossley DA, 2nd, Elsey RM & Gillis TE. (2019). Hypoxia-induced reprogramming of the cardiac phenotype in American alligators (Alligator mississippiensis) revealed by quantitative proteomics. *Sci Rep* **9,** 8592.

Ascuitto RJ, Ross-Ascuitto NT, Chen V & Downing SE. (1989). Ventricular function and fatty acid metabolism in neonatal piglet heart. *Am J Physiol* **256,** H9-15.

Bahtiyar MO & Copel JA. (2008). Cardiac changes in the intrauterine growth-restricted fetus. *Semin Perinatol* **32,** 190-193.

Barker DJ, Winter PD, Osmond C, Margetts B & Simmonds SJ. (1989). Weight in infancy and death from ischaemic heart disease. *Lancet* **2,** 577-580.

Barry JS, Davidsen ML, Limesand SW, Galan HL, Friedman JE, Regnault TR & Hay WW, Jr. (2006). Developmental changes in ovine myocardial glucose transporters and insulin signaling following hyperthermia-induced intrauterine fetal growth restriction. *Exp Biol Med (Maywood)* **231,** 566-575.

Barry JS, Rozance PJ, Brown LD, Anthony RV, Thornburg KL & Hay WW, Jr. (2016). Increased fetal myocardial sensitivity to insulin-stimulated glucose metabolism during ovine fetal growth restriction. *Exp Biol Med (Maywood)* **241,** 839-847.

Bartelds B, Knoester H, Smid GB, Takens J, Visser GH, Penninga L, van der Leij FR, Beaufort-Krol GC, Zijlstra WG, Heymans HS & Kuipers JR. (2000). Perinatal changes in myocardial metabolism in lambs. *Circulation* **102,** 926-931.

Bartelds B, Takens J, Smid GB, Zammit VA, Prip-Buus C, Kuipers JR & van der Leij FR. (2004). Myocardial carnitine palmitoyltransferase I expression and long-chain fatty acid oxidation in fetal and newborn lambs. *Am J Physiol Heart Circ Physiol* **286,** H2243-2248.

Beauchamp B, Thrush AB, Quizi J, Antoun G, McIntosh N, Al-Dirbashi OY, Patti ME & Harper ME. (2015). Undernutrition during pregnancy in mice leads to dysfunctional cardiac muscle respiration in adult offspring. *Biosci Rep* **35**.

Benyshek DC. (2007). The developmental origins of obesity and related health disorders--prenatal and perinatal factors. *Coll Antropol* **31,** 11-17.

Bergman EN. (1990). Energy contributions of volatile fatty acids from the gastrointestinal tract in various species. *Physiol Rev* **70,** 567-590.

Block BS, Schlafer DH, Wentworth RA, Kreitzer LA & Nathanielsz PW. (1990). Regional blood flow distribution in fetal sheep with intrauterine growth retardation produced by decreased umbilical placental perfusion. *J Dev Physiol* **13,** 81-85.

Boehmer BH, Limesand SW & Rozance PJ. (2017). The impact of IUGR on pancreatic islet development and beta-cell function. *J Endocrinol* **235,** R63-R76.

Bortz W, Abraham S, Chaikoff IL & Dozier WE. (1962). Fatty acid synthesis from acetate by human liver homogenate fractions. *J Clin Invest* **41,** 860-870.

Breckenridge RA, Piotrowska I, Ng KE, Ragan TJ, West JA, Kotecha S, Towers N, Bennett M, Kienesberger PC, Smolenski RT, Siddall HK, Offer JL, Mocanu MM, Yelon DM, Dyck JR, Griffin JL, Abramov AY, Gould AP & Mohun TJ. (2013). Hypoxic regulation of hand1 controls the fetal-neonatal switch in cardiac metabolism. *PLoS Biol* **11,** e1001666.

Brosnan JT & Fritz IB. (1971). The oxidation of fatty-acyl derivatives by mitochondria from bovine fetal and calf hearts. *Can J Biochem* **49,** 1296-1300.

Brown LD, Rozance PJ, Bruce JL, Friedman JE, Hay WW, Jr. & Wesolowski SR. (2015). Limited capacity for glucose oxidation in fetal sheep with intrauterine growth restriction. *Am J Physiol Regul Integr Comp Physiol* **309,** R920-928.

Brown NF, Weis BC, Husti JE, Foster DW & McGarry JD. (1995). Mitochondrial carnitine palmitoyltransferase I isoform switching in the developing rat heart. *J Biol Chem* **270,** 8952-8957.

Bubb KJ, Cock ML, Black MJ, Dodic M, Boon WM, Parkington HC, Harding R & Tare M. (2007). Intrauterine growth restriction delays cardiomyocyte maturation and alters coronary artery function in the fetal sheep. *J Physiol* **578,** 871-881.

Call L, Molina T, Stoll B, Guthrie G, Chacko S, Plat J, Robinson J, Lin S, Vonderohe C, Mohammad M, Kunichoff D, Cruz S, Lau P, Premkumar M, Nielsen J, Fang Z, Olutoye O, Thymann T, Britton R, Sangild P & Burrin D. (2020). Parenteral lipids shape gut bile acid pools and microbiota profiles in the prevention of cholestasis in preterm pigs. *J Lipid Res* **61,** 1038-1051.

Cetrullo S, D'Adamo S, Panichi V, Borzi RM, Pignatti C & Flamigni F. (2020). Modulation of Fatty Acid-Related Genes in the Response of H9c2 Cardiac Cells to Palmitate and n-3 Polyunsaturated Fatty Acids. *Cells* **9**.

Chan K, Ohlsson A, Synnes A, Lee DS, Chien LY, Lee SK & Canadian Neonatal N. (2001). Survival, morbidity, and resource use of infants of 25 weeks' gestational age or less. *Am J Obstet Gynecol* **185,** 220-226.

Chang YS, Tsai CT, Huangfu CA, Huang WY, Lei HY, Lin CF, Su IJ, Chang WT, Wu PH, Chen YT, Hung JH, Young KC & Lai MD. (2011). ACSL3 and GSK-3beta are essential for lipid upregulation induced by endoplasmic reticulum stress in liver cells. *J Cell Biochem* **112,** 881-893.

Chattergoon NN, Giraud GD, Louey S, Stork P, Fowden AL & Thornburg KL. (2012a). Thyroid hormone drives fetal cardiomyocyte maturation. *FASEB J* **26,** 397-408.

Chattergoon NN, Louey S, Stork P, Giraud GD & Thornburg KL. (2012b). Mid-gestation ovine cardiomyocytes are vulnerable to mitotic suppression by thyroid hormone. *Reprod Sci* **19,** 642-649.

Clubb FJ, Jr. & Bishop SP. (1984). Formation of binucleated myocardial cells in the neonatal rat. An index for growth hypertrophy. *Lab Invest* **50,** 571-577.

Coburn CT, Hajri T, Ibrahimi A & Abumrad NA. (2001). Role of CD36 in membrane transport and utilization of long-chain fatty acids by different tissues. *J Mol Neurosci* **16,** 117-121; discussion 151-117.

Coburn CT, Knapp FF, Jr., Febbraio M, Beets AL, Silverstein RL & Abumrad NA. (2000). Defective uptake and utilization of long chain fatty acids in muscle and adipose tissues of CD36 knockout mice. *J Biol Chem* **275,** 32523-32529.

Cock ML, Camm EJ, Louey S, Joyce BJ & Harding R. (2001). Postnatal outcomes in term and preterm lambs following fetal growth restriction. *Clin Exp Pharmacol Physiol* **28,** 931-937.

Cock ML & Harding R. (1997). Renal and amniotic fluid responses to umbilicoplacental embolization for 20 days in fetal sheep. *Am J Physiol* **273,** R1094-1102.

Cock ML, Joyce BJ, Hooper SB, Wallace MJ, Gagnon R, Brace RA, Louey S & Harding R. (2004). Pulmonary elastin synthesis and deposition in developing and mature sheep: effects of intrauterine growth restriction. *Exp Lung Res* **30,** 405-418.

Cohn HE, Sacks EJ, Heymann MA & Rudolph AM. (1974). Cardiovascular responses to hypoxemia and acidemia in fetal lambs. *Am J Obstet Gynecol* **120,** 817-824.

Cook GA, Edwards TL, Jansen MS, Bahouth SW, Wilcox HG & Park EA. (2001). Differential regulation of carnitine palmitoyltransferase-I gene isoforms (CPT-I alpha and CPT-I beta) in the rat heart. *J Mol Cell Cardiol* **33,** 317-329.

Corstius HB, Zimanyi MA, Maka N, Herath T, Thomas W, van der Laarse A, Wreford NG & Black MJ. (2005). Effect of intrauterine growth restriction on the number of cardiomyocytes in rat hearts. *Pediatr Res* **57,** 796-800.

Cox KB, Liu J, Tian L, Barnes S, Yang Q & Wood PA. (2009). Cardiac hypertrophy in mice with long-chain acyl-CoA dehydrogenase or very long-chain acyl-CoA dehydrogenase deficiency. *Lab Invest* **89,** 1348-1354.

Davies KL, Camm EJ, Atkinson EV, Lopez T, Forhead AJ, Murray AJ & Fowden AL. (2020). Development and thyroid hormone dependence of skeletal muscle mitochondrial function towards birth. *J Physiol* **598,** 2453-2468.

Dawes GS, Johnston BM & Walker DW. (1980). Relationship of arterial pressure and heart rate in fetal, new-born and adult sheep. *J Physiol* **309,** 405-417.

Dawes GS, Mott JC & Widdicombe JG. (1954). The foetal circulation in the lamb. *J Physiol* **126,** 563-587.

De Blasio MJ, Gatford KL, McMillen IC, Robinson JS & Owens JA. (2007). Placental restriction of fetal growth increases insulin action, growth, and adiposity in the young lamb. *Endocrinology* **148,** 1350-1358.

de Brito Alves JL, Toscano AE, da Costa-Silva JH, Vidal H, Leandro CG & Pirola L. (2017). Transcriptional response of skeletal muscle to a low protein perinatal diet in rat offspring at different ages: The role of key enzymes of glucose-fatty acid oxidation. *J Nutr Biochem* **41,** 117-123.

de Oliveira Lira A, de Brito Alves JL, Pinheiro Fernandes M, Vasconcelos D, Santana DF, da Costa-Silva JH, Morio B, Gois Leandro C & Pirola L. (2020). Maternal low protein diet induces persistent expression changes in metabolic genes in male rats. *World J Diabetes* **11,** 182-192.

Djurhuus CB, Gravholt CH, Nielsen S, Mengel A, Christiansen JS, Schmitz OE & Moller N. (2002). Effects of cortisol on lipolysis and regional interstitial glycerol levels in humans. *Am J Physiol Endocrinol Metab* **283,** E172-177.

Duncan JR, Cock ML, Loeliger M, Louey S, Harding R & Rees SM. (2004). Effects of exposure to chronic placental insufficiency on the postnatal brain and retina in sheep. *J Neuropathol Exp Neurol* **63,** 1131-1143.

Economides DL, Nicolaides KH, Linton EA, Perry LA & Chard T. (1988). Plasma cortisol and adrenocorticotropin in appropriate and small for gestational age fetuses. *Fetal Ther* **3,** 158-164.

El-Wahed MAA, El-Farghali OG, ElAbd HSA, El-Desouky ED & Hassan SM. (2017). Metabolic Derangements in IUGR neonates detected at birth using UPLC-MS. *The Egyptian Journal of Medical Human Genetics* **18,** 281-287.

Ellis JM, Mentock SM, Depetrillo MA, Koves TR, Sen S, Watkins SM, Muoio DM, Cline GW, Taegtmeyer H, Shulman GI, Willis MS & Coleman RA. (2011). Mouse cardiac acyl coenzyme a synthetase 1 deficiency impairs Fatty Acid oxidation and induces cardiac hypertrophy. *Mol Cell Biol* **31,** 1252-1262.

Fisher DJ, Heymann MA & Rudolph AM. (1980). Myocardial oxygen and carbohydrate consumption in fetal lambs in utero and in adult sheep. *Am J Physiol* **238,** H399-405.

Fisher DJ, Heymann MA & Rudolph AM. (1981). Myocardial consumption of oxygen and carbohydrates in newborn sheep. *Pediatr Res* **15,** 843-846.

Gagnon R, Challis J, Johnston L & Fraher L. (1994). Fetal endocrine responses to chronic placental embolization in the late-gestation ovine fetus. *Am J Obstet Gynecol* **170,** 929-938.

Gagnon R, Johnston L & Murotsuki J. (1996). Fetal placental embolization in the late-gestation ovine fetus: alterations in umbilical blood flow and fetal heart rate patterns. *Am J Obstet Gynecol* **175,** 63-72.

Gimeno RE, Ortegon AM, Patel S, Punreddy S, Ge P, Sun Y, Lodish HF & Stahl A. (2003). Characterization of a heart-specific fatty acid transport protein. *J Biol Chem* **278,** 16039-16044.

Girard J, Pintado E & Ferre P. (1979). Fuel Metabolism in the Mammalian Fetus. *Annales de biologie animale, biochimie, biophysique* **19,** 181-197.

Giussani DA. (2016). The fetal brain sparing response to hypoxia: physiological mechanisms. *J Physiol* **594,** 1215-1230.

Giussani DA, Camm EJ, Niu Y, Richter HG, Blanco CE, Gottschalk R, Blake EZ, Horder KA, Thakor AS, Hansell JA, Kane AD, Wooding FB, Cross CM & Herrera EA. (2012). Developmental programming of cardiovascular dysfunction by prenatal hypoxia and oxidative stress. *PLoS One* **7,** e31017.

Giussani DA, Niu Y, Herrera EA, Richter HG, Camm EJ, Thakor AS, Kane AD, Hansell JA, Brain KL, Skeffington KL, Itani N, Wooding FB, Cross CM & Allison BJ. (2014). Heart disease link to fetal hypoxia and oxidative stress. *Adv Exp Med Biol* **814,** 77-87.

Glatz JF & Veerkamp JH. (1982). Postnatal development of palmitate oxidation and mitochondrial enzyme activities in rat cardiac and skeletal muscle. *Biochim Biophys Acta* **711,** 327-335.

Goldberg IJ, Reue K, Abumrad NA, Bickel PE, Cohen S, Fisher EA, Galis ZS, Granneman JG, Lewandowski ED, Murphy R, Olive M, Schaffer JE, Schwartz-

Longacre L, Shulman GI, Walther TC & Chen J. (2018). Deciphering the Role of Lipid Droplets in Cardiovascular Disease: A Report From the 2017 National Heart, Lung, and Blood Institute Workshop. *Circulation* **138,** 305-315.

Gonzalez-Tendero A, Torre I, Garcia-Canadilla P, Crispi F, Garcia-Garcia F, Dopazo J, Bijnens B & Gratacos E. (2013). Intrauterine growth restriction is associated with cardiac ultrastructural and gene expression changes related to the energetic metabolism in a rabbit model. *Am J Physiol Heart Circ Physiol* **305,** H1752-1760.

Grevengoed TJ, Klett EL & Coleman RA. (2014). Acyl-CoA metabolism and partitioning. *Annu Rev Nutr* **34,** 1-30.

Grynberg A & Demaison L. (1996). Fatty Acid Oxidation in the Heart. *Journal of Cardiovascular Pharmacology* **28,** 11-17.

Gupta AK, Savopoulos CG, Ahuja J & Hatzitolios AI. (2011). Role of phytosterols in lipid-lowering: current perspectives. *QJM* **104,** 301-308.

Hanson RW & Ballard FJ. (1967). The relative significance of acetate and glucose as precursors for lipid synthesis in liver and adipose tissue from ruminants. *Biochem J* **105,** 529-536.

Hay WW, Jr. (2008). Strategies for feeding the preterm infant. *Neonatology* **94,** 245-254.

Hoffman DJ, Reynolds RM & Hardy DB. (2017). Developmental origins of health and disease: current knowledge and potential mechanisms. *Nutr Rev* **75,** 951-970.

Huang, Li T, Li X, Zhang L, Sun L, He X, Zhong X, Jia D, Song L, Semenza GL, Gao P & Zhang H. (2014). HIF-1-mediated suppression of acyl-CoA dehydrogenases and fatty acid oxidation is critical for cancer progression. *Cell Rep* **8,** 1930-1942.

Iruretagoyena JI, Davis W, Bird C, Olsen J, Radue R, Teo Broman A, Kendziorski C, Splinter BonDurant S, Golos T, Bird I & Shah D. (2014). Metabolic gene profile in early human fetal heart development. *Mol Hum Reprod* **20,** 690-700.

Jonker SS, Kamna D, LoTurco D, Kailey J & Brown LD. (2018). IUGR impairs cardiomyocyte growth and maturation in fetal sheep. *J Endocrinol* **239,** 253-265.

Jonker SS & Louey S. (2016). Endocrine and other physiologic modulators of perinatal cardiomyocyte endowment. *J Endocrinol* **228,** R1-18.

Jonker SS, Louey S, Giraud GD, Thornburg KL & Faber JJ. (2015). Timing of cardiomyocyte growth, maturation, and attrition in perinatal sheep. *FASEB J* **29,** 4346-4357.

Jonker SS, Zhang L, Louey S, Giraud GD, Thornburg KL & Faber JJ. (2007). Myocyte enlargement, differentiation, and proliferation kinetics in the fetal sheep heart. *J Appl Physiol (1985)* **102,** 1130-1142.

Joyce BJ, Louey S, Davey MG, Cock ML, Hooper SB & Harding R. (2001). Compromised respiratory function in postnatal lambs after placental insufficiency and intrauterine growth restriction. *Pediatr Res* **50,** 641-649.

Kassan A, Herms A, Fernandez-Vidal A, Bosch M, Schieber NL, Reddy BJ, Fajardo A, Gelabert-Baldrich M, Tebar F, Enrich C, Gross SP, Parton RG & Pol A. (2013). Acyl-CoA synthetase 3 promotes lipid droplet biogenesis in ER microdomains. *J Cell Biol* **203,** 985-1001.

Kelly DA. (2006). Intestinal failure-associated liver disease: what do we know today? *Gastroenterology* **130,** S70-77.

Kesavan K & Devaskar SU. (2019). Intrauterine Growth Restriction: Postnatal Monitoring and Outcomes. *Pediatr Clin North Am* **66,** 403-423.

Kiserud T, Ozaki T, Nishina H, Rodeck C & Hanson MA. (2000). Effect of NO, phenylephrine, and hypoxemia on ductus venosus diameter in fetal sheep. *Am J Physiol Heart Circ Physiol* **279,** H1166-1171.

Kolahi K, Louey S, Varlamov O & Thornburg K. (2016). Real-Time Tracking of BODIPY-C12 Long-Chain Fatty Acid in Human Term Placenta Reveals Unique Lipid Dynamics in Cytotrophoblast Cells. *PLoS One* **11,** e0153522.

Kurtz DM, Rinaldo P, Rhead WJ, Tian L, Millington DS, Vockley J, Hamm DA, Brix AE, Lindsey JR, Pinkert CA, O'Brien WE & Wood PA. (1998). Targeted disruption of mouse long-chain acyl-CoA dehydrogenase gene reveals crucial roles for fatty acid oxidation. *Proc Natl Acad Sci U S A* **95,** 15592-15597.

Lalowski MM, Bjork S, Finckenberg P, Soliymani R, Tarkia M, Calza G, Blokhina D, Tulokas S, Kankainen M, Lakkisto P, Baumann M, Kankuri E & Mervaala E.

(2018). Characterizing the Key Metabolic Pathways of the Neonatal Mouse Heart Using a Quantitative Combinatorial Omics Approach. *Front Physiol* **9,** 365.

Lee SJ, Zhang J, Choi AM & Kim HP. (2013). Mitochondrial dysfunction induces formation of lipid droplets as a generalized response to stress. *Oxid Med Cell Longev* **2013,** 327167.

Leger J, Oury JF, Noel M, Baron S, Benali K, Blot P & Czernichow P. (1996). Growth factors and intrauterine growth retardation. I. Serum growth hormone, insulin-like growth factor (IGF)-I, IGF-II, and IGF binding protein 3 levels in normally grown and growth-retarded human fetuses during the second half of gestation. *Pediatr Res* **40,** 94-100.

Lewandowski AJ, Lazdam M, Davis E, Kylintireas I, Diesch J, Francis J, Neubauer S, Singhal A, Lucas A, Kelly B & Leeson P. (2011). Short-term exposure to exogenous lipids in premature infants and long-term changes in aortic and cardiac function. *Arterioscler Thromb Vasc Biol* **31,** 2125-2135.

Li G, Bae S & Zhang L. (2004). Effect of prenatal hypoxia on heat stress-mediated cardioprotection in adult rat heart. *Am J Physiol Heart Circ Physiol* **286,** H1712-1719.

Li T, Li X, Meng H, Chen L & Meng F. (2020). ACSL1 affects Triglyceride Levels through the PPARgamma Pathway. *Int J Med Sci* **17,** 720-727.

Limesand SW, Rozance PJ, Zerbe GO, Hutton JC & Hay WW, Jr. (2006). Attenuated insulin release and storage in fetal sheep pancreatic islets with intrauterine growth restriction. *Endocrinology* **147,** 1488-1497.

Lindgren IM, Drake RR, Chattergoon NN & Thornburg KL. (2019). Down-regulation of MEIS1 promotes the maturation of oxidative phosphorylation in perinatal cardiomyocytes. *FASEB J* **33,** 7417-7426.

Liu J, Chen XX, Li XW, Fu W & Zhang WQ. (2016). Metabolomic Research on Newborn Infants With Intrauterine Growth Restriction. *Medicine (Baltimore)* **95,** e3564.

Lo JO, Roberts VHJ, Schabel MC, Wang X, Morgan TK, Liu Z, Studholme C, Kroenke CD & Frias AE. (2018). Novel Detection of Placental Insufficiency by Magnetic Resonance Imaging in the Nonhuman Primate. *Reprod Sci* **25,** 64-73.

Loeliger M, Duncan J, Louey S, Cock M, Harding R & Rees S. (2005). Fetal growth restriction induced by chronic placental insufficiency has long-term effects on the retina but not the optic nerve. *Invest Ophthalmol Vis Sci* **46,** 3300-3308.

Loeliger M, Louey S, Cock ML, Harding R & Rees SM. (2003). Chronic placental insufficiency and foetal growth restriction lead to long-term effects on postnatal retinal structure. *Clin Exp Ophthalmol* **31,** 250-253.

Lopaschuk GD, Collins-Nakai RL & Itoi T. (1992). Developmental changes in energy substrate use by the heart. *Cardiovasc Res* **26,** 1172-1180.

Lopaschuk GD & Jaswal JS. (2010). Energy metabolic phenotype of the cardiomyocyte during development, differentiation, and postnatal maturation. *J Cardiovasc Pharmacol* **56,** 130-140.

Lopaschuk GD, Spafford MA & Marsh DR. (1991). Glycolysis is predominant source of myocardial ATP production immediately after birth. *Am J Physiol* **261,** H1698-1705.

Lopaschuk GD, Ussher JR, Folmes CD, Jaswal JS & Stanley WC. (2010). Myocardial fatty acid metabolism in health and disease. *Physiol Rev* **90,** 207-258.

Louey S, Cock ML & Harding R. (2005). Long term consequences of low birthweight on postnatal growth, adiposity and brain weight at maturity in sheep. *J Reprod Dev* **51,** 59-68.

Louey S, Cock ML, Stevenson KM & Harding R. (2000). Placental insufficiency and fetal growth restriction lead to postnatal hypotension and altered postnatal growth in sheep. *Pediatr Res* **48,** 808-814.

Louey S, Jonker SS, Giraud GD & Thornburg KL. (2007). Placental insufficiency decreases cell cycle activity and terminal maturation in fetal sheep cardiomyocytes. *J Physiol* **580,** 639-648.

Magee TR, Han G, Cherian B, Khorram O, Ross MG & Desai M. (2008). Down-regulation of transcription factor peroxisome proliferator-activated receptor in programmed hepatic lipid dysregulation and inflammation in intrauterine growth-restricted offspring. *Am J Obstet Gynecol* **199,** 271 e271-275.

Makrecka-Kuka M, Sevostjanovs E, Vilks K, Volska K, Antone U, Kuka J, Makarova E, Pugovics O, Dambrova M & Liepinsh E. (2017). Plasma acylcarnitine concentrations reflect the acylcarnitine profile in cardiac tissues. *Sci Rep* **7,** 17528.

Mallard EC, Rees S, Stringer M, Cock ML & Harding R. (1998). Effects of chronic placental insufficiency on brain development in fetal sheep. *Pediatr Res* **43,** 262-270.

Maritz GS, Cock ML, Louey S, Suzuki K & Harding R. (2004). Fetal growth restriction has long-term effects on postnatal lung structure in sheep. *Pediatr Res* **55,** 287-295.

Mashek DG, Li LO & Coleman RA. (2006). Rat long-chain acyl-CoA synthetase mRNA, protein, and activity vary in tissue distribution and in response to diet. *J Lipid Res* **47,** 2004-2010.

Mayhew TM, Gregson C & Fagan DG. (1999). Ventricular myocardium in control and growth-retarded human fetuses: growth in different tissue compartments and variation with fetal weight, gestational age, and ventricle size. *Hum Pathol* **30,** 655-660.

Mdaki KS, Larsen TD, Wachal AL, Schimelpfenig MD, Weaver LJ, Dooyema SD, Louwagie EJ & Baack ML. (2016a). Maternal high-fat diet impairs cardiac function in offspring of diabetic pregnancy through metabolic stress and mitochondrial dysfunction. *Am J Physiol Heart Circ Physiol* **310,** H681-692.

Mdaki KS, Larsen TD, Weaver LJ & Baack ML. (2016b). Age Related Bioenergetics Profiles in Isolated Rat Cardiomyocytes Using Extracellular Flux Analyses. *PLoS One* **11,** e0149002.

Meyburg J, Schulze A, Kohlmueller D, Linderkamp O & Mayatepek E. (2001). Postnatal changes in neonatal acylcarnitine profile. *Pediatr Res* **49,** 125-129.

Mitchell EK, Louey S, Cock ML, Harding R & Black MJ. (2004). Nephron endowment and filtration surface area in the kidney after growth restriction of fetal sheep. *Pediatr Res* **55,** 769-773.

Moody L, Xu GB, Chen H & Pan YX. (2019). Epigenetic regulation of carnitine palmitoyltransferase 1 (Cpt1a) by high fat diet. *Biochim Biophys Acta Gene Regul Mech* **1862,** 141-152.

Morrison JL, Botting KJ, Dyer JL, Williams SJ, Thornburg KL & McMillen IC. (2007). Restriction of placental function alters heart development in the sheep fetus. *Am J Physiol Regul Integr Comp Physiol* **293,** R306-313.

Most AS, Brachfeld N, Gorlin R & Wahren J. (1969). Free fatty acid metabolism of the human heart at rest. *J Clin Invest* **48,** 1177-1188.

Muralimanoharan S, Li C, Nakayasu ES, Casey CP, Metz TO, Nathanielsz PW & Maloyan A. (2017). Sexual dimorphism in the fetal cardiac response to maternal nutrient restriction. *J Mol Cell Cardiol* **108,** 181-193.

Murotsuki J, Challis JR, Han VK, Fraher LJ & Gagnon R. (1997). Chronic fetal placental embolization and hypoxemia cause hypertension and myocardial hypertrophy in fetal sheep. *Am J Physiol* **272,** R201-207.

Mylonis I, Simos G & Paraskeva E. (2019). Hypoxia-Inducible Factors and the Regulation of Lipid Metabolism. *Cells* **8**.

Nardozza LM, Caetano AC, Zamarian AC, Mazzola JB, Silva CP, Marcal VM, Lobo TF, Peixoto AB & Araujo Junior E. (2017). Fetal growth restriction: current knowledge. *Arch Gynecol Obstet* **295,** 1061-1077.

Neely JR & Morgan HE. (1974). Relationship between carbohydrate and lipid metabolism and the energy balance of heart muscle. *Annu Rev Physiol* **36,** 413-459.

Neely JR, Rovetto MJ & Oram JF. (1972). Myocardial utilization of carbohydrate and lipids. *Prog Cardiovasc Dis* **15,** 289-329.

Nicolaides KH, Economides DL & Soothill PW. (1989). Blood gases, pH, and lactate in appropriate- and small-for-gestational-age fetuses. *Am J Obstet Gynecol* **161,** 996-1001.

Noble RC, Shand JH & Calvert DT. (1982). The role of the placenta in the supply of essential fatty acids to the fetal sheep: studies of lipid compositions at term. *Placenta* **3,** 287-295.

Nose F, Yamaguchi T, Kato R, Aiuchi T, Obama T, Hara S, Yamamoto M & Itabe H. (2013). Crucial role of perilipin-3 (TIP47) in formation of lipid droplets and PGE2 production in HL-60-derived neutrophils. *PLoS One* **8,** e71542.

O'Brien T, Dinneen SF, O'Brien PC & Palumbo PJ. (1993). Hyperlipidemia in patients with primary and secondary hypothyroidism. *Mayo Clin Proc* **68,** 860-866.

Owens JA, Thavaneswaran P, De Blasio MJ, McMillen IC, Robinson JS & Gatford KL. (2007). Sex-specific effects of placental restriction on components of the metabolic syndrome in young adult sheep. *Am J Physiol Endocrinol Metab* **292,** E1879-1889.

Partridge EA, Davey MG, Hornick MA, McGovern PE, Mejaddam AY, Vrecenak JD, Mesas-Burgos C, Olive A, Caskey RC, Weiland TR, Han J, Schupper AJ, Connelly JT, Dysart KC, Rychik J, Hedrick HL, Peranteau WH & Flake AW. (2017). An extra-uterine system to physiologically support the extreme premature lamb. *Nat Commun* **8,** 15112.

Peleg D, Kennedy CM & Hunter SK. (1998). Intrauterine growth restriction: identification and management. *Am Fam Physician* **58,** 453-460, 466-457.

Piquereau J & Ventura-Clapier R. (2018). Maturation of Cardiac Energy Metabolism During Perinatal Development. *Front Physiol* **9,** 959.

Rajabi M, Kassiotis C, Razeghi P & Taegtmeyer H. (2007). Return to the fetal gene program protects the stressed heart: a strong hypothesis. *Heart Fail Rev* **12,** 331-343.

Rambold AS, Cohen S & Lippincott-Schwartz J. (2015). Fatty acid trafficking in starved cells: regulation by lipid droplet lipolysis, autophagy, and mitochondrial fusion dynamics. *Dev Cell* **32,** 678-692.

Rasanen J, Debbs RH & Huhta JC. (1997). Echocardiography in intrauterine growth restriction. *Clin Obstet Gynecol* **40,** 796-803.

Razeghi P, Young ME, Alcorn JL, Moravec CS, Frazier OH & Taegtmeyer H. (2001). Metabolic gene expression in fetal and failing human heart. *Circulation* **104,** 2923-2931.

Reller MD, Morton MJ, Reid DL & Thornburg KL. (1987). Fetal lamb ventricles respond differently to filling and arterial pressures and to in utero ventilation. *Pediatr Res* **22,** 621-626.

Roberts VH, Rasanen JP, Novy MJ, Frias A, Louey S, Morgan TK, Thornburg KL, Spindel ER & Grigsby PL. (2012). Restriction of placental vasculature in a non-human primate: a unique model to study placental plasticity. *Placenta* **33,** 73-76.

Rolph TP & Jones CT. (1983). Regulation of glycolytic flux in the heart of the fetal guinea pig. *J Dev Physiol* **5,** 31-49.

Rueda-Clausen CF, Dolinsky VW, Morton JS, Proctor SD, Dyck JR & Davidge ST. (2011a). Hypoxia-induced intrauterine growth restriction increases the susceptibility of rats to high-fat diet-induced metabolic syndrome. *Diabetes* **60,** 507-516.

Rueda-Clausen CF, Morton JS, Lopaschuk GD & Davidge ST. (2011b). Long-term effects of intrauterine growth restriction on cardiac metabolism and susceptibility to ischaemia/reperfusion. *Cardiovasc Res* **90,** 285-294.

Ruiz M, Labarthe F, Fortier A, Bouchard B, Thompson Legault J, Bolduc V, Rigal O, Chen J, Ducharme A, Crawford PA, Tardif JC & Des Rosiers C. (2017). Circulating acylcarnitine profile in human heart failure: a surrogate of fatty acid metabolic dysregulation in mitochondria and beyond. *Am J Physiol Heart Circ Physiol* **313,** H768-H781.

Sack MN, Rader TA, Park S, Bastin J, McCune SA & Kelly DP. (1996). Fatty acid oxidation enzyme gene expression is downregulated in the failing heart. *Circulation* **94,** 2837-2842.

Salama GS, Kaabneh MA, Almasaeed MN & Alquran M. (2015). Intravenous lipids for preterm infants: a review. *Clin Med Insights Pediatr* **9,** 25-36.

Sandoval A, Fraisl P, Arias-Barrau E, Dirusso CC, Singer D, Sealls W & Black PN. (2008). Fatty acid transport and activation and the expression patterns of genes involved in fatty acid trafficking. *Arch Biochem Biophys* **477,** 363-371.

Sayre NL & Lechleiter JD. (2012). Fatty acid metabolism and thyroid hormones. *Curr Trends Endocinol* **6,** 65-76.

Schiff M, Haberberger B, Xia C, Mohsen AW, Goetzman ES, Wang Y, Uppala R, Zhang Y, Karunanidhi A, Prabhu D, Alharbi H, Prochownik EV, Haack T, Haberle J, Munnich A, Rotig A, Taylor RW, Nicholls RD, Kim JJ, Prokisch H & Vockley J. (2015). Complex I assembly function and fatty acid oxidation

enzyme activity of ACAD9 both contribute to disease severity in ACAD9 deficiency. *Hum Mol Genet* **24,** 3238-3247.

Schlaepfer IR & Joshi M. (2020). CPT1A-mediated Fat Oxidation, Mechanisms, and Therapeutic Potential. *Endocrinology* **161**.

Schulz LC. (2010). The Dutch Hunger Winter and the developmental origins of health and disease. *Proc Natl Acad Sci U S A* **107,** 16757-16758.

Schulze PC, Drosatos K & Goldberg IJ. (2016). Lipid Use and Misuse by the Heart. *Circulation research* **118,** 1736-1751.

Selak MA, Storey BT, Peterside I & Simmons RA. (2003). Impaired oxidative phosphorylation in skeletal muscle of intrauterine growth-retarded rats. *Am J Physiol Endocrinol Metab* **285,** E130-137.

Smith EH & Matern D. (2010). Acylcarnitine analysis by tandem mass spectrometry. *Curr Protoc Hum Genet* **Chapter 17,** Unit 17 18 11-20.

Smolich JJ. (1995). Ultrastructural and functional features of the developing mammalian heart: a brief overview. *Reprod Fertil Dev* **7,** 451-461.

Spray JW. (2016). Review of Intravenous Lipid Emulsion Therapy. *J Infus Nurs* **39,** 377-380.

Stahl A. (2004). A current review of fatty acid transport proteins (SLC27). *Pflugers Arch* **447,** 722-727.

Stahl A, Hirsch DJ, Gimeno RE, Punreddy S, Ge P, Watson N, Patel S, Kotler M, Raimondi A, Tartaglia LA & Lodish HF. (1999). Identification of the major intestinal fatty acid transport protein. *Mol Cell* **4,** 299-308.

Su Z, Liu Y & Zhang H. (2021). Adaptive Cardiac Metabolism Under Chronic Hypoxia: Mechanism and Clinical Implications. *Front Cell Dev Biol* **9,** 625524.

Suzuki M, Shinohara Y, Ohsaki Y & Fujimoto T. (2011). Lipid droplets: size matters. *J Electron Microsc (Tokyo)* **60 Suppl 1,** S101-116.

Taegtmeyer H, Sen S & Vela D. (2010). Return to the fetal gene program: a suggested metabolic link to gene expression in the heart. *Ann N Y Acad Sci* **1188,** 191-198.

Thompson JA, Richardson BS, Gagnon R & Regnault TR. (2011). Chronic intrauterine hypoxia interferes with aortic development in the late gestation ovine fetus. *J Physiol* **589,** 3319-3332.

Thornburg KL & Reller MD. (1999). Coronary flow regulation in the fetal sheep. *Am J Physiol* **277,** R1249-1260.

Thureen PJ & Hay WW. (2006). *Neonatal nutrition and metabolism*. New York : Cambridge University Press, Cambridge, UK.

Uhlen M, Fagerberg L, Hallstrom BM, Lindskog C, Oksvold P, Mardinoglu A, Sivertsson A, Kampf C, Sjostedt E, Asplund A, Olsson I, Edlund K, Lundberg E, Navani S, Szigyarto CA, Odeberg J, Djureinovic D, Takanen JO, Hober S, Alm T, Edqvist PH, Berling H, Tegel H, Mulder J, Rockberg J, Nilsson P, Schwenk JM, Hamsten M, von Feilitzen K, Forsberg M, Persson L, Johansson F, Zwahlen M, von Heijne G, Nielsen J & Ponten F. (2015). Proteomics. Tissue-based map of the human proteome. *Science* **347,** 1260419.

Van Duyne CM, Parker HR, Havel RJ & Holm LW. (1960). Free fatty acid metabolism in fetal and newborn sheep. *Journal of Physiology* **199,** 987-990.

Vieira Neto E, Fonseca AA, Almeida RF, Figueiredo MP, Porto MA & Ribeiro MG. (2012). Analysis of acylcarnitine profiles in umbilical cord blood and during the early neonatal period by electrospray ionization tandem mass spectrometry. *Braz J Med Biol Res* **45,** 546-556.

Vlaardingerbroek H, Vermeulen MJ, Carnielli VP, Vaz FM, van den Akker CH & van Goudoever JB. (2014). Growth and fatty acid profiles of VLBW infants receiving a multicomponent lipid emulsion from birth. *J Pediatr Gastroenterol Nutr* **58,** 417-427.

von Bergen NH, Koppenhafer SL, Spitz DR, Volk KA, Patel SS, Roghair RD, Lamb FS, Segar JL & Scholz TD. (2009). Fetal programming alters reactive oxygen species production in sheep cardiac mitochondria. *Clin Sci (Lond)* **116,** 659-668.

Wang H, Lei M, Hsia RC & Sztalryd C. (2013). Analysis of lipid droplets in cardiac muscle. *Methods Cell Biol* **116,** 129-149.

Wang H, Sreenivasan U, Hu H, Saladino A, Polster BM, Lund LM, Gong DW, Stanley WC & Sztalryd C. (2011). Perilipin 5, a lipid droplet-associated protein,

provides physical and metabolic linkage to mitochondria. *J Lipid Res* **52,** 2159-2168.

Wang H, Wei E, Quiroga AD, Sun X, Touret N & Lehner R. (2010a). Altered lipid droplet dynamics in hepatocytes lacking triacylglycerol hydrolase expression. *Mol Biol Cell* **21,** 1991-2000.

Wang Z, Ying Z, Bosy-Westphal A, Zhang J, Schautz B, Later W, Heymsfield SB & Muller MJ. (2010b). Specific metabolic rates of major organs and tissues across adulthood: evaluation by mechanistic model of resting energy expenditure. *Am J Clin Nutr* **92,** 1369-1377.

Wells RJ, Friedman WF & Sobel BE. (1972). Increased oxidative metabolism in the fetal and newborn lamb heart. *Am J Physiol* **222,** 1488-1493.

Wendel AA, Lewin TM & Coleman RA. (2009). Glycerol-3-phosphate acyltransferases: rate limiting enzymes of triacylglycerol biosynthesis. *Biochim Biophys Acta* **1791,** 501-506.

Werner JC & Sicard RE. (1987). Lactate metabolism of isolated, perfused fetal, and newborn pig hearts. *Pediatr Res* **22,** 552-556.

Werner JC, Sicard RE & Schuler HG. (1989). Palmitate oxidation by isolated working fetal and newborn pig hearts. *Am J Physiol* **256,** E315-321.

Werner JC, Whitman V, Musselman J & Schuler HG. (1982). Perinatal changes in mitochondrial respiration of the rabbit heart. *Biol Neonate* **42,** 208-216.

Widdowson EM & McCance RA. (1963). The Effect of Finite Periods of Undernutrition at Different Ages on the Composition and Subsequent Development of the Rat. *Proc R Soc Lond B Biol Sci* **158,** 329-342.

Williams PJ, Marten N, Wilson V, Litten-Brown JC, Corson AM, Clarke L, Symonds ME & Mostyn A. (2009). Influence of birth weight on gene regulators of lipid metabolism and utilization in subcutaneous adipose tissue and skeletal muscle of neonatal pigs. *Reproduction* **138,** 609-617.

Willis DM, Anderson DF, Thornburg KL & Faber JJ. (1985). Alteration of arterial gas composition by positive pressure ventilation in the unanesthetized fetal lamb in utero. *Biol Neonate* **47,** 295-304.

Wulf A, Harneit A, Kroger M, Kebenko M, Wetzel MG & Weitzel JM. (2008). T3-mediated expression of PGC-1alpha via a far upstream located thyroid hormone response element. *Mol Cell Endocrinol* **287,** 90-95.

Xiao J, Gregersen S, Kruhoffer M, Pedersen SB, Orntoft TF & Hermansen K. (2001). The effect of chronic exposure to fatty acids on gene expression in clonal insulin-producing cells: studies using high density oligonucleotide microarray. *Endocrinology* **142,** 4777-4784.

Yamada M, Wolfe D, Han G, French SW, Ross MG & Desai M. (2011). Early onset of fatty liver in growth-restricted rat fetuses and newborns. *Congenit Anom (Kyoto)* **51,** 167-173.

Yamaguchi S, Indo Y, Coates PM, Hashimoto T & Tanaka K. (1993). Identification of very-long-chain acyl-CoA dehydrogenase deficiency in three patients previously diagnosed with long-chain acyl-CoA dehydrogenase deficiency. *Pediatr Res* **34,** 111-113.

Yang Q, Hohimer AR, Giraud GD, Van Winkle DM, Underwood MJ, He GW & Davis LE. (2008). Effect of fetal anaemia on myocardial ischaemia-reperfusion injury and coronary vasoreactivity in adult sheep. *Acta Physiol (Oxf)* **194,** 325-334.

Zou X, Huang J, Jin Q, Guo Z, Liu Y, Cheong L, Xu X & Wang X. (2013). Lipid composition analysis of milk fats from different mammalian species: potential for use as human milk fat substitutes. *J Agric Food Chem* **61,** 7070-7080.

BIOGRAPHICAL SKETCH

NAME OF APPLICANT: Rachel Drake

ERA COMMONS USER NAME (credential, e.g., agency login): drakra

POSITION TITLE: MD/PhD student, 7th year student, 5th year graduate

EDUCATION/TRAINING

INSTITUTION AND LOCATION	DEGREE	Completion	FIELD OF STUDY
University of Minnesota, Minneapolis, MN	BA	12/2013	Spanish Studies
University of Minnesota, Minneapolis, MN	BS	06/2014	Biochemistry
Oregon Health and Science University, Portland, OR	MD, PhD	08/2022	Fetal Development & Metabolism

PERSONAL STATEMENT

My love for science and medicine has been cultivated through a variety of unique experiences that have culminated in a career path towards becoming a physician scientist. Each undergraduate research experience opened my eyes to the multifaceted nature of scientific discovery. My first research experience studying Usherin piqued my interest

about how small genetic errors could have dire functional consequences. The next year, I was fascinated throughout my summer internship in the Rabinovitch lab which introduced me to the intricacies and challenges of formulating and testing research questions including experimental design, rationale/literature review, practical skills (survival mouse surgery, reading echocardiographs, tissue harvest and appropriate preservation), data analysis/interpretation and manuscript preparation. I chose that lab because I wanted to work closely with a physician scientist so I could better understand how to successfully navigate a career that involves both research and clinical components. I was thrilled to be part of a basic science research project that had clinical implications and I realized that this union of science and medicine was where I wanted to steer my career. I am grateful to Dr. Rabinovitch who continues to provide career mentorship and guidance. An extended research project mapping the coronary venous system in 121 human hearts was a wonderful opportunity to immerse myself in a project at a deeper level and taught me the value of computational and imaging skills and knowledge of cardiac anatomy. This project confirmed my plan to pursue a career at the interface of science and medicine.

I chose Oregon Health and Science University's (OHSU) Medical Scientist Training Program to follow this passion due its highly collaborative environment and a strong partnership between basic science research and clinical care. The culture at OHSU facilitates interactions with experts in various fields, stimulating translational research in a nurturing learning environment. Throughout my undergraduate education and first two years of medical school, I have taken advantage of the many opportunities presented to

me which has provided me with techniques in molecular biology, molecular metabolism and cardiovascular imaging.

OHSU is the premier location to conduct my thesis research because it has a long history of fetal physiology expertise using a large animal model, which now partners with newly developed imaging and bioanalytical techniques. For my thesis project, I am pairing *in vitro* with *in vivo* studies and examining lipid handling in a multifaceted manner which will allow rigorous scientific testing. With a plethora of techniques available, this has taught me to critically select the most appropriate methods to answer my research question. I feel fortunate to be mentored by Kent Thornburg, PhD who is a world expert of the developmental origins of disease. Dr. Thornburg and I developed an Individual Development Plan when I joined his lab two years ago and we follow this religiously to guide my progress and remain on track. My mentorship team is further strengthened by our lab community of postdoctoral fellows and research assistants, a partnership with Sergio Fazio, MD/PhD, an expert in lipidology, and regular interactions with the MD/PhD program director David Jacoby and MD/PhD students.

One of the reasons I was drawn to OHSU was their strong neonatology division, which has proven to be a vital aspect of my development as a physician scientist. My training is supplemented by a team of outstanding neonatologists including Brian Scottoline, MD/PhD and Cindy McEvoy, MD who provide guidance with both career advice and study design to ensure clinical relevance of my basic science project. These encounters reinforce the valuable partnership between scientific discovery, understanding

mechanistic underpinnings of disease, diagnosis and treatment which has been instrumental in formulating the focus of my thesis project. My thesis project has already given me a large appreciation for how critical the perinatal period is for determining perinatal and long term health. My ultimate goal is to be an independently funded scientist specializing in optimizing nutrition strategies for infants undergoing treatment in neonatal intensive care units. It is too early to predict the research direction, but will involve mechanistic studies designed with translation in mind.

POSITIONS AND HONORS

Undergraduate Research Intern	08/2012	06/2014	Cardiovascular Imaging	University of Minnesota	Paul Iaizzo, PhD
Summer Research Intern	06/2012	08/2012	Neuroscience	University of Oregon	Monte Westerfield, PhD
Summer Research Intern	06/2013	08/2013	Pathology	University of Washington	Peter Rabinovitch, MD/PhD
Student Health Advisory Committee Co-chair	09/2012	05/2013	Public Health	University of Minnesota	Dave Golden
Teaching Assistant	09/2013	12/2012	Biochemistry	University of Minnesota	Janet Schottel, PhD
Teaching Assistant	01/2014	05/2014	Biochemistry	University of Minnesota	Paul Siliciano, PhD
NCAA Division I Cross Country Team Captain	09/2012	05/2014	Athletics	University of Minnesota	Gary Wilson

Wilderness Medicine Interest Group Leader	09/2015	05/2016	Leadership	Oregon Health and Science University	Craig Warden, MD
Women's Leadership Development Program Peer Mentor	09/2016	current	Leadership	Oregon Health and Science University	Megan Furnari, MD
MD Program Interviewer	09/2017	current	Admissions	Oregon Health and Science University	Kari Kriedberg
MD/PhD Committee Student Representative	08/2018	current	Admissions	Oregon Health and Science University	David Jacoby, MD

Academic and Professional Honors

2009-2014 Dean's List: Awarded by the University of Minnesota College of Biological Sciences and College of Liberal Arts

2013 Rhodes Scholarship Finalist: Awarded by the Rhodes Trust

2014 Big Ten Postgraduate Scholarship: Awarded by the Big Ten Conference

2014 Wayne Duke Postgraduate Award Nominee: Awarded by the University of Minnesota Athletic Department

2016 Tartar Trust Grant Awardee

CONTRIBUTIONS TO SCIENCE

I was part of three research projects as an undergraduate student, all of which have clinical ties: 1) mapping the coronary venous system in human hearts, 2) determining electron

transport protein turnover rates in mice to better understanding mitochondrial dysfunction and 3) studying domains of proteins whose mutations can lead to hereditary deaf-blindness. In my PhD thesis lab at Oregon Health and Science University, I am investigating cardiomyocyte metabolism in a fetal sheep model. I have spent the past two years mastering an array of techniques in the laboratory relevant to both my own projects and to other ongoing projects in the lab. One such project with a postdoctoral fellow (Isa Lindgren, PhD) is focused on the metabolic switch from carbohydrate to fatty acid metabolism in the perinatal period. I used siRNA knockdown *in vitro* to suppress the transcription factor, MEIS1 and determine the impact on fatty acid metabolism using a Seahorse extracellular flux analyzer, which measures oxygen consumption in response to fatty acid substrate. I also imaged mitochondrial morphology in the presence and absence of MEIS1 and measured myocardial gene and protein expression.

1. Thornburg KL, Kolahi K, Pierce M, Valent A, **Drake R**, Louey S. “Biological Features of Placental Programming.” Placenta, 2016 Dec; 48 [Supplement 1]: S48-S53. PMC5278807
2. Lindgren I, **Drake R**, Thornburg KL. “MEIS1 promotes the maturation of oxidative phosphorylation in perinatal cardiomyocytes.” FASEB J. 2019 Jun, 33(6): 7417-7426. PMC6529342.
3. Thornburg KL, **Drake R**, Valent AM. “Maternal Hypertension Affects Heart Growth in Offspring.” J Am Heart Assoc. 2020 May 5; 9(9):e016538. PMC7428588.

Mapping the coronary venous system for aiding the development of medical devices University of Minnesota, Mentor: Paul Iaizzo, PhD

This translational project involved mapping out the coronary venous system using perfusion fixed human hearts. Access to the coronary venous system is required for the delivery of several cardiac therapies including cardiac resynchronization therapy, coronary sinus ablation, and coronary drug delivery. However, current devices are not always able to navigate the coronary venous system appropriately. The goal of the project was to better understand the implications of coronary venous anatomy for the development of devices deployed within these vessels. My role in the project was to assist the graduate student at the time (Julianne Spencer, PhD) by cannulating the coronary sinus of 121 hearts with a venogram balloon catheter and injecting contrast in order to obtain computed tomographic images. For each major coronary vein, I measured the distance to the coronary sinus, branching angle, arc length, tortuosity, number of branches, and ostial diameter from the reconstructed anatomy in MATLAB.

1. Spencer JH, Larson AA, **Drake R**, Iaizzo PA. A detailed assessment of the human coronary venous system using contrast computed tomography of perfusion-fixed specimens. Heart Rhythm. 2014 Feb;11(2):282-8. PMC24144884.

Measuring protein turnover rates of electron transport chain proteins to better understand mitochondrial dysfunction University of Washington, Mentor: Peter Rabinovitch, MD/PhD

This project focused on measuring the protein turnover rates of the electron transport proteins. Mitochondrial dysfunction has a central role in aging and a wide range of diseases. As a biochemistry major, I was eager to apply my knowledge of fundamental

molecular metabolism to an animal model that allowed me to follow tissue from *in vivo* all the way to *in vitro* and molecular analyses. My role in the project was to localize electron transport chain subunits to intermembrane, inner mitochondrial membrane or mitochondrial matrix. This project on respiratory chain protein dynamics *challenged the notion that all mitochondrial proteins turnover at similar rates and that RC complexes and supercomplexes are maintained in unitary solid states.* I presented this project as a poster at the 2013 LifeScience Alley Conference in Minneapolis.

1. Karunadharma PP, Basisty N, Chiao YA, Dai DF, **Drake R**, et al. Respiratory chain protein turnover rates in mice are highly heterogeneous but strikingly conserved across tissues, ages, and treatments. FASEB J. 2015 Aug;29(8):3582-92. PMC4511201.

Determining functional significance of protein domains of Usherin, a protein involved in Usher Syndrome (hereditary deafblindness): University of Oregon, Mentor: Monte Westerfield, PhD

This project involved studying protein domains of Usherin, which when mutated can lead to Usher syndrome, the most prevalent cause of hereditary deafblindness. Usher type 2A is the most widespread form of the syndrome, caused by mutations in the *USH2A* gene. *USH2A* consists of 72 exons encoding the protein Usherin, with several functional domains have been identified. Determining the relative importance of these functional domains is crucial to the development of effective therapies. My role was to design morpholino oligonucleotides to alter splice sites at either the 5' and 3' region, inject them and establish phenotypic traits to categorize each defect. The key finding from this study is that the PDZ binding domain is essential for photoreceptor survival and truncating this

domain induces cell death. I presented this project at the 2012 LifeScience Alley Conference in Minneapolis and the 2013 American Biochemistry and Molecular Biology Conference in Boston.

Complete List of Published Work

https://www.ncbi.nlm.nih.gov/sites/myncbi/1dU2biUeU8h5k/collections/56099211/public/

SCHOLASTIC PERFORMANCE

YEAR	SCIENCE COURSE TITLE	GRADE	YEAR	OTHER COURSE TITLE	GRADE
	University of Minnesota				
2009	Introduction to Chemistry + Lab	A	2007	Intermediate Spanish I	A
2009	Precalculus II	A	2008	Intermediate Spanish II	A
2010	Chemical Principles I	A	2008	Introduction to Literature	A
2010	Calculus I	A	2009	Spanish Composition and Communication	A
2010	Chemical Principles II	A	2010	Advanced Communication Skills (Spanish)	A-
2010	Calculus II	B+	2010	Writing and Academic Inquiry	A
2011	Foundations of Biology I	A	2010	Introduction to Psychology	A
2011	Organic Chemistry I	A	2010	Hispanic Cultures	B+
2011	Organic Chemistry II	A-	2011	Mexican Art History	A

YEAR	SCIENCE COURSE TITLE	GRADE	YEAR	OTHER COURSE TITLE	GRADE
2011	Organic Chemistry Lab	A	2011	Introduction to the Study of Hispanic Literature	A
2011	Physics I	A-	2011	Hispanic Linguistics	A
2012	Introduction to Biochemistry	A	2011	Spanish Film Studies	A
2012	Foundations of Biology II + Lab	A	2011	Modern Latin America	A
2012	Animal Diversity Lab	A	2012	Topics in Spanish American Literature	A
2012	Physiology	B+	2012	Latinos in the United States	A
2012	Biochemistry: Structure, Catalysis, Metabolism	A	2012	Hispanic Issues	A-
2012	Genetics	A	2013	Medical Spanish and Community Health Service	A
2012	Directed Research	P	2013	Drugs and the U.S. Healthcare System	A
2013	Biochemistry Research Topics	P	2013	Public Health: From Lab to Bedside to Populations	A
2013	Laboratory in Biochemistry	A	2013	Spanish Graduation Seminar	A-
2013	Physics II	A			
2013	Biochemistry: Signal Transduction and Gene Expression	A			
2013	Cell Biology	A-			
2013	Speech Language Hearing Sciences: Talking Brain	A			

YEAR	SCIENCE COURSE TITLE	GRADE	YEAR	OTHER COURSE TITLE	GRADE
2014	Introduction to Physical Biochemistry	A-			

Oregon Health and Sciences University 2014–present

Physiology and Pharmacology Graduate Program			**Medicine**		
YEAR	COURSE TITLE	GRADE	YEAR	COURSE TITLE	GRADE
2016	Practice and Ethics of Science	P	2014	Fundamentals of Medicine	P
2016-2018	Physiology and Pharmacology Departmental Seminar	P	2014	Blood and Host Defense	P
2016-2018	Physiology and Pharmacology Journal Club	P	2015	Skin, Bones and Musculature	P
2018	Developmental Origins of Health and Disease	P	2015	Cardiopulmonary and Renal	P
2018	Biostatistics	A	2015	Hormones and Digestion	P
			2015	Nervous System and Function	P
			2015	Developing Human	P
			2016	Transition to Clinical Experiences	P
MD/PhD Coursework					
2014-2021	MD/PhD Journal Club	P			
2016-2018	MD/PhD Longitudinal Clerkship	P			

Undergraduate and Graduate Grading: A-F; Medical School Grading: Pass (P)/Fail (F), In Progress (IP)

Standardized Test Scores

MCAT: Phy Sci 10 Bio Sci 10 Verbal 8 : 28

US Medical Licensing Exam I (01/2016): 235 (passing 192)